

FABRICATION OF ECO-FRIENDLY DYE SENSITIZED SOLAR CELLS  
USING NATURAL DYE AS LIGHT-HARVESTING PIGMENTS



PHITCHAPHORN KHAMMEE

MASTER OF ENGINEERING IN RENEWABLE ENERGY ENGINEERING  
MAEJO UNIVERSITY  
2021

FABRICATION OF ECO-FRIENDLY DYE SENSITIZED SOLAR CELLS  
USING NATURAL DYE AS LIGHT-HARVESTING PIGMENTS



PHITCHAPHORN KHAMMEE

A THESIS SUBMITTED IN PARTIAL FULFILLMENT  
OF THE REQUIREMENTS FOR THE DEGREE OF MASTER OF ENGINEERING  
IN RENEWABLE ENERGY ENGINEERING  
ACADEMIC ADMINISTRATION AND DEVELOPMENT MAEJO UNIVERSITY

2021

Copyright of Maejo University

FABRICATION OF ECO-FRIENDLY DYE SENSITIZED SOLAR CELLS  
USING NATURAL DYE AS LIGHT-HARVESTING PIGMENTS

PHITCHAPHORN KHAMMEE

THIS THESIS HAS BEEN APPROVED IN PARTIAL FULFLLMENT  
OF THE REQUIREMENTS FOR THE DEGREE OF MASTER OF ENGINEERING  
IN RENEWABLE ENERGY ENGINEERING

APPROVED BY

**Advisory Committee**

Chair .....

(Dr. Rameshprabu Ramaraj)

...../...../.....

Committee .....

(Assistant Professor Dr. Natthawud Dussadee)

...../...../.....

Committee .....

(Assistant Professor Dr. Yuwalee Unpaprom)

...../...../.....

Committee .....

(Associate Professor Dr. Theerapol Thurakitseree)

...../...../.....

Program Chair, Master of Engineering .....

in Renewable Energy Engineering (Assistant Professor Dr. Tanate Chaichana)

...../...../.....

**CERTIFIED BY ACADEMIC**

.....

**ADMINISTRATION AND DEVELOPMENT**

(Associate Professor Dr. Yanin Opatpatanakit)

Vice President for the Acting President of Maejo

University

...../...../.....

ชื่อเรื่อง	การประดิษฐ์เซลล์แสงอาทิตย์ชนิดสีย้อมไวแสงที่เป็นมิตรต่อสิ่งแวดล้อม โดยใช้สีย้อมธรรมชาติเป็นรงควัตถุสำหรับเก็บเกี่ยวแสง
ชื่อผู้เขียน	นางสาวพิชชาพร คำมี
ชื่อปริญญา	วิศวกรรมศาสตรมหาบัณฑิต สาขาวิชาวิศวกรรมพลังงานทดแทน
อาจารย์ที่ปรึกษาหลัก	Dr. Rameshprabu Ramaraj

### บทคัดย่อ

หนึ่งในอุปกรณ์พลังงานหมุนเวียนที่น่าสนใจคือ เซลล์แสงอาทิตย์ที่ไวต่อการย้อมสี (DSSC) ซึ่งสามารถเปลี่ยนรังสีดวงอาทิตย์เป็นพลังงานไฟฟ้า โดยใช้เม็ดสีจากธรรมชาติเป็นสารไวแสง เทคนิคการเตรียมที่เรียบง่าย ต้นทุนต่ำ กระบวนการสกัดที่เป็นไปได้ เม็ดสีที่ไม่เป็นอันตราย การย่อยสลายทางชีวภาพที่สมบูรณ์และเป็นมิตรต่อสิ่งแวดล้อม ซึ่งเป็นข้อดีของ DSSC นอกจากนี้กระบวนการสกัดสีจากธรรมชาตินั้นง่ายและราคาไม่แพง เมื่อเทียบกับสีสังเคราะห์ เม็ดสีธรรมชาติเหล่านี้ เช่น คลอโรฟิลล์ แอนโทไซยานิน แคโรทีนอยด์ และฟลาโวนอยด์ ถูกสกัดจากดอกไม้ ใบ ราก และผลไม้ จากแหล่งพืช เนื่องจากความได้เปรียบของเม็ดสีใน DSSC การใช้สีย้อมธรรมชาติจึงเป็นวัตถุประสงค์หลักในการศึกษานี้ ดังนั้นงานวิจัยนี้จึงศึกษาการสกัดสีย้อมธรรมชาติ จากพืชเขตร้อน (ใบหูกวาง; *Terminalia catappa*, ดอกสุพรรณิการ์; *Cochlospermum regium*, ใบลำไย; *Dimocarpus longan* และ ใบอินทนิลบก; *Lagerstroemia macrocarpa*) โดยใช้วิธีการสกัดด้วยตัวทำละลายเมทานอล และวิเคราะห์ประสิทธิภาพของชั้นที่แตกต่างกัน (1, 2 และ 3 ชั้น) และอุณหภูมิ (100, 200 และ 300 °C) ของไททาเนียมไดออกไซด์ที่เคลือบบนกระจกที่นำไฟฟ้าซึ่งคือ ดีบุกออกไซด์ที่เจือฟลูออรีน (FTO, SnO<sub>2</sub>: F) เพื่อประเมินประสิทธิภาพของเซลล์แสงอาทิตย์ที่ไวต่อการย้อมสี (DSSC) โดยเครื่องสเปกโตรมิเตอร์ที่มองเห็นได้ด้วยรังสี UV ใช้สำหรับวิเคราะห์ความยาวคลื่น การดูดซับสีย้อมธรรมชาติสำหรับการใช้งาน DSSC ผลการวิจัยพบว่า เม็ดสีที่สกัดจากใบลำไยมีปริมาณเม็ดสีสูงกว่าสีย้อมธรรมชาติอื่น ๆ ประกอบด้วยคลอโรฟิลล์ - เอมากที่สุดคือ  $85.213 \pm 0.403 \mu\text{g} / \text{ml}$  ตามด้วยคลอโรฟิลล์ - บี และแคโรทีนอยด์มีค่า  $28.083 \pm 0.079$  และ  $13.128 \pm 0.125 \mu\text{g} / \text{ml}$  ตามลำดับ นอกจากนี้สภาพของอนุภาคนาโนไททาเนียมไดออกไซด์ ที่ความหนาหนึ่งชั้นและใช้ อุณหภูมิในการหลอม 300 °C ด้วยสีย้อมธรรมชาติที่สกัดจากใบลำไย มีประสิทธิภาพสูงสุดโดยมีค่า  $0.4735 \pm 0.043\%$  เครื่องเอ็กซ์เรย์สเปกโทรสโกปีแบบกระจายพลังงาน (EDX) ใช้สำหรับยืนยันองค์ประกอบของอนุภาคนาโนไททาเนียมไดออกไซด์ และสีย้อมธรรมชาติ กล้องจุลทรรศน์อิเล็กตรอน



แบบส่องกราด (SEM) และกล้องจุลทรรศน์เลเซอร์สแกน ที่ใช้สำหรับวิเคราะห์ลักษณะทางสัณฐานวิทยาของอนุภาคนาโนไททาเนียมไดออกไซด์ และสีย้อมธรรมชาติ นอกจากนี้ไบอินทิลบคยังมีประสิทธิภาพสูงสุดด้วย  $1.138\% \pm 0.018$  ซึ่งสภาพของอนุภาคนาโนไททาเนียมไดออกไซด์ 1 ชั้น และอุณหภูมิ  $300\text{ }^{\circ}\text{C}$  เมื่อเปรียบเทียบกับ ไบหูกวาง, ดอกสุพรรณิการ์ และใบลำไย ดังนั้นการใช้สารสกัดเหล่านี้จะช่วยเพิ่มประสิทธิภาพและลดต้นทุนการผลิตสำหรับการผลิต DSSC

คำสำคัญ : การสกัดเม็ดสี, คลอโรฟิลล์, แคโรทีนอยด์, สีย้อมธรรมชาติ, เซลล์แสงอาทิตย์ชนิดสีย้อมไวแสง



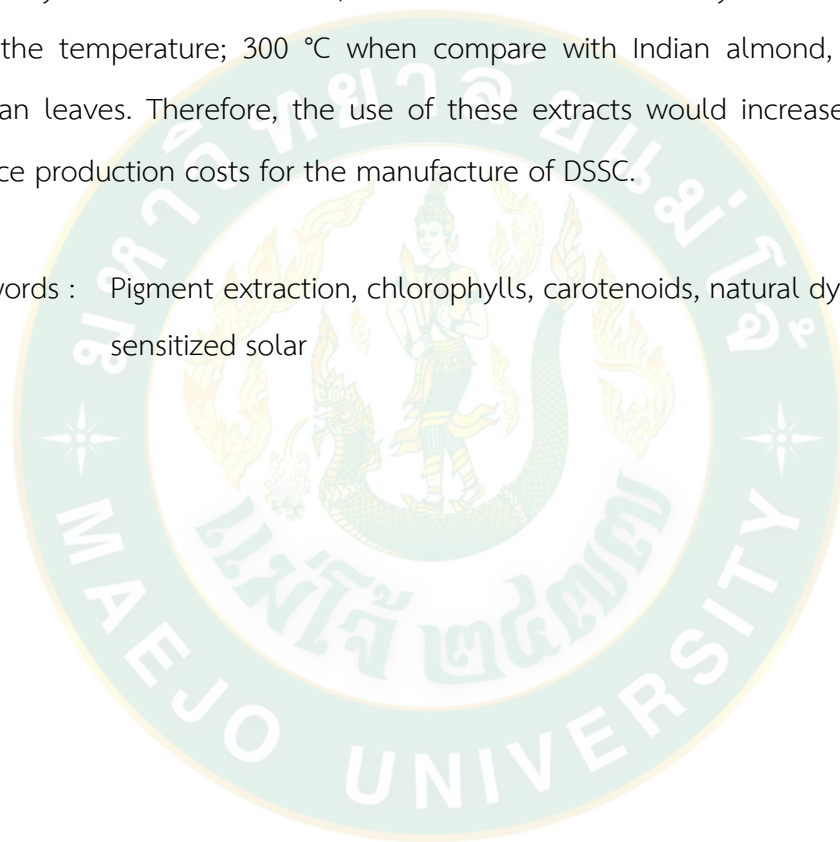
<b>Title</b>	FABRICATION OF ECO-FRIENDLY DYE SENSITIZED SOLAR CELLS USING NATURAL DYE AS LIGHT-HARVESTING PIGMENTS
<b>Author</b>	Miss Phitchaphorn Khammee
<b>Degree</b>	Master of Engineering in Renewable Energy Engineering
<b>Advisory Committee Chairperson</b>	Dr. Rameshprabu Ramaraj

### ABSTRACT

One of the interesting renewable energy devices is dye-sensitized solar cells (DSSC), which can convert solar radiation into electricity by using natural pigments as sensitizers. The simple preparation technique, low cost, feasible extraction processes, innocuous pigments, complete biodegradation and environmentally friendly are the advantage of DSSC. Besides, the extraction process of natural pigments is simple and inexpensive compared with synthetic dyes. These natural pigments such as chlorophylls, anthocyanin, carotenoids, and flavonoids were extracted from flowers, leaves, roots, and fruits from the plant source. Due to pigment advantage on DSSC, natural dyes utilization is the main objective in this study. Thus, this research study on the extraction of natural dye from tropical plants (*Terminalia catappa*, *Cochlospermum regium*, *Dimocarpus longan* and *Lagerstroemia macrocarpa*) by using solvent extraction method. Moreover, analyze the effectiveness of the different layers (1, 2 and 3 layers) and temperature (100, 200 and 300 °C) of TiO<sub>2</sub> on fluorine-doped tin oxide (FTO, SnO<sub>2</sub>: F) to evaluate the efficiency of dye-sensitized solar cells (DSSC). A UV-visible spectrometer was used for analyzing the natural dye's absorption wavelength for the DSSC application. The result showed the pigment extracted from longan leaves had the highest pigment content than other natural dyes. The most composed of chlorophyll-a, which is  $85.213 \pm 0.403$  µg/ml, followed by chlorophyll-b and carotenoids with is  $28.083 \pm 0.079$  and  $13.128 \pm 0.125$  µg/ml, respectively. The

condition of one layer and 300 °C of the TiO<sub>2</sub> nanoparticle with natural dye extracted from longan leaves have the highest efficiency with 0.4735 ±0.043%. The energy-dispersive X-ray spectroscopy (EDX) was used for confirmed the elemental of the TiO<sub>2</sub> nanoparticles and natural dyes. The scanning electron microscope (SEM) and the laser scanning microscope used for analyzed morphological characteristics of TiO<sub>2</sub> nanoparticles and natural dyes. Moreover, Inthanin bok leaves have the highest efficiency with 1.138% ± 0.018, which the condition of 1 layer of TiO<sub>2</sub> nanoparticles and the temperature; 300 °C when compare with Indian almond, Yellow cotton, Longan leaves. Therefore, the use of these extracts would increase efficiency and reduce production costs for the manufacture of DSSC.

Keywords : Pigment extraction, chlorophylls, carotenoids, natural dyes, dye-sensitized solar



## ACKNOWLEDGEMENTS

First of all, I would like to express my sincere thanks to my advisor Dr. Rameshprabu Ramaraj as well as my co-advisor Asst. Prof. Dr. Yuwalee Unpaprom who gave me the great opportunity for doing a Master's Degree. Their suggestions and invaluable guidance helped me all the time of research and this wonderful thesis of Fabrication Of Eco-Friendly Dye Sensitized Solar Cells Using Natural Dye As Light-Harvesting Pigments. Without their persistent, this Master's study could not be completed.

Secondly, I gratefully acknowledge my co-advisor: Asst. Prof. Dr. Natthawud Dussadee and Asst. Prof. Dr. Theerapol Thurakitseree for their kindness and encouragement to carry out my thesis work. I also extend my gratefulness to external examiner Dr. Rattanachai Pairintra, Assistant Professor, Division of Biochemical Technology, School of Bioresources and Technology, King Mongkut's University of Technology Thonburi, Bangkok, Thailand for meticulously criticized my research for better output.

In additional, I would like to thank my parents, my family, my boyfriend, friends and everyone who helped me a lot in finishing this project within the allotted time. Lastly, I gratefully acknowledged the School of Renewable Energy, Program in Biotechnology, Energy Research Center and the Department of Graduate Studies, Office of Academic Administration and Development, Maejo University, Chiang Mai, Thailand, for the research fund and facilities to accomplish this experimental study.

Phitchaphorn Khammee

## TABLE OF CONTENTS

	Page
ABSTRACT (THAI).....	C
ABSTRACT (ENGLISH).....	E
ACKNOWLEDGEMENTS.....	G
TABLE OF CONTENTS.....	H
LIST OF TABLES.....	K
LIST OF FIGURE.....	L
CHAPTER 1 INTRODUCTION.....	1
1.1 Research objectives.....	4
1.2 Scope of research.....	5
1.3 Benefits of study.....	5
CHAPTER 2 LITERATURE REVIEW.....	6
2.1 Solar energy.....	6
2.2 Generation of solar cell.....	7
2.2.1 First generation of photovoltaics (1970s).....	7
2.2.2 Second generation of photovoltaics (1980s).....	8
2.2.3 Third generation of photovoltaics (1990s).....	9
2.3 Dye-sensitized solar cells (DSSC).....	10
2.4 Structure of dye-sensitized solar cell (DSSCs).....	11
2.5 Operation principle of dye-sensitized solar cell (DSSCs).....	12
2.6 Components of dye-sensitized solar cell (DSSCs).....	14
2.6.1 Transparent and conductive substrate.....	14

2.6.2 Photoelectrode (Titanium dioxide).....	14
2.6.3 Dye-sensitized photosensitizer .....	15
2.6.3.1 Natural dye-sensitizers .....	16
2.6.3.1.1 Anthocyanin .....	17
2.6.3.1.2 Flavonoids .....	17
2.6.3.1.3 Carotenoids .....	18
2.6.3.1.4 Chlorophyll .....	18
2.6.3.2 Plants material.....	19
2.6.4 Electrolyte.....	24
2.6.5 Counter electrode.....	24
2.7 Technique of fabrication DSSC.....	25
2.7.1 Physical methods.....	26
2.7.1.1 Dip coating.....	26
2.7.1.2 Spin coating.....	26
2.7.1.3 Doctor blade printing.....	27
2.7.2 Chemical methods .....	28
2.7.2.1 Sol-gel coating.....	28
2.8 Performance of the dye-sensitized solar cells.....	28
CHAPTER 3 MATERIALS AND METHODS.....	31
3.1 Materials and chemicals .....	31
3.2 Materials preparation.....	32
3.3 Pigment extraction processes.....	33
3.4 Pigment analysis and characterization.....	34
3.5 Preparation of FTO glass substrates .....	35

3.6 Preparation of TiO <sub>2</sub> nanoparticle paste as a photoanode.....	35
3.7 Preparation of electrolyte .....	36
3.8 Characterization techniques .....	38
3.9 Statistical analysis.....	38
CHAPTER 4 RESULTS AND DISCUSSION .....	39
4.1 Spectrophotometric analysis of pigments extraction.....	39
4.1.1 Indian almond.....	40
4.1.2 Yellow cotton.....	41
4.1.3 Longan.....	42
4.1.4 Inthanin bok.....	43
4.2 The pigment extraction content and estimation of natural dyes.....	44
4.3 The effect of different nanostructure layers of photoanode .....	47
4.4 The effect of different temperature of photoanode.....	49
4.5 The surface and morphology analysis of TiO <sub>2</sub> nanoparticles with natural dyes.....	53
4.6 Performance of DSSC with the natural dyes .....	62
CHAPTER 5 SUMMARY AND CONCLUSION .....	69
REFERENCES .....	71
APPENDIX A PUBLICATIONS .....	84
APPENDIX B CERTIFICATES .....	110
CURRICULUM VITAE.....	115



## LIST OF TABLES

	<b>Page</b>
Table 1 The amount of pigment extract from natural dyes .....	45
Table 2 The DSSC parameters of the devices obtained with different thicknesses (1,2 and 3 layers) with natural dyes extracted from Longan leaves .....	48
Table 3 The DSSC parameters of the devices obtained with different thicknesses (1,2 and 3 layers) with natural dyes extracted from Longan leaves .....	50
Table 4 The area under a graph ( $\mu\text{m}^2$ ) of longan dyes coated on $\text{TiO}_2$ layers.....	52
Table 5 The elemental composition of $\text{TiO}_2$ coated on FTO glass substrate with natural dyes immersion of Indian almond, Yellow cotton, Longan and Inthanin bok leaves.....	57
Table 6 The area under a graph ( $\mu\text{m}^2$ ) of natural dyes coated on $\text{TiO}_2$ layers .....	61
Table 7 The DSSC parameters of the devices obtained with different thicknesses and temperature with natural dyes extracted from Indian almond, yellow cotton, longan and inthanin bok.....	63
Table 8 The DSSC parameters of the devices obtained with different natural dyes extraction .....	67

## LIST OF FIGURE

	Page
Figure 1 Estimated finite and renewable planetary energy reserves (Terawatt-years) (Perez and Perez, 2015).....	2
Figure 2 Basic structure and operating principle of DSSC (Gong et al., 2017).....	12
Figure 3 Schematic structure of DSSC (Ludin et al., 2014).....	13
Figure 4 The chemical structure of (A) Anthocyanin, (B) Flavonoid, (C) $\beta, \beta$ - Carotene and (D) Chlorophyll (Ludin et al., 2014) .....	17
Figure 5 Indian almond ( <i>Terminalia catappa</i> ).....	19
Figure 6 Yellow cotton ( <i>Cochlospermum regium</i> ).....	20
Figure 7 Longan ( <i>Dimocarpus longan</i> ) .....	22
Figure 8 Inthanin bok ( <i>Lagerstroemia macrocarpa</i> ) .....	23
Figure 9 Schematic diagram of dip coating methods (A) Batch type and (B) Continuous type dip coating (a) immersion (b) startup and (c) pull-up steps (Ahmad et al., 2017). .....	26
Figure 10 Schematic of spin coating technique (Ahmad et al., 2017).....	27
Figure 11 Schematic of the doctor blade technique (Ahmad et al., 2017).....	28
Figure 12 Illustration of current-voltage (J-V) curve of a solar cell (Dawoud, 2016) ....	29
Figure 13 The framework of DSSC fabrication .....	31
Figure 14 Materials collection of (a) Indian almond, (b) Yellow cotton, .....	32
Figure 15 Materials preparation of (a) Indian almond, (b) Yellow cotton,.....	33
Figure 16 The extraction processes (a) Cut to small pieces, (b) The sample mixed with methanol by using a blender, (c) The vacuum filter was separated solid and liquid and (d) The pigments extraction .....	34
Figure 17 The natural dyes from (a) Indian almond, (b) Yellow cotton, .....	34

Figure 18 (a) Soap solution, (b) Distilled water and (c) Methanol for clean FTO glass	35
Figure 19 The preparation of TiO <sub>2</sub> nanoparticle paste; (a) Weigh TiO <sub>2</sub> powder, (b) The mixer of 5 g of TiO <sub>2</sub> powder, 10 ml of 5% acetic acid and 0.5 ml of surfactant.....	36
Figure 20 Immersed in natural dye sensitizer solution at room temperature; (a) Indian almond, (b) Yellow cotton, (c) Longan and (d) Inthanin bok.....	36
Figure 21 The processes of assembly DSSC and measurement.....	37
Figure 22 Schematic circuit diagram of the experimental setup used to measure the current-voltage characteristics of DSSC with variable resistance (10 k $\Omega$ ).....	38
Figure 23 The absorption wavelength of pigments (Carvalho et al., 2011).....	40
Figure 24 The absorption wavelength of pigments extraction (Indian almond leaves) .....	40
Figure 25 The absorption wavelength of pigments extraction (Yellow cotton flower)	41
Figure 26 The absorption wavelength of pigments extraction (Longan leaves).....	42
Figure 27 The absorption wavelength of pigments extraction (Inthanin bok leaves) ..	43
Figure 28 The amount of pigment extract from natural dyes .....	45
Figure 29 The pH of pigment extract from natural dyes.....	46
Figure 30 The photocurrent–voltage characteristics curve for the DSSC extraction natural pigment (Longan leaves).....	48
Figure 31 The photocurrent–voltage characteristics curve for the DSSC extraction natural pigment (Longan leaves).....	51
Figure 32 The laser scanning microscope analyzed the surface and morphology of longan dyes coated on TiO <sub>2</sub> layers (1 layer and 100 °C ) .....	51
Figure 33 The laser scanning microscope analyzed the surface and morphology of longan dyes coated on TiO <sub>2</sub> layers (1 layer and 300 °C).....	52
Figure 34 Scanning electron microscope of morphological characteristics of TiO <sub>2</sub> thin films annealed at 300 °C.....	54

Figure 35 Scanning electron microscope of morphological characteristics of TiO <sub>2</sub> thin films with natural dye extraction from (a) Indian almond, (b) Yellow cotton, (c) Longan and (d) Inthanin bok leaves dye annealed at 300 °C .....	54
Figure 36 The energy-dispersive X-ray spectroscopy (EDX) analysis of TiO <sub>2</sub> coated on FTO glass substrate (a1,2) .....	55
Figure 37 The energy-dispersive X-ray spectroscopy (EDX) analysis of TiO <sub>2</sub> coated on FTO glass substrates with natural dyes immersion (a1,2) Indian almond, (b1,2) Yellow cotton, (c1,2) Longan and (d1,2) Inthanin bok leaves. ....	56
Figure 38 The laser scanning microscope analyzed the surface and morphology of Indian almond dyes coated on TiO <sub>2</sub> layers; (a1-3) 1 layer and 100 °C .....	59
Figure 39 The laser scanning microscope analyzed the surface and morphology of yellow cotton dyes coated on TiO <sub>2</sub> layers; (a1-3) 1 layer and 100 °C .....	59
Figure 40 The laser scanning microscope analyzed the surface and morphology of longan dyes coated on TiO <sub>2</sub> layers; (a1-3) 1 layer and 100 °C .....	60
Figure 41 The laser scanning microscope analyzed the surface and morphology of inthanin bok dyes coated on TiO <sub>2</sub> layers; (a1-3) 1 layer and 100 °C .....	60
Figure 42 The photocurrent–voltage characteristics curve for the DSSC extraction ....	65
Figure 43 The photocurrent–voltage characteristics curve for the DSSC .....	65
Figure 44 The photocurrent–voltage characteristics curve for the DSSC .....	66
Figure 45 The photocurrent–voltage characteristics curve for the DSSC .....	66
Figure 46 Scanning electron microscope of morphological characteristics of TiO <sub>2</sub> thin films with natural dye extraction from longan (stored pigment) .....	67

## CHAPTER 1

### INTRODUCTION

Human activities emphatically relied upon the wealth of natural assets (mainly water, minerals, and vitality). A continued populace development and the longing for improved living conditions cause individuals to have an expanding vitality request that might be a long way past the accessible customary vitality supply, for example, coal, oil, and flammable gas. The assessed vitality utilization of the world will arrive at 27 Terawatt-years in 2050 (Perez and Perez, 2015). This implies the vitality utilization design needs be moved from limited vitality stores to inexhaustible assets in a progressively productive way, and this way, lessen our reliance on conventional petroleum derivatives, mineral, and natural assets. In such a manner, using a sustainable power source is of significance for a practical advancement of our general public and the insurance of our planet/condition. Looking at different vitality assets of our planet figure 1, the capability of sun oriented vitality predominates the potential from some other vitality asset on the planet (Perez and Perez, 2015).

Solar energy delivered from daylight striking the earth in 1h is higher than all the vitality devoured by people on the planet in one year. In this way, sun based vitality, as the most plenteous sustainable power source on the planet, can be collected and changed into different types of vitality for reasonable applications by thermoelectric, photocatalytic, photovoltaic (PV), and photo electrochemical (PEC) innovations. Among them, the PV innovation as one model of sun oriented vitality usage is by and large regarded to assume a first job in catching sunlight based vitality and straightforwardly changing it into electrical vitality (Yun et al., 2018).



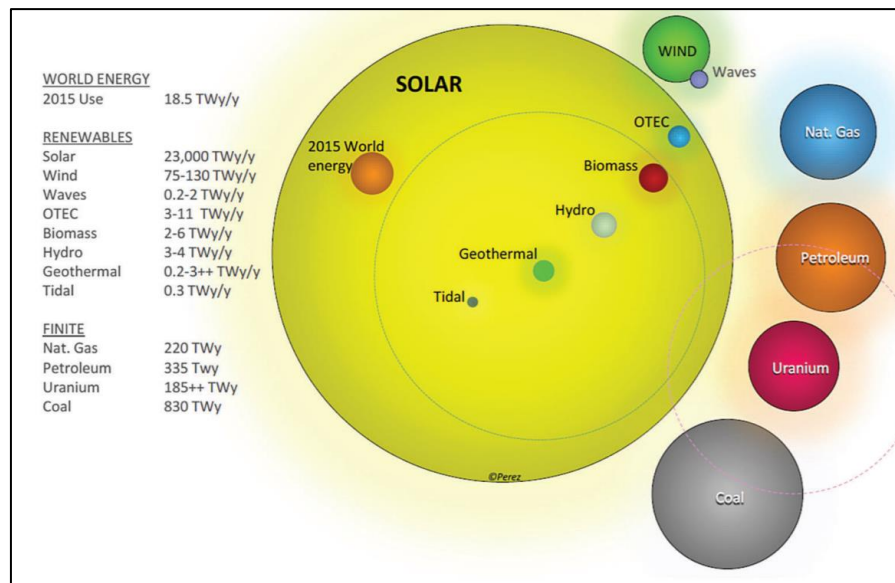


Figure 1 Estimated finite and renewable planetary energy reserves (Terawatt-years) (Perez and Perez, 2015)

Photovoltaic technologies are growing fast in fundamental research and industrialization. Solar cell formation can be organized into three stages. The word "first generation" refers to p-n intersection photovoltaics, which are usually made of monocrystalline silicon and polycrystalline silicon doped with various components. (Spath et al., 2003; Yun et al., 2018). In monocrystalline and polycrystalline photovoltaic solar systems, a long and demanding manufacturing process is used for each crystal and piece of silicon. The solar cell modules that have done the best were initial monocrystalline silicon. Whatever, these cells do not.

Thin-film photovoltaic (PV) cells Amorphous semiconductors are built on polycrystalline. So far, this generation has been considering as key thin-film candidates. (Ludin et al., 2014). Thin-film substance layers with various bandgaps improve the efficiency. However, the cost also increase due to many processes or technique relate to the coating each layer of materials during fabrication (Zainudin et al., 2011).

Most recently, low-cost solar cells have taken center stage in R&D. The third generation of solar cell technologies differs from their predecessors in that they have a higher yield, which, however are much more expensive and more scarce costs (Green,

2006; Marti and Luque, 2003; Zhao et al., 1999). The more significant part of the third-generation photovoltaic cells are still remains in the early phases of growth, with respect to their several of these methods, and that includes different types of dyes sensitized solar cells (DSSC), photonic solar cells, hybrid solar cells, and perovskite solar cells (PSCs) (Ludin et al., 2014).

One of these devices gained considerable interest as an alternative technology to silicon-based solar cells and is called dye-sensitized solar cells, which are known to be the third generation of solar cells. The dye-sensitized solar cell works superior to silicon solar cell, particularly under low light levels (Albrecht et al., 2016; Lee et al., 2015). The DSSC free on light episode point, it displays the most noteworthy change productivity under low light conditions. However, the most noteworthy transformation effectiveness for silicon cells was seen at high irradiance; it shows terrible showing under low-light conditions, for example, overcast day, early morning and sunset of the day. A valuable photocurrent age is seen for the DSSC for expanding frequency edges, which might be translated as the impact of the expanded light way inside the dynamic layers (Lee et al., 2015).

The silicon cells display a decrease in relative photocurrent for expanding frequency edges because of the expanded reflection at the outside of the top-glass. Besides, the low-light sun oriented cell (DSSCs) empowers new indoor applications, for example, shrewd home and original structure. Until this point in time, the most considerable force transformation proficiency (PCEs) of DSSCs on unbending conductive glass substrates has reached 13% (Hadi, 2018; Mathew et al., 2014; Watson et al., 2011).

For the assembly of DSSC, which consists of a photoanode coated with FTO glass, the counter electrode, which is platinum coated with FTO glass and between the photoanode and the counter electrode, is electrolyte (Yildiz et al., 2019). The photoanode is made from the semiconductor oxides layers such as TiO<sub>2</sub> and ZnO. Sensitizers are photoactive compounds derived from industrial and organic colorings. In addition, the cost of production is low, simple to manufacture and energy conversion efficiency is fair. In the past decades, the enhancement of dye-sensitized solar cells has been widely studied (Maurya et al., 2019). In addition, DSSC cells are



advantageous in that they contain more energy when exposed to normal sunlight than previous generations. Thus, It makes the DSSCs ideal for many types of architecture (Arulraj et al., 2019; Rajan and Cindrella, 2019).

As far as semiconductor dyes are concerned, researchers have been doing research on using many different methods and applying dyes to a wide range of semiconductors. Scientists have experimented with different natural pigments such as anthocyan, carotenoid, chlorophyll, and flavonoids to see how they may have improved the tints of the flowers. There was no clear preference given protocol for the order in which the pigments were used, but some (but not all) of them showed promise in light absorbance (Hug et al., 2014; Ludin et al., 2014; Rekha et al., 2019).

The objective of this work is to utilize tropical plants such as *Terminalia catappa*, *Cochlospermum regium*, *Dimocarpus longan* and *Lagerstroemia macrocarpa* for produce natural dyes. Furthermore, I will select potential and efficient plants from them. Furthermore, analyzing the different layers of  $\text{TiO}_2$  on fluorine-doped tin oxide (FTO) also find out the suitable temperature condition of the photoanode and fabrication approach.

### 1.1 Research objectives

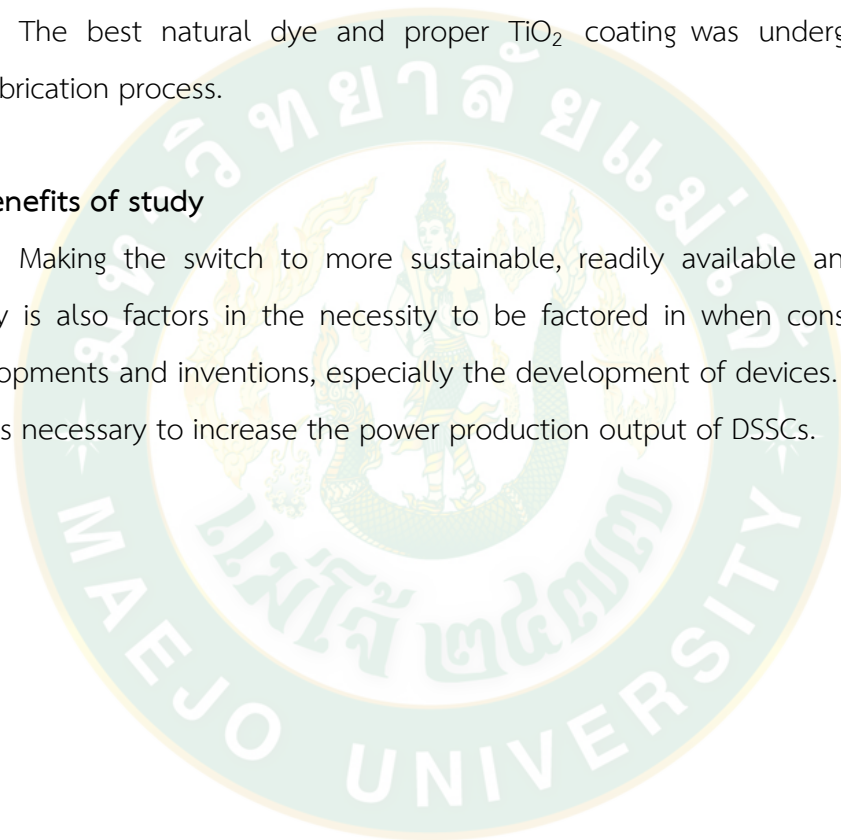
- Study on extraction of natural dye from tropical plants (*Terminalia catappa*, *Cochlospermum regium*, *Dimocarpus longan* and *Lagerstroemia macrocarpa*) by using solvent extraction method.
- To analyze the effectiveness of the different layers of  $\text{TiO}_2$  on fluorine-doped tin oxide (FTO,  $\text{SnO}_2$ : F).
- To figure out the suitable temperature condition of  $\text{TiO}_2$  coated on fluorine-doped tin oxide (FTO,  $\text{SnO}_2$ : F), and evaluate the efficiency of dye-sensitized solar cells (DSSC).

## 1.2 Scope of research

- Utilize tropical plants such as *Terminalia catappa*, *Cochlospermum regium*, *Dimocarpus longan* and *Lagerstroemia macrocarpa* to produce natural dyes by using solvent extraction method.
- This research using doctor blade technique to produce for different test thicknesses of the titanium dioxide (TiO<sub>2</sub>) layer (1, 2 and 3 layers) and using different temperature condition of photoanode (100, 200 and 300 °C).
- The best natural dye and proper TiO<sub>2</sub> coating was undergone by using fabrication process.

## 1.3 Benefits of study

Making the switch to more sustainable, readily available and longer-term energy is also factors in the necessity to be factored in when considering a new developments and inventions, especially the development of devices. In order to do so, it is necessary to increase the power production output of DSSCs.



## CHAPTER 2

### LITERATURE REVIEW

#### 2.1 Solar energy

Worldwide environmental concerns and the heightening interest for vitality, combined with consistent advancement in sustainable renewable energy, are opening up new open doors for the use of sustainable power source assets. Sun oriented vitality is the most bounteous, endless and clean of all the sustainable power source assets to date. The force from the sun caught by the earth is about  $1.8 \times 10^{11}$  MW, which is commonly more significant than the present pace of all the vitality utilization (Parida et al., 2011).

Sun based vitality is a steady, sustainable asset accessible in numerous zones of the world and offers a nonstop increment of attainable efficiencies. Of all the accessible innovations creating sustainable power sources, photo voltaic vitality is a hotly debated issue in flow explores (Parida et al., 2011). All sustainable power sources have numerous favorable circumstances, yet sun oriented vitality is the main in this challenge, which can satisfy the worldwide need by furnishing full ghastly synthesis of daylight with an immense measure of clean vitality. While silicon-based advances have been created to bridle sun oriented vitality proficiently, they are not yet focused on petroleum derivatives chiefly because of the high generation costs. It is an urgent errand to grow a lot less expensive photovoltaic gadgets with sensible proficiency for the widespread use of photovoltaic innovation (Parida et al., 2011).

In this unique situation, dye-sensitized solar cells (DSSCs) have risen as a significant option in contrast to customary silicon sun-powered cells inferable from their captivating highlights, for example, low creation cost and generally high effectiveness. At present, constant utilization of these put-away vitality assets has caused shortage as well as a severe effect on nature because of expanding CO<sub>2</sub> levels delivering issues, for example, those displayed by ozone harming substances and by ecological toxins (Parida et al., 2011).

Tending to such issues and the consistently expanding human interest for vitality has prompted the need to grow new direct sunlight based vitality

transformation strategies. Sun powered vitality speaks to a spotless, vast and sustainable power source and is subsequently a superb contender for a future ecologically cordial vitality source. In any case, the enormous scale accessibility of sunlight based vitality will hence rely upon a district's geographic position, average climate conditions, moderately high generation expenses of traditional sun oriented cells and land accessibility, which have constrained their far-reaching commercialization. We obviously should push toward a progressively manageable vitality economy (Parida et al., 2011).

Thus, with developing requests for vitality, the need for stemming increments in carbon dioxide discharges and the need to create inexhaustible, clean wellsprings of vitality are getting progressively significant. Sun powered vitality holds the plausibility of tending to these vitality concerns. Manufacture of color sharpened sun-powered 7 cells (DSSCs) offers a potential answer for this issue, as these novel cells can be delivered all the more modestly contrasted with standard Si-based cells. Late research and mechanical improvements of DSSCs have pulled in much consideration due to their attributes of being economical and having the ability for colossal scale sun based vitality transformation (Parida et al., 2011).

## **2.2 Generation of solar cell**

the effect of exposure of an of the photovoltaic (PV) process was discovered by Bequerel in 1839, who found a photovoltaic (PV) current being generated at the intersection of two cathodes in an electrolyte medium by the application of light Photovoltaic is defined as the significance of light and as a unit of power equal to one volt. In light of the idea of the material, most significant change proficiency reachable, and the related expense of photovoltaic force, Martin Green has assembled different photovoltaic solar cells in three significant classifications (Radwan, 2015).

### **2.2.1 First generation of photovoltaics (1970s)**

Solar cells produced by using crystalline silicon is the first of locate a significant application providing satellites with vitality. Silicon stays an alluring substance wherewith there is one of the bounteous components on earth which is 20% of the

world outside layer, for the most part, as sand ( $\text{SiO}_2$ ). There are semiconductor material appropriate for PV applications with a vitality band hole of 1.1 eV. This cells are group of two fundamental sorts relying upon the Si wafers was made.

1. Monocrystalline which is the additionally called single-crystalline
2. Polycrystalline in some cases are as multi-crystalline

Almost 90% of the photovoltaics nowadays depend on variety of silicon. Monocrystalline sun powered boards has the most elevated effectiveness rates wherewith there has the most elevated evaluation silicon. The productivity paces of monocrystalline sunlight based boards are ordinarily 20-25%. While the productivity of polycrystalline-based sun based boards are commonly 13-16% (Radwan, 2015).

Due to bring down silicon immaculateness, polycrystalline sun oriented boards are not exactly as effective as monocrystalline sun oriented boards. These high proficiency advancements, be that as it may, for the most part, cause higher creation costs contrasted with standard silicon cells because of high work costs for the material handling and the noteworthy vitality input required, cost per watt is likewise the most noteworthy.

### 2.2.2 Second generation of photovoltaics (1980s)

Crystalline silicon developments need long and several steps to put in place. Second layer manufacturing implementation, for example, may use semiconductor materials as thin as a few micrometers on various substrates, such as glass, flexible plastic, or in steel. as a result, they reduce the semiconductor content requirement to the same measure. Additionally, extraneous bundles can be rendered lightweight and compact. The three major sources of thin films are Amorphous (a-Silicon), Cadmium Telluride, and Copperindiumselen ( $\text{CuInGaSe}$  and  $\text{CuInGaSe}$ ) (CIGS). Using thin-film modules, companies' new approaches, have achieved efficiencies of 7-15% (Radwan, 2015).

Practically the entirety of the present thin-film innovation depends on indistinct silicon in which there is next to no structure to the game plan of iotas. CdTe meager film PV sun oriented cells have lower generation costs and higher cell efficiencies



(15.8%) than amorphous silicon thin film innovations (Britt and Ferekides, 1993). This blend makes CdTe meager movies the most affordable thin-film innovation as of now accessible. The compound CdTe has unexpected characteristics in comparison to the two components, cadmium and tellurium, taken independently. Lethality finds the CdTe is less toxic than normal cadmium. CIS and CIGS PV cells deliver the most remarkable efficiency of all thin film PV technologies. Current module efficiency ranges from 7 per cent to 16 per cent, while efficiencies of up to 20.3 per cent have been achieved in the testing center, close to that of the C-Si cells. The competition is currently to develop the know-how of industry modules (Green et al., 2010).

### 2.2.3 Third generation of photovoltaics (1990s)

Recently, new photovoltaic proposals were considered. These developments include, for the most part, concentrated photovoltaic innovation, DSSCs, organic solar cells, and novel and emerging solar cell ideas, which are currently known as third-age photovoltaics, since they are meant to consolidate the upsides of all era gadgets. On account of the minimal effort materials and simple manufacture, these advancements are required to take a massive offer in the quickly developing photovoltaic zones (Ananthakumar et al., 2019).

These solar cells was focused on accomplishing with high effectiveness and low cost. Latest methodologies utilizing semiconductor oxide nanoparticles were used in this sort of photovoltaic cell. Dueto, the semiconductor nanoparticles could deliver of the high current utilizing the novel ideas like effect ionization, gadgets utilizing this idea are profoundly fascinating. The thermodynamic vitality change breaking point of solar cell shifts from 31% to 41%, which is named Shockley-Queisser proficiency utmost, and, usually, this farthest point can be overwhelmed by utilizing the semiconductor nanoparticles (Saravanan, 2019). Third-generation solar cells include dye-sensitized solar cells, quantum-dot sensitized solar cells (QDSCs), and newly emerging perovskite cells. In the first two examples, a ruthenium complex Titania coating is also added to aid optical absorption. To date, almost 14% of the DSSC goals have been met; of these, this, almost 8% has been the DSSC in any case, producing greater efficiency using novel colors, counter terminals, and electrolytes leads to have

been embraced, resulting in greater gadgets. Nearby particles or as affidavits detectors approach possible benefactors if the configuration is set up that allows for natural sunlight-based cells to occur. roughly, only about 10% of the target has been completed. Note: The production of perovskite coated with half a dynamic layer of  $\text{CH}_3\text{NH}_3\text{Br}$  and I, as of late, have produced over 20% output (Saravanan, 2019). Extra, hot-high-intrumped cells, multiband cells, and pair-solar cells are being investigated for increasing photosynthetic current (Ananthakumar et al., 2019).

### 2.3 Dye-sensitized solar cells (DSSC)

DSSCs belongs to the third generation of solar cells. In 1990, at the Ecole Polytechnique Federale de Lausanne (EPFL), Grätzel and his colleagues developed a new kind of solar cell known as the DSSC or Grätzel cell, which uses nano-particulate titanium dioxide ( $\text{TiO}_2$ ) films with ruthenium (Ru) bipyridyl complex (Grätzel, 2003; Nazeeruddin et al., 1993; O'regan and Grätzel, 1991).

The good things about distributed DSSCs of the drawback is that they provide, simplicity in manufacturing, lower payback period in manufacture, low energy expenditure, and high efficiency are attractive because of those three, and those three they often provide as a free-of-charge (PCEs). Additionally, it is possible to play diffusely if you have quick, medium, and darker textured hair and still want to appear multicolored. Similarly, several diverse dyes (e.g., biotin) are more and more likely to be found appealing for solar concentrators as immense kinds (i.e. a. natural) can be used to capture charge, including numerous dyes (specifically, small) existent dyes (Higashino and Imahori, 2015; Hug et al., 2014).

In recent years, incredible advancement has been made in essential research and the mechanical application for DSSCs (Yun et al., 2018). The objective of focused research ventures identified with dye- sensitized solar cells is to upgrade the mechanical use of DSSCs. Advances made in the plan, joining on various substrates, modules, security, and clever creation strategies, have permitted DSSC innovation to move from the research facility to viable applications (Fakharuddin et al., 2014; Yun et al., 2018)



The photoanode, which consists of photoactive atoms (sensitizers) bound to the surface of a large bandgap semiconductor oxide, absorbs sunlight in DSSC (fundamentally  $\text{TiO}_2$  or  $\text{ZnO}$ ). DRSC uses a transparent oxide conductor (TCO) in two stages: a photoanode sheet of indium oxide or trifluorine tin oxide sandwiched between two phosphors, and a counter electrode containing the indium trichloride ( $\text{I}^-/\text{I}_3^+$ ) redox couple (Eshaghi and Aghaei, 2015; Guerin et al., 2010; Selopal et al., 2014).

In response to being excited by light, the dye molecules emit electrons into the conductive band of the semiconductor oxide. From there, the electron spreads through the conduction (FTO-coated) layer to the substrate glass, eventually diffusing into the interior of the substrate glass. The triiodide is used to reactivate the oxidized dye molecules from the electrolyte, and they are made once more active once more. The overall charge loop is accomplished by the decrease of the oxidized electrolyte at the electrode and electron from the external circuit (Maurya et al., 2019).

#### **2.4 Structure of dye-sensitized solar cell (DSSCs)**

The dye-sensitized cell is distinctly different from the other solar cells in production and procedures behind their operation. Instead of using only solid-state semiconductor materials, DSSC photovoltaic devices take place (Adedokun et al., 2016; Bauer et al., 2002; Luque and Hegedus, 2011). The basic component of DSSC is made of a semiconductor photoanode, a dye sensitizer mixture in the middle of two conducting glass substrate layers, and an electrolyte which is used as the working electrode, both arranged in a sandwich-like fashion (Jamalullail et al., 2018; Siddiquee et al., 2019)

A schematic portrayal of Dye-sensitized solar cell is delineated in figure 2. The framework is made out of four principal parts (Gong et al., 2017):

1. A photoanode made up of a mesoporous oxide layer (commonly,  $\text{TiO}_2$ ) stored on a transparent conductive glass substrate.
2. A monolayer of dye sensitizer covalently attached to the outside of the  $\text{TiO}_2$  layer to reap light and create photon-energized electrons.

3. An electrolyte is containing redox couple (commonly,  $I^-/I_3^-$ ) in a natural dissolvable to gather electrons at the counter anode and affecting dye reconstruct.
4. A counter electrode which is platinum or activated carbon covered conductive glass substrate.

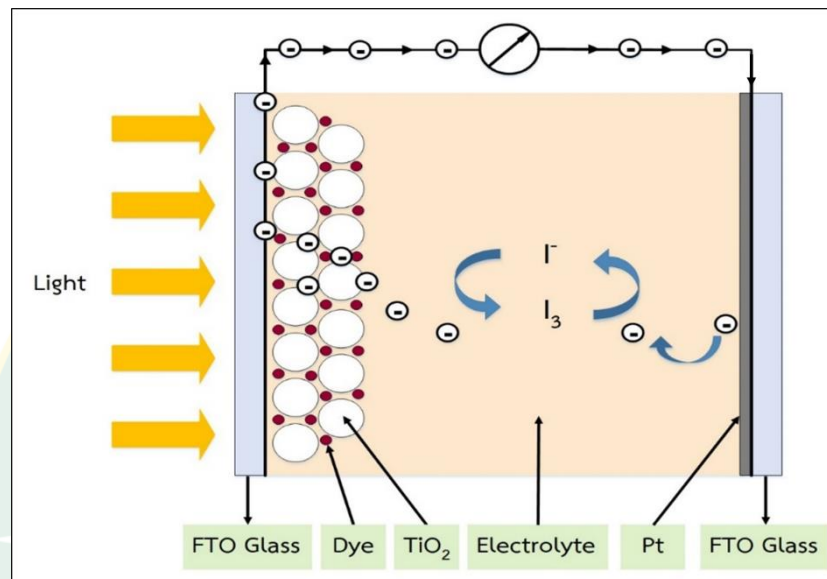


Figure 2 Basic structure and operating principle of DSSC (Gong et al., 2017)

## 2.5 Operation principle of dye-sensitized solar cell (DSSCs)

The light absorption in the DSSC occurs in the dye molecule (sensitizers). The dye molecules are attached to the nanocrystalline  $TiO_2$ , which provides electrical conduction and a large surface area for maximum light absorption. Photons excite the electrons of the dye molecules from the highest occupied molecular orbital (HOMO) in the ground state to the lowest unoccupied molecular orbital (LUMO) in the excited state and oxidize them (Figure 3). (Eq.1) describes that process. The released electrons are discharged through the  $TiO_2$  (Eq. 2) towards the conducting layer of the FTO glass (anode) and to a load where the work performed is delivered as electrical energy (Eq. 3) (Alhamed et al., 2012; Calogero and Di Marco, 2008; Matthews et al., 1996; Narayan, 2012; Smestad, 1998).

The oxidized dye molecules are reduced by the iodide from the electrolyte, leading to regeneration of the ground state. Two iodide-ions are oxidized by reducing the dye molecules to elemental iodine. The iodine reacts with another iodide-ion to form the oxidized state triiodide ( $I_3^-$ ). This was shown in equation 4.

The triiodide diffuses towards the platinum of the cathode (platinum covered FTO glass), where it is reduced by three iodide-ions ( $3I^-$ ; Eq.5) (Ito, Seigo et al., 2008; Wang et al., 2005). The electrons for this reduction reach the cathode from an external load and thereby closing the electric cycle (Bauer et al., 2002).

A charge-compensate cation diffusion escorts the electron motion in the  $TiO_2$  layer in the electrolyte relative to the sensitized  $TiO_2$ . Therefore, electric power generation in DSSC does not cause permanent chemical transformation (Grätzel, 2005; Ludin et al., 2014).

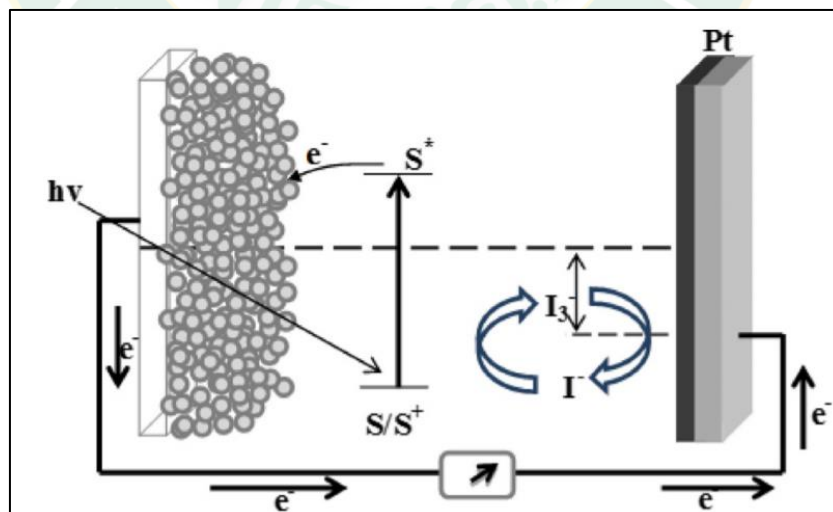


Figure 3 Schematic structure of DSSC (Ludin et al., 2014)

## 2.6 Components of dye-sensitized solar cell (DSSCs)

The transfer of light in-to-power vitality by DSSC relies on the sensitization of wideband hole semiconductors and is essentially made up of dye, photoelectrode, electrolyte, counter-electrode and transparent conductive oxide (TCO) layer glass substrates. The streamlining of both of them is deeply important to the improvement of general competence (Adedokun et al., 2016).

### 2.6.1 Transparent and conductive substrate

Dye-sensitized cells are typically two layers of conducting glass that assist in the electric current collector and as well as the semiconductor statements. To begin, there are two things to consider in a DSSC: Substrates must be high-transparent (preferably more than 80 percent) in order to allow sunlight to easily flow to the active region of the cell; to enable the movement of optimal current, the substrate must be highly conductive (Mehmood et al., 2014; Sharma et al., 2018)

DSSCs conductive substrate is typically used for fluorine-doped tin oxide (FTO,  $\text{SnO}_2:\text{F}$ ) and indium-doped tin oxide (ITO,  $\text{In}_2\text{O}_3:\text{Sn}$ ). Soda-lime glass of indium oxide and tin-fluorine oxide is used to this day as a primary substrate for preparing photosensitive glasses for plate and film, because of the effects of fluorine. The indium-doped tin oxide (ITO) has a transmittance of approximately 80% and sheet resistance of  $18 \Omega/\text{cm}^2$ . The problem of ITO with this cathode is that indium is a seldom discovered metal; also, ITO anodes delivered have weak properties and are less compatible with solid corrosive, and are less steady at high temperature. While fluorine-doped tin oxide (FTO) is cheaper than ITO and has a transmittance of roughly 75% in the visible area and sheet resistance of  $8.5 \Omega/\text{cm}^2$  (Gupta et al., 2018).

### 2.6.2 Photoelectrode (Titanium dioxide)

The photoelectrode consists of wideband semiconducting metal oxides, such as  $\text{TiO}_2$ ,  $\text{Nb}_2\text{O}_5$ ,  $\text{ZnO}$  or  $\text{SnO}_2$ , that is sensitized with photoactive molecules and attached to a transparent, conducting glass plate made of FTO or ITO (Grant, 1959; Sayama et al., 1998; Tennakone et al., 1999). The most widely used oxide is  $\text{TiO}_2$ , as it is an abundant, inexpensive, and non-toxic material. Its favorable crystal structure, the

anatase phase, has a bandgap of about 3.2eV (Desilvestro et al., 1985). The semiconducting oxide layer is transparent and comprises nanoparticles with a size of 15-30 nm and an average thickness of the layer of 10-15  $\mu\text{m}$ . By using screen printing, the doctor blade method or spin coating an oxide layer is deposited onto the FTO glass. The film of viscous colloidal  $\text{TiO}_2$  is then sintered at temperatures between 450-500°C. Due to the high temperatures of the sintering process, the nanoparticles form a porous but electrical interconnection (Sharma et al., 2018).

Since the semiconducting oxide layer consumes just a tiny fraction of UV radiation, photosensitive molecules are used to sensitize it. The oxide layer is immersed in a solution containing photosensitive molecules and solvent for this purpose. These molecules can bind to the  $\text{TiO}_2$  surface covalently. The oxide layer's surface area is enormous due to its porous composition. This results in a large number of molecules adhering to the nanocrystalline surface, enhancing the photoelectrode's light absorption properties (Adedokun et al., 2016; Radwan, 2015).

### 2.6.3 Dye-sensitized photosensitizer

In dye sensitized solar (DSSC), dye-sensitizers act as a solar energy absorber, which has a significant influence on light collection performance and overall photoelectric transition effectiveness. The ideal dye-sensitized solar cell sensitizer can hold all light only below a limit wavelength of 920 nm, be immovably attached to the semiconductor oxide surface, and infuse electrons into the transmitting band with a quantum yield of solidarity (Kong et al., 2007; Sokolský and Círák, 2010). Its redox potential ought to be adequately high that it tends to be recovered quickly using an electron gift from the electrolyte or an opening conductor. At last, it should be sufficiently steady to support at any rate of 10<sup>8</sup> redox turnovers under brightening, relating to around 20 years of exposure to natural light (Jasim, 2011).

The explanation for dyeing is to assimilate light and commercial electrons to the semiconductor conduction band. It is artificially attached to the permeable surface of the semiconductor. It should be an appropriate photosensitizer (Gong et al., 2017; Mehmood et al., 2014)



1. The dye ought to have a wide ingestion range; to catch however much as could be expected of the solar radiation.
2. The termination coefficient ( $\epsilon$ ) of dyes ought to high over the entire assimilation range, to retain the more significant part of the light with at least color.
3. The energized condition of the dye should vigorously lie over the conduction band edge of the semiconductor, to ensure quick electron infusion.
4. The energized lifetime of dyes essential long enough for the proficient electron infusion.
5. The positive potential of oxidized dye must have more than the redox couple in the electrolyte. To forestall recombination of infused electron with the oxidized dye. Then again, the redox capability of the electrolyte would rather somewhat positive. Due to, it decides the capability of the counter anode and, accordingly, the voltage of cell.
6. The dyes must joining gatherings (- COOH, - H<sub>2</sub>PO<sub>3</sub>, - SO<sub>3</sub>H, etc.) to improve the substance holding with the semiconductor and perhaps to fill in as extensions for electron infusion.
7. The dye ought to be dissolvable in some dissolvable for adsorption on the cathode, and ought not to be desorbed by the electrolyte redox.
8. The photosensitizer ought to have synthetic, warm and electrochemical steadiness during the introduction to sun radiation and in the electrolyte media. (Mehmood et al., 2014).

#### 2.6.3.1 Natural dye-sensitizers

Flowers, leaves, and fruits in nature come in a variety of colors and contain a variety of pigments that can be extracted and used to make DSSCs quickly (Ludin et al., 2014). Natural pigments have been suggested as potential DSSC elective sensitizer colors due to their clear preparation scheme, low cost, full biodegradation, easy accessibility, virtue rating, ecological friendliness, and, in particular, a high decrease in noble metal and material amalgamation costs (Kishimoto et al., 2005; Nishantha et al., 2012; Sinha et al., 2012). Plant pigmentation is made up of the electrical structure of colors, which changes wavelengths in response to sunlight. The coloring is determined

by the observer's limitations. The most intense absorption wavelength ( $\lambda_{\text{max}}$ ) can be used to represent the pigment (Davies, 2004). Many pigments (natural dyes) that are used as sensitizers in DSSC, such as chlorophyll, carotenoid, anthocyanin, flavonoid, cyanine, and tannin, have been studied.

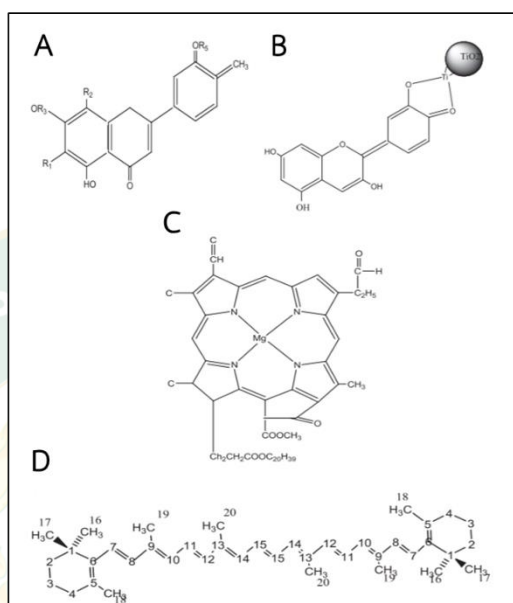


Figure 4 The chemical structure of (A) Anthocyanin, (B) Flavonoid, (C)  $\beta,\beta$ - Carotene and (D) Chlorophyll (Ludin et al., 2014)

#### 2.6.3.1.1 Anthocyanin

An anthocyanin is a natural group that the color of purple-red range (Andersen and Markham, 2005; Chang and Lo, 2010; Ludin et al., 2014). Anthocyanin can find in another plant for example the tubers, seeds, roots, leaves and stems (Patrocínio et al., 2009) There have carbonyl and hydroxyl bunches bound to semiconductor surface which is energize electron move from the sensitizer (anthocyanin particles) go through the conduction band of porous semiconductor (Patrocínio et al., 2009).

#### 2.6.3.1.2 Flavonoids

Flavonoids is the term that portrays an incredible assortment of characteristic colors which incorporates a  $C_6C_3C_6$  carbon structure, or all the more extraordinarily, phenylbenzopyran usefulness (Grotewold, 2006). Flavonoids have been extracted from numerous plants over 5000 naturally occurring and portion according to their chemical structure. The flavonoids contain of 15-carbon established structure with two phenyl



rings associated with three carbon spans, framing the third ring. The level of phenyl ring oxidation recognizes the various shades of flavonoids.

Nevertheless, not all flavonoids can ingest visible light, even though they have similar structures. Free electrons describe flavonoid atoms; hence, the vitality required for electron excitation to LUMO is brought down, permitting pigment particles to be invigorated by the apparent light (Narayan and Raturi, 2011). A variety of pigment that call flavonoid was controlled by the wavelengths of apparent light consumed by color particles and reflected. Flavonoid was adsorbed the mesoporous of  $\text{TiO}_2$  surface are quick, uprooting an OH counter particle from the Ti locales which join with proton gave by pigment structure (flavonoid) (Narayan and Raturi, 2011).

#### 2.6.3.1.3 Carotenoids

Carotenoids are natural pigments found in plants and microorganisms. Related organs also contain carotenoids, flavonoids, and anthocyanin. Carotenoid hues are responsible for yellow to orange petal hues in flowers and natural goods of red, yellow, and orange hues (Davies, 2004; Kishimoto et al., 2005; Ruiz-Anchondo et al., 2010). Carotenoid is comprising of 8-isoprenoid units which is boundless and incredible potential as vitality reapers and sensitizers for DSSCs (Ruiz-Anchondo and Glossman-Mitnik, 2009).

#### 2.6.3.1.4 Chlorophyll

Chlorophyll (Chl) is a green pigment that can found in the leaves. Mostly in green plants, algae, and cyanobacteria. It has six different types of chlorophyll pigment exist, and the most happening type is Chl . The sub-atomic structure incorporates a chlorine ring with Mg center, alongside various side chains and a hydrocarbon trail, contingent upon the chlorophyll type. Chlorophyll ingests light from red, blue, and violet wavelengths, and determines its pigment by reflecting green. Chlorophylls are the chief shades in natural photosynthetic systems (Chang et al., 2011; Wang et al., 2005). Their capacities incorporate collecting daylight, converting solar energy (to chemical energy), and moving electrons. Chlorophyll incorporates a gathering of more than 50 pigments (Green and Parson, 2003). Chlorophyll and their derivatives are

maneuvers into DSSC as dye-sensitizers as a result of their useful light assimilation propensity modes; the most efficiency is Chl and absorption maximum of chlorophyll is 670 nm. Xiao et al. revealed that chlorine two could lead to semiconductors  $\text{TiO}_2$  and ZnO surfaces through various modes (Wang et al., 2010).

#### 2.6.3.2 Plants material

- Indian almond (*Terminalia catappa*) that show in the figure 5.

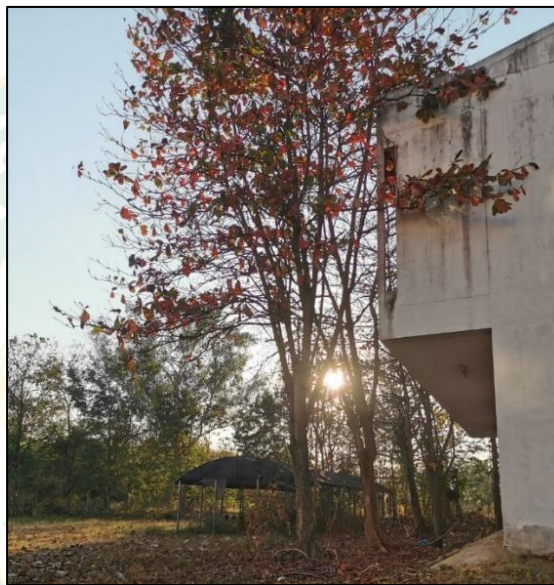


Figure 5 Indian almond (*Terminalia catappa*)

#### Scientific classification

Kingdom:	Plantae
Clade:	Tracheophytes
Clade:	Angiosperms
Clade:	Eudicots
Clade:	Rosids
Order:	Myrtales
Family:	Combretaceae
Genus:	<i>Terminalia</i>
Species:	<i>T. catappa</i>
Binomial name:	<i>Terminalia catappa</i> L.

*Terminalia catappa* is a huge tropical tree in the leadwood tree family, Combretaceae, which generally grows in tropical area such as Asia, Africa, and Australia. Country almond, Indian almond, Malabar almond, Sea almond, Tropical almond, Beach almond and False kamani are common names in English of this plant (Chitnis, 2013). The tree grows to 35 m in tall, with a straight, symmetrical crown and horizontal branches. *Terminalia catappa* has corky, light fruit that is spread by water. The seed within the fruit is eatable when completely mellow, savor, nearly like almond. As the tree secure older, the crown turns into flattened to form an augmentation, vase shape. Its branches are distinctively arranged in rating. The leaves are big, 15–25 cm (5.9–9.8 in) long and 10–14 cm (3.9–5.5 in) broad. Leaves are obovate with short petioles spirally grouped at the branch tips, glossy dark green, and leathery. When dry-season will become deciduous before falling, they turn into pinkish-reddish or yellow-brown, due to pigments such as violaxanthin, lutein, and zeaxanthin. The leaves of *Terminalia catappa* include various flavonoids (for example, kaempferol or quercetin), various tannins (such as punicalin, punicalagin or tercatin), saponines and phytosterols (Chitnis, 2013).

- Yellow cotton (*Cochlospermum regium*) that show in the figure 6.



Figure 6 Yellow cotton (*Cochlospermum regium*)

### Scientific classification

Kingdom:	Plantae
Clade:	Tracheophytes
Clade:	Angiosperms
Clade:	Eudicots
Clade:	Rosids
Order:	Malvales
Family:	Bixaceae
Genus:	<i>Cochlospermum</i>
Species:	<i>C. regium</i>
Binomial name:	<i>Cochlospermum regium</i> (Mart. ex Schrank) Pilg.

*Cochlospermum regium*, also known as the name yellow cotton tree and another name from each country such as Portuguese call *Algodao do cerrado* and Thailand call *suphannika*. Initially, this flowering plant has origins in the Cerrado tropical savanna of South America (Bolivia, Brazil, Paraguay). These plants also commonly available in Southeast Asia. In Thailand, it is the provincial flower of Nakhon Nayok, Sara Buri, Buri Ram, Suphan Buri and Uthai Thani Provinces (Nunes et al., 2003; Solon et al., 2012). *Cochlospermum regium* (Mart. & Schrank) Pilg. is a ornamental plant belongs to family Cochlospermaceae. The root extract from *C. regium* was reported to contain various phenolic compounds and flavonoids (Correa de Oliveira et al., 1996).



- Longan (*Dimocarpus longan*) that show in figure 7.



Figure 7 Longan (*Dimocarpus longan*)

#### Scientific classification

Kingdom:	Plantae
Clade:	Tracheophytes
Clade:	Angiosperms
Clade:	Eudicots
Clade:	Rosids
Order:	Sapindales
Family:	Sapindaceae
Genus:	<i>Dimocarpus</i>
Species:	<i>D. longan</i>
Binomial name:	<i>Dimocarpus longan</i>

*Dimocarpus longan*, regularly known as the longan, is a tropical tree varieties that produce eatable fruit. It is one of the better-known tropical individuals from the soapberry family (Sapindaceae). It is local to Southern Asia. They are rich in bioactive polysaccharides, phenolic acids, and flavonoids (He et al., 2016; Morton and Dowling, 1987). The tree grows to over 30 m (in height) is depending on weather and soli, but stands typically is around 30–40 ft (9–12 m) in height. (He et al., 2016; Morton and Dowling, 1987). The phytochemical analysis demonstrates the result that the crude

extract of Longan contains high amounts of triterpenes, tannins, flavonoids, and carbohydrates. *D. longan* leaves were reported to contain eight polyphenolic compounds: ellagic acid, 3,4-O-dimethyl ellagic acid, (+) -catechin, ethyl gallate, gallic acid, kaempferol, quercetin and kaempferol-3-O- $\alpha$ -L-rhamnoside (Apriyanto et al., 2015).

- Inthanin bok (*Lagerstroemia macrocarpa*) that show in the figure 8.

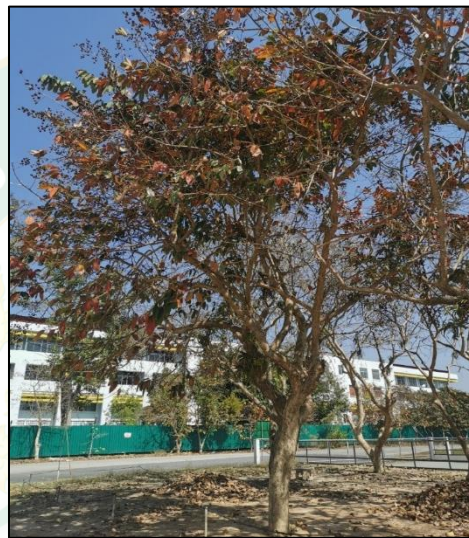


Figure 8 Inthanin bok (*Lagerstroemia macrocarpa*)

#### Scientific classification

Kingdom:	Plantae
Family:	Lythraceae
Genus:	<i>Lagerstroemia</i>
Species:	<i>macrocarpa</i>
Binomial name:	<i>Lagerstroemia macrocarpa</i> Wall
Common name:	Inthanin bok

*Lagerstroemia* is the most economically class in Lythraceae and includes around 55 species, which, for the most part, dispersed in tropical and sub-tropical natural surroundings of southern China, Japan and upper east Australia. Most *Lagerstroemia* species bloom from summer till fall with great highlights of beautiful



blossoms. Especially as an ornamental estimation of *Lagerstroemia*, above, before 260 cultivars have been registered in the universal authority of *Lagerstroemia* cultivars (Gu et al., 2016). *Lagerstroemia macrocarpa* is a deciduous tree with a many-flowered terminal bundle that has a worth ornamental feature and disorderly in dry dipterocarp forest and open forests in Burma (Myanmar) and Laos (Khammouan) (Gu et al., 2016).

#### 2.6.4 Electrolyte

The reason for the electrolyte is to revitalize the dye after it infuses electrons into the conduction band of the semiconductor. It additionally goes about as a charge entry medium to transfer positive charges for the counter cathodes. The long-practical lifetime steadiness of DSSCs unequivocally relies upon the properties of the electrolyte. In this way, the electrolyte might have the following characteristic (Jasim, 2011; Mehmood et al., 2014)

1. Incredible electrical conductivity and low consistency for quicker dissemination of electrons.
2. Great interfacial contact with the nanocrystalline semiconductor and the counter electrode.
3. It ought not to be the reason for the desorption of the dye from the oxidized surface and the debasement of the color.
4. It might not assimilate light in the visible region.

Many of the options are being proposed to improve the faults of electrolytes, but among all of the electrolytes redox couple electrolyte  $I^-/I_3^-$  is the maximum efficiency. Due to  $I_3^-/I^-$  is viewed as a perfect redox couple as a result of its phenomenal dissolvability, quick color recovery, low absorbance of light in the prominent locale, appropriate redox potential, and extremely moderate recombination energy between infused electrons into the semiconductor and triiodide (Zulkifili et al., 2015).

#### 2.6.5 Counter electrode

The counter electrode is used for the regeneration of the electrolyte. To transfer the electrons arriving from the external circuit back to the redox electrolyte,

which is the function of the counter electrode. Thus, the conducting must be well and exhibit a low overvoltage for the reduction of the redox couple. Moreover, it might operate as a mirror, mirroring the light transmitted by the photoelectrode to cross it a second time. In this way, it increases light absorption with an offering amount of dye (Anandan, 2007; Veerappan et al., 2012). Normally, Transparent conducting oxide (TCO) is used fluorine-doped tin oxide (FTO), silver or platinum, or carbon is coated onto the glass.

One of the materials often used for the counter electrode as a catalyst is a platinum. Platinum (Pt) is a counter-electrode that obtain high conversion efficiency. However, there are few limitations in this is due to its expensive price, scarceness, contingency with redox-electrolyte and high sintering in temperature (Semalti and Sharma, 2020; Yue et al., 2013).

Thus, the demanding alternative of the catalyst of the counter electrode is cheaper materials, efficient, steady counter-electrode with the high catalytic quality such as graphene, graphite, carbon, activated carbon and carbon nanotubes (Mubarak et al., 2018; Puspitasari et al., 2017). The kind of carbon material was changed to see the impact on the efficiency of monolithic structured solar cells. There have many advantages of the carbon material used as a counter electrode; for example, it is moderate and simpler to give than other materials, such as platinum. Moreover, carbon likewise has a consumption of safe properties and has a great electro-catalytic ability (Gong et al., 2017; Jasim, 2011; O'regan and Grätzel, 1991).

## **2.7 Technique of fabrication DSSC**

Picking an ideal fabrication method for DSSC relies upon different factors, for example, generation volume, size, shape intricacy, capital speculation, generation adaptability, vitality request, human factor, etc. (Krebs, 2009). Notwithstanding its points of interest over spin-coating, it additionally has a few constraints which incorporate low molecule focus and low dissipation rate. Plan and choice of manufacture strategy is always an exchange off among properties and cost, so it is essential to have considerable information on different classes of procedures (Hubka, 2015).

### 2.7.1 Physical methods

Physical techniques for coated depend on physical spectacle to plan and store the material on the substrate surface. Physical techniques are comprehensively named liquid phase deposition and gas-phase deposition. This grouping depends on the forerunner stage. Following sub-segments, the point by point working of physical techniques will be portrayed.

#### 2.7.1.1 Dip coating

Dip coating are a simple and most likely established procedure for covering purposes (Menning and Aegerter, 2004). This is commonly used to cover various metals of steel sheets. On a basic level, a steady arrangement is first arranged to utilize nanoparticles of any material with unstable dissolvable (Pinsly, 2001).

A cleaned substrate is drenched at a consistent speed in arrangement and kept it there for the recommended time. Then the substrate was pulled out from arrangement and let it dried. Batch type dip coating and continuous dip coating as shown in Figure 9. are gives a smoothly and thin layer of nanoparticles on substrate.

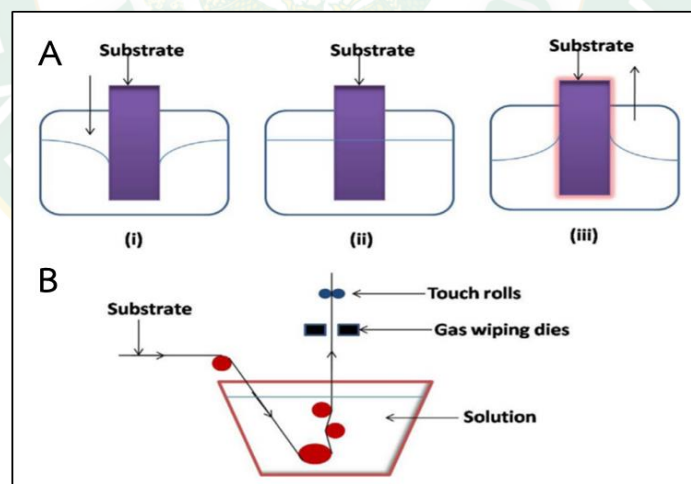


Figure 9 Schematic diagram of dip coating methods (A) Batch type and (B) Continuous type dip coating (a) immersion (b) startup and (c) pull-up steps (Ahmad et al., 2017).

#### 2.7.1.2 Spin coating

The spin coating method uses centrifugal forces to store the material coated on substrate (Sato and Fujii, 1978). Usually, substrate was kept on a spin coate

machine. There conduct vacuum underneath the substrate was fix on position and pivot the substrate with the fast (Birnie, 2004). The high diffusive powers which spread out on the substrate that coated it completely. The schematic of the spin coat process was shown in Figure 10. The solution was deposit on substrate and eventually, the evaporation of solution which is departure after a thin film of nanoparticles (Ahmad et al., 2017).

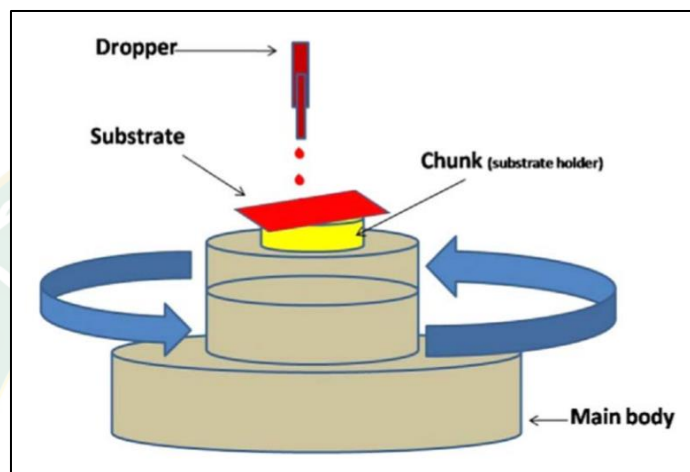


Figure 10 Schematic of spin coating technique (Ahmad et al., 2017)

### 2.7.1.3 Doctor blade printing

Doctor blade coating technique defined as tape casting is the most utilized coating method for the lab-scale of DSSCs presumably because of its cheap, effortless activity and less moving parts (Padinger et al., 2000). Due to its adaptability and cost worth, it has additionally been utilized by novices. This device comprises a phase where the substrate are kept, a sharp moving blade and a few apparatuses. The substrate are set on the stage and a sharp edge is situated on the substrate with required separating among cutting edges and dispersing, which eventually characterizes the thickness of the coating. The semiconductor was dropped on substrate that diffuses of the paste by using a blade. This process can innovate and increase the thickness for the development of the multi-layer. The procedure outline was shown in Figure 11. A nanoparticles paste was dropped on substrate and moved, identically expand by using blade. After uniform spreading, the substrate is expelled from the phase for consequent dry (Ahmad et al., 2017).

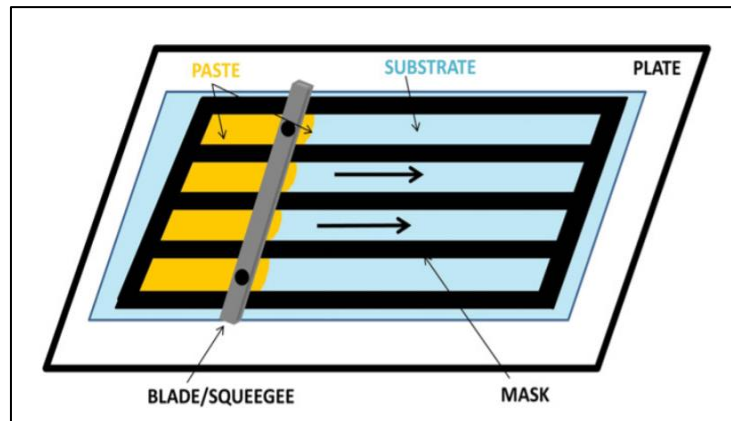


Figure 11 Schematic of the doctor blade technique (Ahmad et al., 2017)

## 2.7.2 Chemical methods

Chemical techniques are depend on the chemical reactions of substrate-forerunner and antecedent, another compound medium to get ready and store the nanoparticles on the substrate surface. Chemical techniques are divide into classified as liquid phase coated and gas-phase coated (Ahmad et al., 2017).

### 2.7.2.1 Sol-gel coating

The sol-gel method, can call molecular level mix which has outstanding strategy to deliver better size of the particles including the planning of sol and with time this sol change to gel which is then dried and squashed to frame nano-sized oxide particles (Saelim et al., 2011). In the middle of the procedure of hydrolysis and precipitation is gel shaping advance. There gel can directly coated on the substrate and ensuing drying will deliver excellent covering. The doped of nanoparticle and composites have much of the time been set up with the sol-gel system (Ahmad et al., 2017).

## 2.8 Performance of the dye-sensitized solar cells

After the manufacture of dye-sensitized solar cells, it is presently imperative to assess its performance. The essential estimation required to decide the effectiveness of a DSSC is the current and capability of the cell estimated through an outside variant resistance and intensity of the incident light (Dawoud, 2016).

The fundamental of performance parameters of the solar cell is achieved from current-voltage (J-V) measurements, as shown in figure 12.

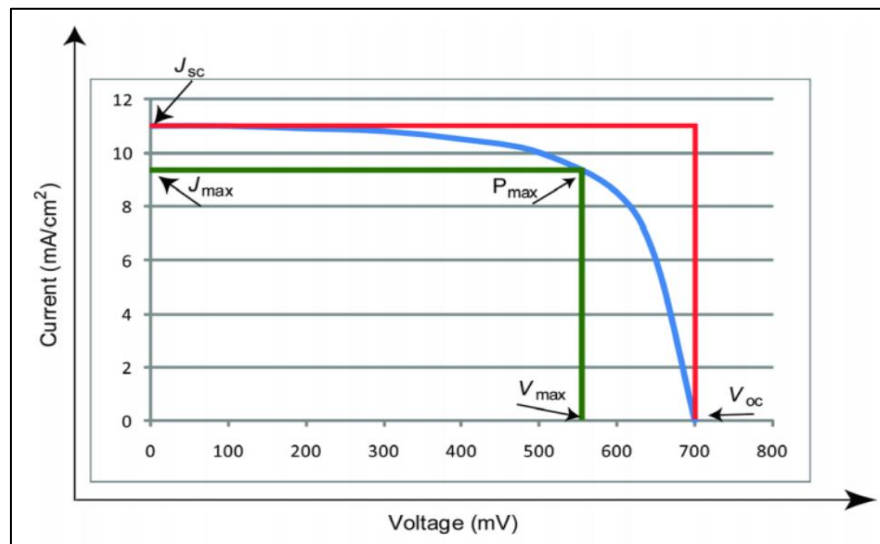


Figure 12 Illustration of current-voltage (J-V) curve of a solar cell (Dawoud, 2016)

The achievement of a dye-sensitized solar cell can be assessed by short circuit current ( $J_{sc}$ ), open-circuit voltage ( $V_{oc}$ ), maximum current density ( $J_{max}$ ), maximum voltage ( $V_{max}$ ), maximum power output ( $P_{max}$ ), efficiency ( $\eta$ ), and fill factor (FF) can be obtained using the following equations:

$$P_{max} = J_{max} \times V_{max} \quad (\text{Eq. 6})$$

Where,  $P_{max}$  is the maximum output power and the voltage ( $V_{max}$ ) and current ( $J_{max}$ ) at the maximum power point can be determined by computing the product of  $I$  and  $V$  at various points along the curve and selecting the point where the product is maximum (Prakash, 2012).

The fill factor, all the more ordinarily known by its acronym "FF", is essentially a proportion of solar cells. The FF is comparing by the maximum power ( $P_{max}$ ) to the theoretical power ( $P_T$ ) which is output obtained at the open-circuit voltage ( $V_{oc}$ ) is the maximum voltage accessible from a solar cell, and this happens at zero current and the short circuit current ( $J_{sc}$ ) is the current through the solar cell per unit area when



the voltage across the solar cell is zero (Sharma et al., 2018). The FF is normally determined as:

$$FF = \frac{P_{\max}}{J_{sc} \times V_{oc}} \quad (\text{Eq. 7})$$

The efficiency of the solar cell is the ordinarily used parameter to compare the performance of one solar cell to another cell and it is determined as the ratio of maximum power output to the energy input from the sun (solar radiation,  $P_{in}$ ) or input power (incident light) measured in  $\text{mW}/\text{cm}^2$  by the following conversion efficiency formula (Dawoud, 2016) :

$$\eta = \frac{P_{\max}}{P_{in}} \times 100 \quad \text{or} \quad \frac{J_{sc} \times V_{oc} \times FF}{P_{in}} \times 100 \quad (\text{Eq. 8})$$

## CHAPTER 3

### MATERIALS AND METHODS

This study was divided into three subsections, including the experimental and analysis parts: 1) natural dye preparations, 2) DSSC fabrications and 3) material characterizations.

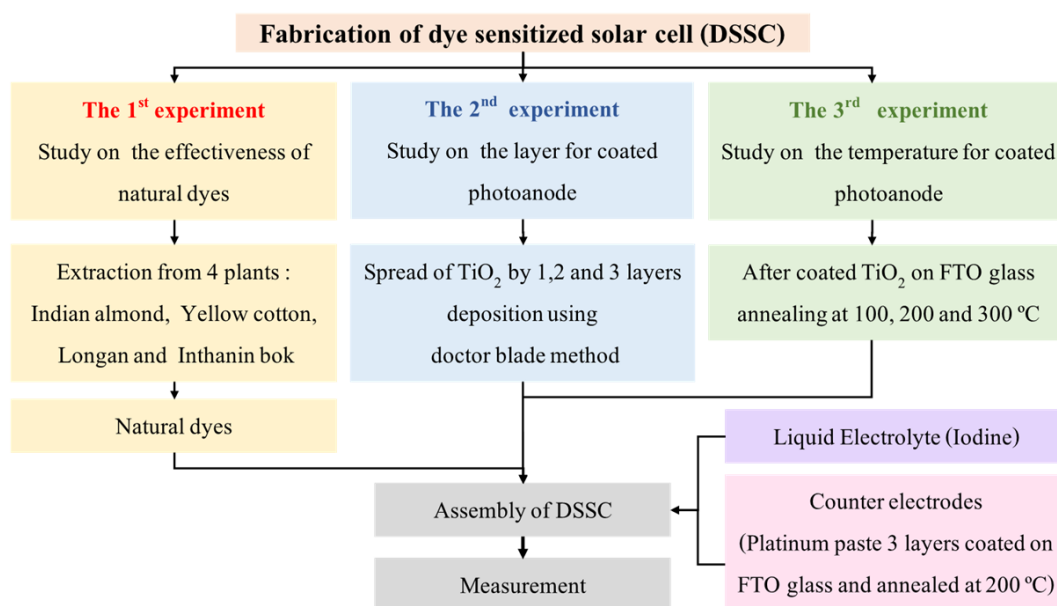


Figure 13 The framework of DSSC fabrication

### 3.1 Materials and chemicals

All materials and chemicals were purchased from commercial sources and the chemical was used without additional purification. Natural dyes were extracted by using methanol (RCI Labscan). Fluorine-doped tin oxide (FTO) glass substrate of 10  $\Omega$ /sq surface resistivity and 2.2 mm thickness purchased from Hangzhou DCT Hardware Industry Co., Ltd. (China) was used as a conductive surface in the photoanode and counter electrodes. For the preparation of Titanium dioxide (TiO<sub>2</sub>) nanoparticle paste was used TiO<sub>2</sub> powder, which has the particle 20 nm, Acetic Acid Glacial (RCI Labscan) and Tween 20 (Polysorbate 20) was used as the binder for thin film deposition on the photoanode. Platinum (Pt) paste from Sigma Aldrich was used as a counter electrode side. Potassium iodide; KI (Ajax), iodine; I<sub>2</sub> (KemAus), acetonitrile (Duksan) and ethylene

glycol (KemAus) were used to prepare the electrolyte solution and executed as a charge transport intermediary between the two electrodes. Scotch tape 3M has a thickness of 60  $\mu\text{m}$  used in the doctor's blade technique to control the film's thickness and used as a separator layer between the two electrodes.

### 3.2 Materials preparation

Fresh leaves and flowers of Indian almond (*Terminalia catappa*), Yellow cotton (*Cochlospermum regium*), Longan (*Dimocarpus longan*) and Inthanin bok (*Lagerstroemia macrocarpa*) were collected from the Faculty of Animal Science and Technology, Maejo Fram, Energy Research Center and Inthanin field respectively. The leaves and flowers were around Maejo University, Chiang Mai, Thailand, as shown in figure 14. After that, the leaves and flowers were transferred to Saowaran Nittayawattana Building, Faculty of Science, Maejo University, Chiang Mai, Thailand. Then, the leaves and flowers were washed with tap water to remove the duct and then blotted dry with paper toweling, as shown in figure 15. Then, the leaves were removed from the middle parts to prepare for the pigment extraction process.



Figure 14 Materials collection of (a) Indian almond, (b) Yellow cotton, (c) Longan and (d) Inthanin bok

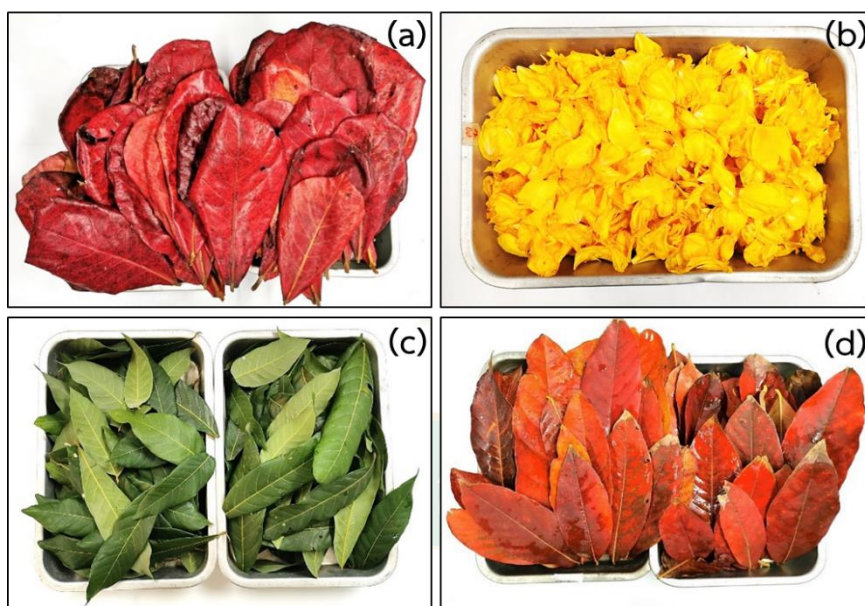


Figure 15 Materials preparation of (a) Indian almond, (b) Yellow cotton, (c) Longan and (d) Inthanin bok

### 3.3 Pigment extraction processes

The extraction process was adopted by (Sumanta et al., 2014) and modified. For the extraction of leaves and flowers was used and the solvent for the extraction procedure is methanol. After that, the 20 g of leaves and flowers were mixed with methanol 100 ml by using a blender and set the time for 10 min for this process. Subsequently, the vacuum filter was applying for separated solid and liquid. Afterward, the pigment extraction was adjusted volume to 100 ml in a volumetric flask. The experiment was operated with triplications, and the experiment processes are shown in Figures 16 and 17. Furthermore, the natural dyes were stored in the refrigerator at 4 °C and avoid light exposure.





Figure 16 The extraction processes (a) Cut to small pieces, (b) The sample mixed with methanol by using a blender, (c) The vacuum filter was separated solid and liquid and (d) The pigments extraction



Figure 17 The natural dyes from (a) Indian almond, (b) Yellow cotton, (c) Longan and (d) Inthanin bok

### 3.4 Pigment analysis and characterization

The pigment extracted from Indian almond, Yellow cotton, Longan and Inthanin bok was measured using the absorbance wavelength by using a UV-visible spectrophotometer (SPECORD 200 PLUS, Analytik Jena, Germany. Analysis of the

determination of chlorophylls (chlorophyll a (Chl-a) and chlorophyll b (Chl-b)) and carotenoids content by using Eqs. 10–12.

$$\text{The amount of chlorophyll a} = (12.25 \times A_{663} - 2.79 \times A_{645}) \times \text{DF} \quad (\text{Eq. 10})$$

$$\text{The amount of chlorophyll b} = (21.50 \times A_{645} - 5.10 \times A_{663}) \times \text{DF} \quad (\text{Eq. 11})$$

$$\text{The amount of carotenoids} = \frac{(1000 \times A_{470} - 1.43 \times C_a - 35.87 \times C_b) \times \text{DF}}{205} \quad (\text{Eq.12})$$

### 3.5 Preparation of FTO glass substrates

The FTO substrates were washed with soap solution, distilled water and methanol for 15 min in an ultrasonic bath, as shown in Figure 18. After that, dried at room temperature and measurement the resistance by Multimeter.

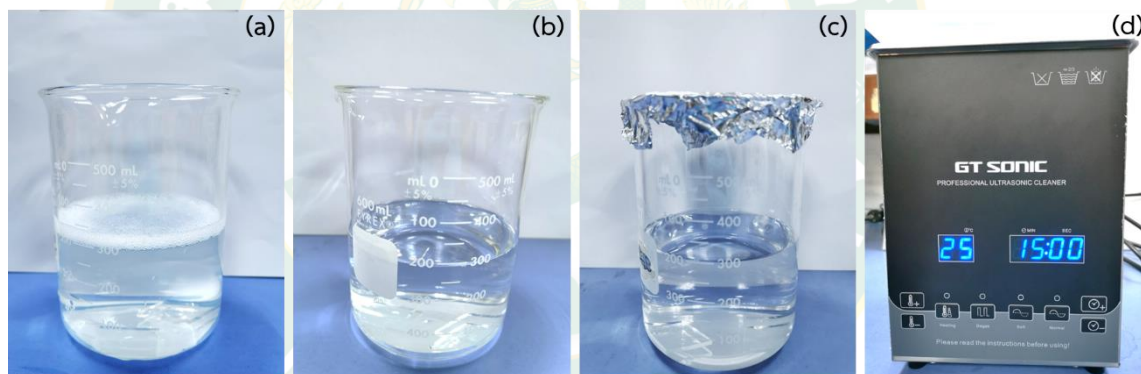


Figure 18 (a) Soap solution, (b) Distilled water and (c) Methanol for clean FTO glass

### 3.6 Preparation of TiO<sub>2</sub> nanoparticle paste as a photoanode

To prepare TiO<sub>2</sub> nanoparticle paste, need to reduce the particle size of TiO<sub>2</sub> powder by using a magnetic mixer and set the time for 1 hr. The mixer of TiO<sub>2</sub> nanoparticle paste consists of 5g of TiO<sub>2</sub> powder, 10 ml of 5% acetic acid and 0.5 ml of surfactant (Tween 20) which fully mix magnetic stirrer for 1hr and kept in a sealed container to avoid evaporation of TiO<sub>2</sub> nanoparticle paste. After that, Scotch tape 3M (60 μm) was used to control the film thickness layers, which is 1, 2 and 3 layers on FTO glass substrate and the active area is 3 cm<sup>2</sup>. Then, TiO<sub>2</sub> nanoparticle paste was deposited on the FTO glass substrate by using the doctor's blade technique and dried



in room temperature. After that, remove the tape before annealing the film at 100, 200 and 300 °C for 1 hour. The preparation of TiO<sub>2</sub> nanoparticle paste as a photoanode was presented in figure 19. Subsequently, the natural dyes were dropped on the front of the film at room temperature for 1 hour under the dark condition, as presented in figure 20.

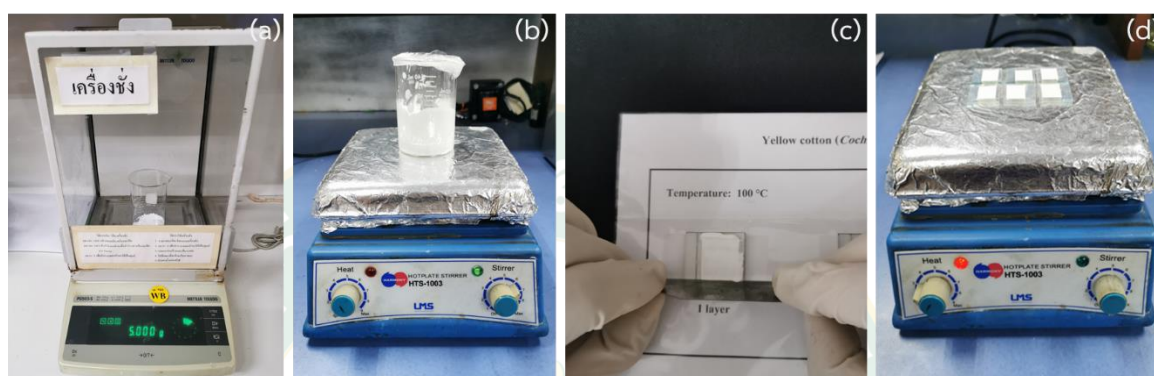


Figure 19 The preparation of TiO<sub>2</sub> nanoparticle paste; (a) Weigh TiO<sub>2</sub> powder, (b) The mixer of 5 g of TiO<sub>2</sub> powder, 10 ml of 5% acetic acid and 0.5 ml of surfactant (c) TiO<sub>2</sub> paste coated on FTO conductive glass by doctor blade method and (d) Anneal photoanodes by using a hot plate

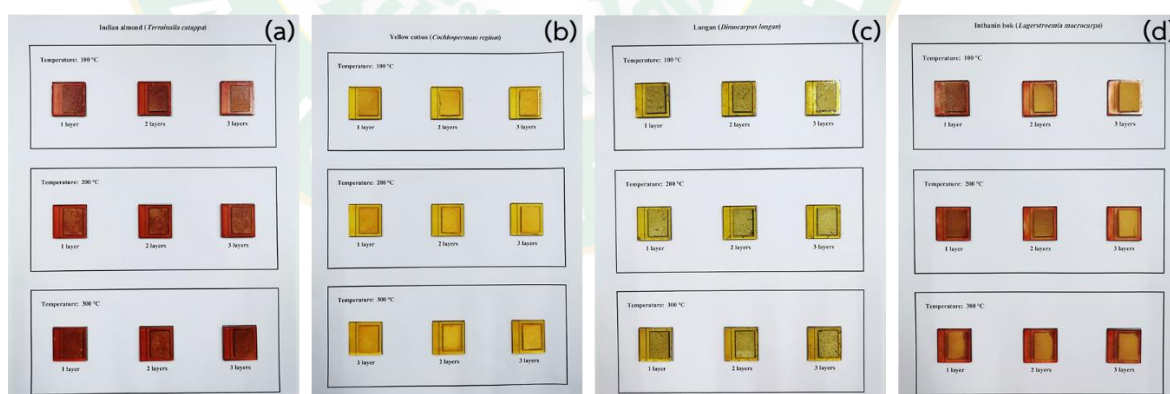


Figure 20 Immersed in natural dye sensitizer solution at room temperature; (a) Indian almond, (b) Yellow cotton, (c) Longan and (d) Inthanin bok

### 3.7 Preparation of electrolyte

The electrolyte was prepared by adding 1.08 g KI powder is solved in a mixture solvent of acetonitrile (80 ml) and ethylene glycol (20 ml) and was stirred for a few

minutes. Then, add a 0.21 g of Iodine into this solution individually, allowing them to stir for 30 minutes (Gu et al., 2017).

### 3.9 Assembly and measurement of the DSSC

This DSSC device assembly consist of a photoanode, which is a  $\text{TiO}_2$  nanoparticle paste with natural dyes coated on conductive glass (FTO glass), an electrolyte, and the counter electrode, which is platinum paste coated on FTO glass annealed at  $200\text{ }^\circ\text{C}$  for 1 hr. DSSC in this study was assembled by used hot-melt glue to sealed the sandwich of the photoanode and a counter electrode. Finally, the electrolyte was injected inside DSSC and sealed very well to avoid leakage of electrolyte in the cell, as shown in figure 21. Besides, the current-voltage characteristics were measured by using a digital multimeter (UNI-T UT61E) with variable resistance ( $10\text{ k}\Omega$ ) under illuminated with the yellow light of 24000 LUX ( $0.03504\text{ W/cm}^2$ ) in the ambient atmosphere and the schematic circuit diagram of the experimental setup shown in figure 22.

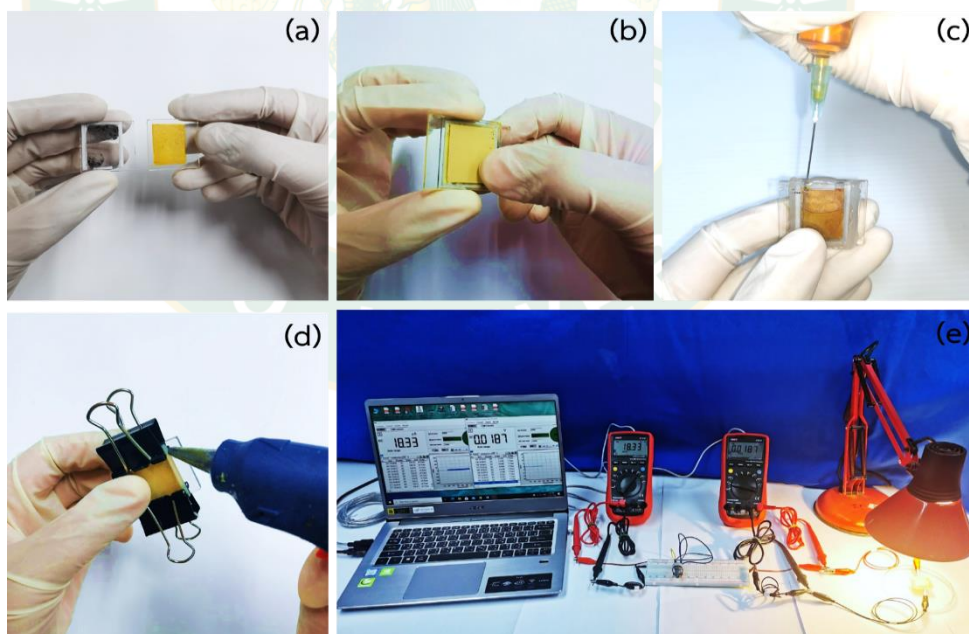


Figure 21 The processes of assembly DSSC and measurement

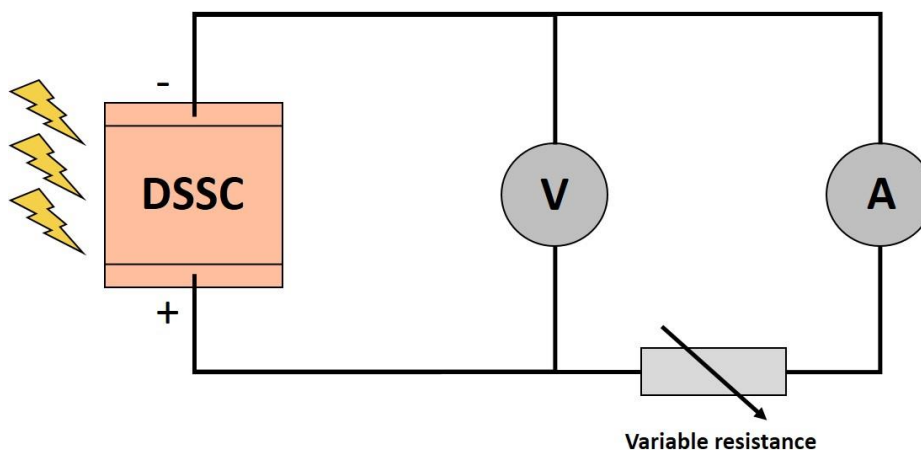


Figure 22 Schematic circuit diagram of the experimental setup used to measure the current-voltage characteristics of DSSC with variable resistance (10 k $\Omega$ )

### 3.8 Characterization techniques

The characterization of the TiO<sub>2</sub> coated on FTO glass substrate with natural dyes immersion from Indian almond, Yellow cotton, Longan, and Inthanin bok leaves was investigated under the scanning electron microscope (SEM) for the determination of the morphology. Besides, the energy-dispersive X-ray spectroscopy (EDX) analyzed the elemental composite of the samples. The laser scanning microscope (Olympus; OLS 5100) was examined the surface and morphology of natural dyes coated on TiO<sub>2</sub> layers.

### 3.9 Statistical analysis

Data are reported as mean  $\pm$  SE from triplicate observations. Significant differences between means were analyzed. All statistical analyses were performed using SPSS Version 20.0. A correlation was assumed significant when  $P < 0.05$ .

## CHAPTER 4

### RESULTS AND DISCUSSION

#### 4.1 Spectrophotometric analysis of pigments extraction

The generally of the biological processes is depending on the portion of the electromagnetic spectrum called visible light (or simply light). The human eye can detect the light spectrum. The wavelengths from 380 nm, which is provide violet color to 700 nm, which is, provide red color. However, many species are able correspond to wavelengths that fall outside the visible spectrum, such as shorter wavelengths (ultraviolet light-UV;400 nm) and longer wavelengths [far red (FR); 700–800 nm]. Therefore, as light is possibly a critical condition for life on earth, its interaction with organisms (Carvalho et al., 2011).

The plant pigment structure was interacted with sunlight and the wavelengths were transformed by transmitted or reflected from the plant tissue. This procedure leads to the occurrence of plant pigmentation. The natural pigments such as chlorophylls, carotenoid, flavonoids specified, and anthocyanin was specified from the maximum absorbance of wavelength ( $\lambda_{max}$ ) and the colors perceived by humans (Kumara et al., 2013; Shalini et al., 2015) as shown in figure 23. In this study, the absorption wavelength of pigments extraction was examined by the UV-Vis spectrophotometer that the wavelength between 380 to 800 nm and used the methanol as a solvent for extraction process. Due to, methanol is an excellent solvent extracting for chlorophylls, especially from recalcitrant vascular plants and algae (Ritchie, 2006).

Also Şükran et al. was an experiment for pigment extraction by used different solvent that is methanol, acetone and diethyl ether to extract algal was found that the solvents used were important in the pigment extraction, and the best solvent was methanol. It was observed that the extraction with methanol was nearly complete in *Cladophora glomerata* and *Ulva rigita* because of the diversity of the cell wall structures. Although it was seen that acetone was a better solvent in comparison with



diethyl ether, no significant difference was determined between two solvents (Şükran et al., 1998).

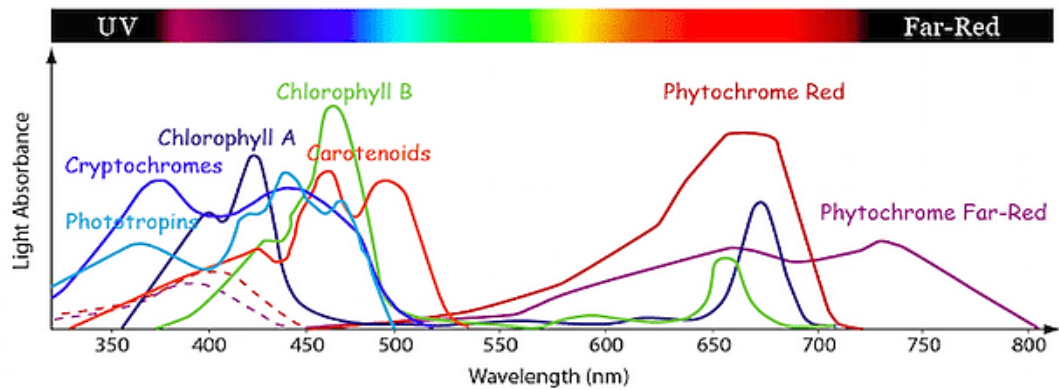


Figure 23 The absorption wavelength of pigments (Carvalho et al., 2011).

#### 4.1.1 Indian almond

Indian almond had peaks with wavelengths of 470 nm, as displayed in figure 24. Indian almond is a possibility that had the functional group of carotenoids. Generally, carotenoids absorption wavelengths between 400 to 550 nm (violet to green light). The compounds had colored yellow, orange, or red (Khammee et al., 2020) Thus, the structure of the pigments extraction from Indian almond consists of the functional group of carotenoids.

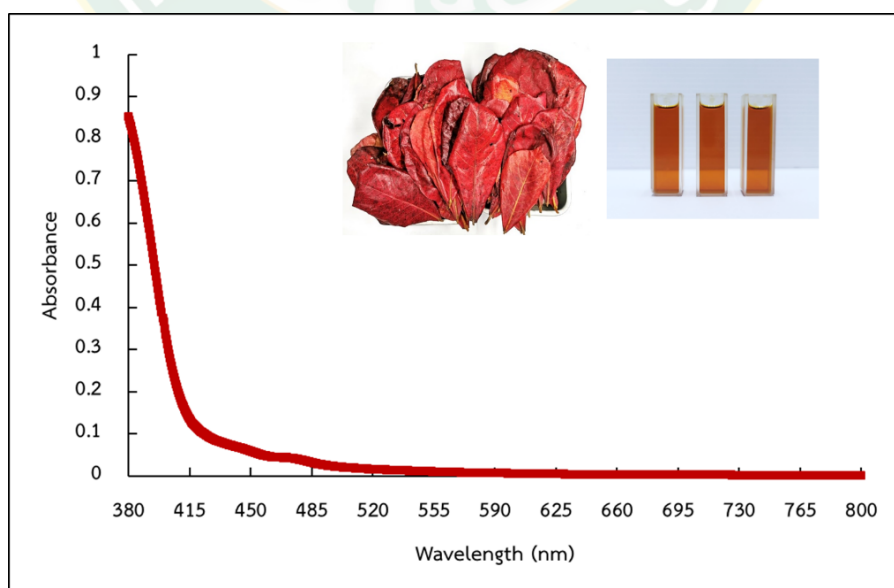


Figure 24 The absorption wavelength of pigments extraction (Indian almond leaves)

#### 4.1.2 Yellow cotton

Yellow cotton had two peaks with 396.5 nm and 420.5 nm, as shown in figure 25. The wavelengths 396.5 presume that it is the functional group of flavonoids. Due to comprised absorption bands of flavonoids are near 350 to 400 nm (Vachali et al., 2016). Therefore, the yellow cotton flower is a possibility that had the functional group of flavonoids as the pigments. While the wavelengths of 420.5 nm are feasible, that is, the chlorophylls and carotenoids. Owing to the characteristic absorption maximum of chlorophyll a is 420 nm, 490 nm and 660 nm. The wavelength range of carotenoids is 420 nm, 440 nm and 470 nm. Thus, the peaks at 420 nm correspond to the absorption bands of chlorophylls and carotenoids (Britton, 1992; Solovchenko et al., 2001). The pigment extraction structure from yellow cotton flower containing chlorophylls, flavonoids, and carotenoids can be considered an investigation dyes sensitizer material for fabrication DSSC.

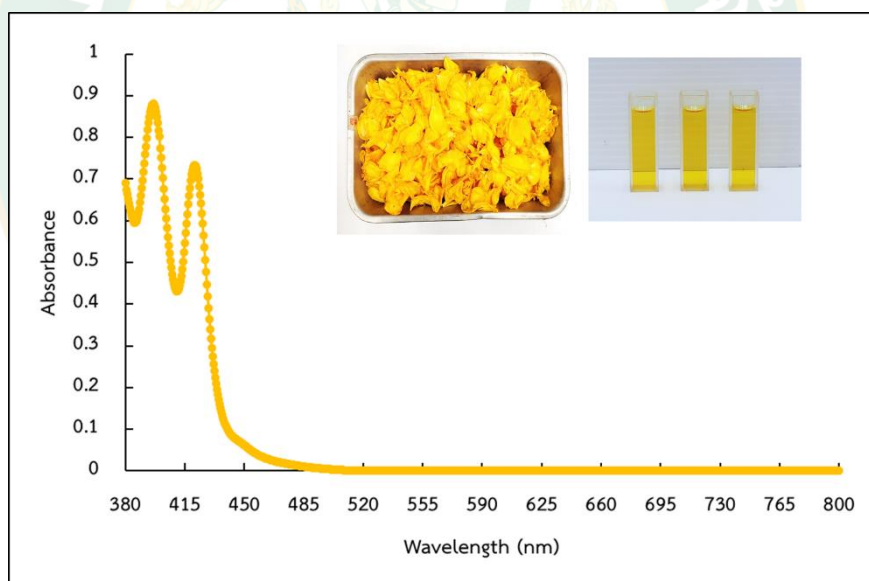


Figure 25 The absorption wavelength of pigments extraction (Yellow cotton flower)



#### 4.1.3 Longan

In this study, the absorption qualification of the pigment extraction from longan leaves were examined and an aliquot of the natural dye extract was diluted by methanol and was examined by the UV-Vis spectrophotometer that has a wavelength between 380 and 800 nm, as shown in figure 26. The results show that the longan leaves have a wide peak at 664 nm. The result matches the standard absorption wavelength of chlorophyll, the main peak at 662–666 nm and chlorophyll b the shoulder near 650 nm; both were present in the absorption wavelength's red band. In the blue region, the visible absorption wavelength between 430 and 440 nm and 470 and 480 nm is the light absorption by chlorophyll and carotenoids (Lichtenthaler, 1987; Merzlyak et al., 1996; Solovchenko et al., 2001). Moreover, considering the absorption wavelength of carotenoid pigments in the blue region of the spectrum is considerably sophisticated due to an overlapping absorption of chlorophyll appear in most plant tissues (Merzlyak et al., 2003). However, carotenoids' absorption wavelength peak is at 420, 450, and 480 nm (Solovchenko et al., 2001). The longan leaves extraction had three absorption peaks at 415 nm, 440 nm, and 470 nm, similar to the functional group of carotenoids. Consequently, the pigment extraction from longan leaves consist of Chl-a, Chl-b, and carotenoids.

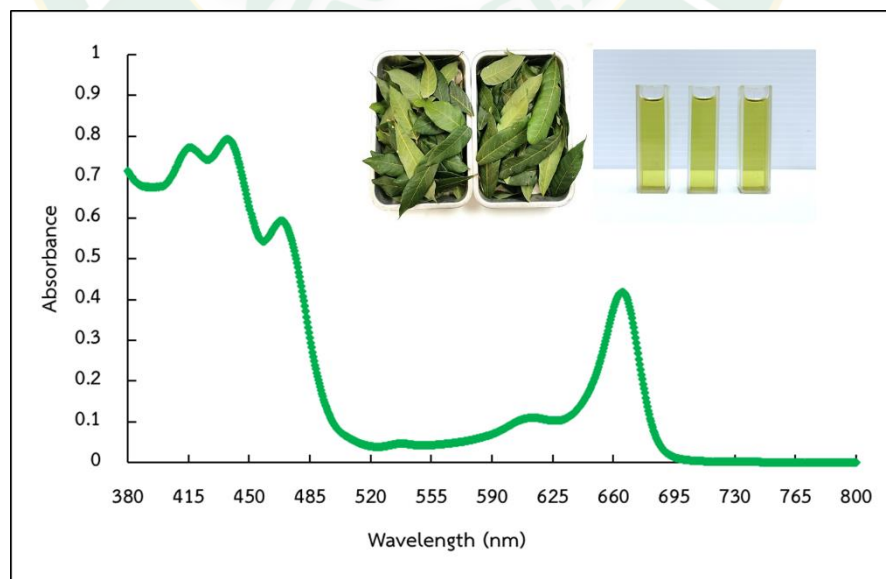


Figure 26 The absorption wavelength of pigments extraction (Longan leaves)

#### 4.1.4 Inthanin bok

The absorbance spectra curves from the inthanin bok dyes shown in figure 27 had three peaks of absorption at the wavelength of 420 nm, 440 nm and 470 nm. The wavelength of 420 nm, 490 nm and 660 nm is the standard maximum absorption wavelength of chlorophylls (Khammee et al., 2020). Thus, the maximum absorption wavelength of inthanin bok dyes feasibility is chlorophylls. On the other hand, the absorption peak of inthanin bok was also matched with the absorption bands of carotenoids, which is 420 nm, 440 nm and 470 nm. In most plant tissues, the considerably sophisticated blue region of the spectrum owing to the absorption wavelength of chlorophylls and carotenoid pigments overlaps absorption wavelength (Khammee et al., 2020). It indicates that the pigments extraction from inthanin bok consists of chlorophylls and carotenoid pigments.

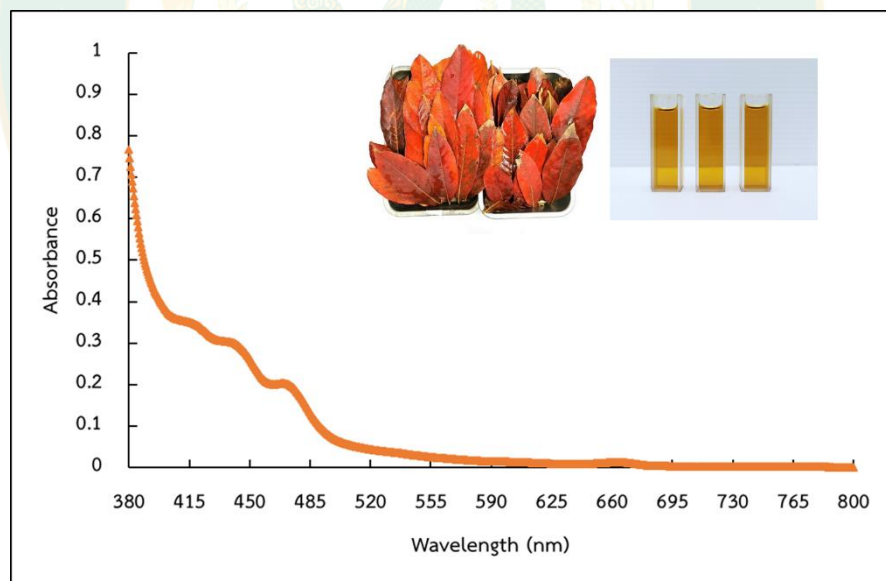


Figure 27 The absorption wavelength of pigments extraction (Inthanin bok leaves)

## 4.2 The pigment extraction content and estimation of natural dyes

Chlorophylls are photosynthetic pigments that provide a green color. The primary functions of chlorophylls are harvesting light energy, spectral properties, and energy transduction for photosynthesis processes. Chlorophylls have two main types, which are chlorophyll-a and chlorophyll-b. Their derivatives of chlorophylls are consumed as sensitizers in DSSC because of their absorbed blue and red light. The most efficient is the chlorophyll-a derivative, which is the carboxyl group. There are directly attached to the conjugated macrocycle to facilitate efficient electron injection to  $\text{TiO}_2$  (Shalini et al., 2015; Wang et al., 2005). Moreover, Carotenoids (Cars) are a huge group that has over 600 members. They provide the red, orange and yellow color for fruits and flowers. Carotenoids have essential roles in photosynthesis that complementary to chlorophylls. The functional consist of light-harvesting, photo-protective functions, and redox function (Frank and Cogdell, 1996; Koyama and Fujii, 1999; Wang et al., 2005). In this study, the natural dye from Indian almond, Yellow cotton, Longan and Inthanin bok are composed of pigments which are chlorophyll-a (Chl-a), chlorophyll-b (Chl-b) and carotenoids (Cars).

The pigments extraction content by using UV-Vis spectrophotometer and used the equations (10, 11 and 12) and the amount of pigment extract from natural dyes shown in table 1 and figure 28. The result showed the pigment extracted from longan leaves had the highest pigment content than other natural dyes. The most composed of chlorophyll-a, which is  $85.213 \pm 0.403 \mu\text{g/ml}$ , followed by chlorophyll-b and carotenoids with is  $28.083 \pm 0.079$  and  $13.128 \pm 0.125 \mu\text{g/ml}$ , respectively. Inthanin bok has a higher pigment content of chlorophyll-a than Indian almond and yellow cotton with  $2.708 \pm 0.251$ ,  $2.008 \pm 0.031$  and  $0.719 \pm 0.061 \mu\text{g/ml}$ , respectively. On the other hand, Indian almond has a higher pigment content of chlorophyll-b and carotenoids than inthanin bok and yellow cotton. The chlorophyll-b content was  $4.209 \pm 0.055$ ,  $2.500 \pm 0.102$  and  $1.484 \pm 0.107 \mu\text{g/ml}$  respectively. Followed by carotenoids with  $11.300 \pm 0.107$ ,  $10.666 \pm 0.324$  and  $7.743 \pm 0.141 \mu\text{g/ml}$  respectively. These natural colorants have been of interest in different fields and applications. Most useful is the

use of natural dyes as sensitizers in DSSCs, their key benefits being a simple extraction procedure, low cost, wide availability, and their environmentally friendly nature. Therefore, in this study, longan pigment extracted has the highest pigments content consisting of chlorophyll-a, chlorophyll-b and carotenoids, and other natural dyes.

In addition, Natural dyes extracted from Indian almond, Yellow cotton, Longan and Inthanin bok leaves (figure 29) was examined the pH by using pH meter. The results found that Longan has the highest pH with 5.33, followed by Yellow cotton, Indian almond and Inthanin bok with 5.30, 4.97 and 4.32.

Table 1 The amount of pigment extract from natural dyes

Dyes	The amount of pigments ( $\mu\text{g/ml}$ )		
	Chlorophyll-a	Chlorophyll-b	Carotenoids
Indian almond	$2.008 \pm 0.031$	$4.209 \pm 0.055$	$11.300 \pm 0.107$
Yellow cotton	$0.719 \pm 0.061$	$1.484 \pm 0.107$	$7.743 \pm 0.141$
Longan	$85.213 \pm 0.403$	$28.083 \pm 0.079$	$13.128 \pm 0.125$
Inthanin bok	$2.708 \pm 0.251$	$2.500 \pm 0.102$	$10.666 \pm 0.324$

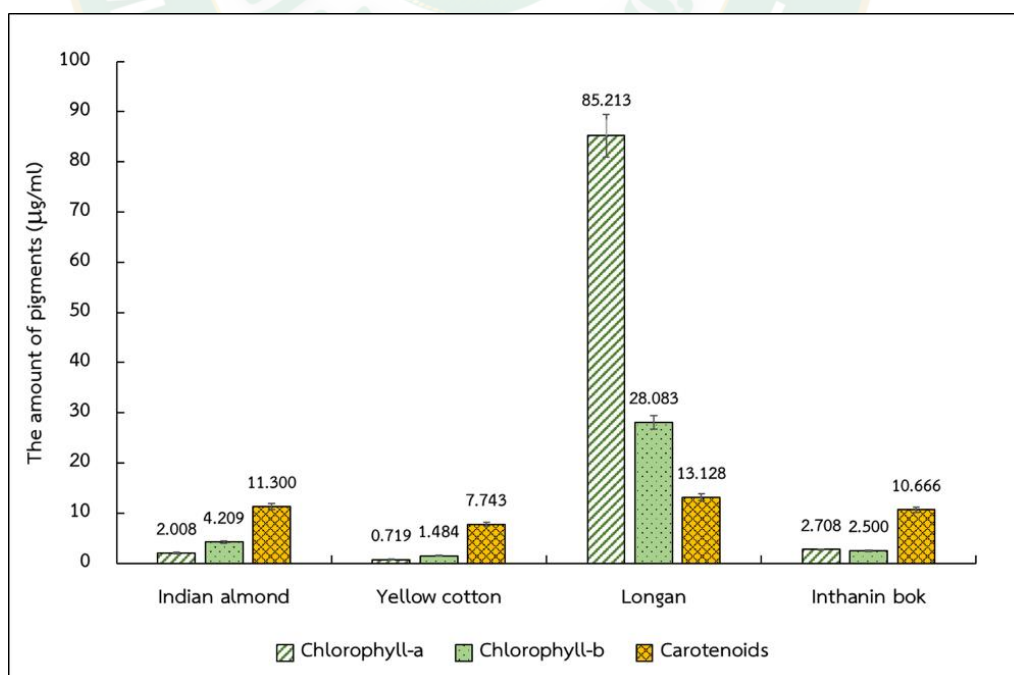


Figure 28 The amount of pigment extract from natural dyes

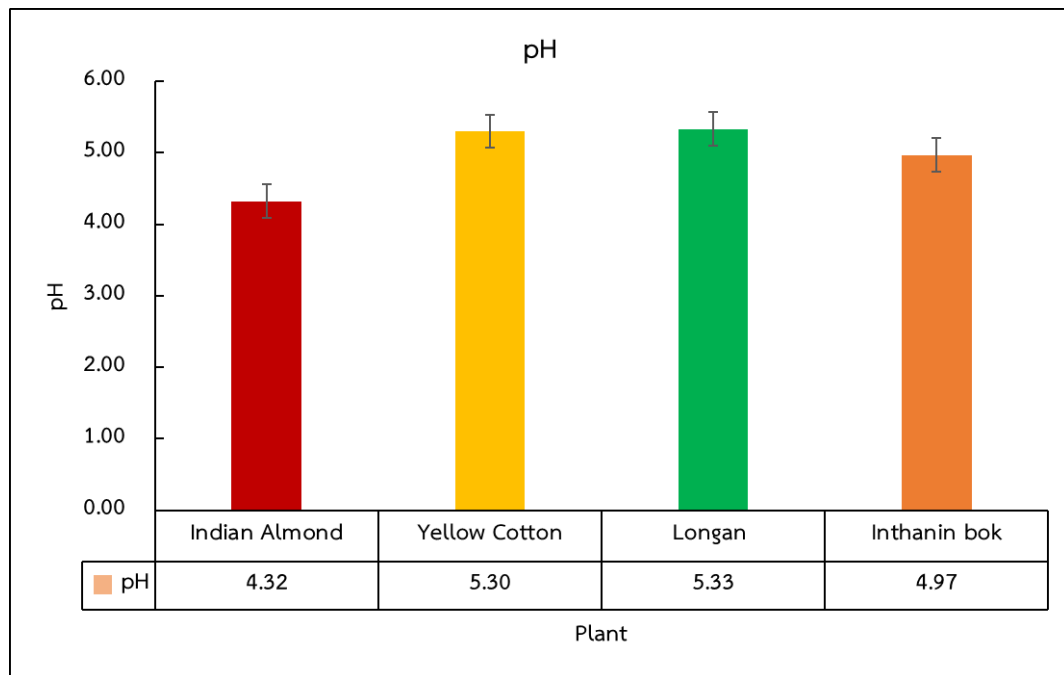
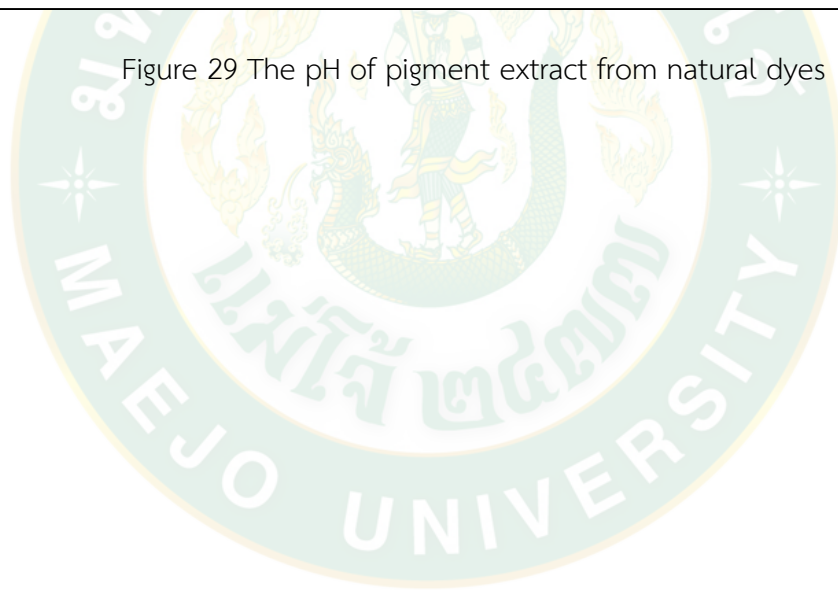


Figure 29 The pH of pigment extract from natural dyes





### 4.3 The effect of different nanostructure layers of photoanode

Nowadays, many innovations in this technology (DSSC), such as the new natural dyes that can absorb a more extended range of wavelengths and the titanium oxides ( $\text{TiO}_2$ ) nanostructure for increase surface areas and etc (Ito et al., 2008; Kuang et al., 2006; Zhang and Cao, 2011; Zhang et al., 2009). The research's main improvement is by introducing natural dyes extracted instead of  $\text{TiO}_2$  and using different nanostructure layers (1, 2 and 3 layers) and temperatures (100, 200 and 300 °C) to improve the absorption collection and efficiency of DSSC. Consequently, the optimized photoanode ( $\text{TiO}_2$  nanostructure) is necessary for developing high solar efficiency of DSSCs (Jeng et al., 2013).

Table 2 and figure 30 show the DSSC parameters of the devices obtained with different thicknesses (1,2 and 3 layers) with natural dyes extracted from Longan leaves and the photocurrent–voltage characteristics curve for the DSSC extraction natural pigment (Longan leaves). The result shows that one layer of the  $\text{TiO}_2$  nanoparticle with natural dye extracted from longan leaves has the highest efficiency with  $0.4735 \pm 0.043\%$ , followed by  $0.4121 \pm 0.024 \%$  of two layers and  $0.2883 \pm 0.056 \%$  of three-layer respectively. The increase of the thickness of  $\text{TiO}_2$  layers will adsorb more natural dyes. However, the results have shown that the established electron in natural dyes extracted from longan leaves cannot be effectively injected into electrodes due too long-distance when the thickness of  $\text{TiO}_2$  layers is too thick. In addition, the thicker  $\text{TiO}_2$  layers will result in a dwindle transmittance and reduce the absorption of light intensity of the pigment dyes. Also, the resistance of charge transfer might be increasing when the thickness of  $\text{TiO}_2$  layers increases. Furthermore, the thicker layers of  $\text{TiO}_2$  will become difficult for the charge recombination between electrons from the excited dye to the conduction band of  $\text{TiO}_2$  and the  $\text{I}_3^-$  ions in the electrolyte (Jeng et al., 2013)

Table 2 The DSSC parameters of the devices obtained with different thicknesses (1,2 and 3 layers) with natural dyes extracted from Longan leaves

Thickness (layers)	Temperature (°C)	$I_{sc}$ (mA/cm <sup>2</sup> )	$V_{oc}$ (V)	$I_{max}$ (mA)	$V_{max}$ (V)	FF (%)	$\eta$ (%)
1	300	0.0317	1.0045	0.0622	0.8002	52.086	0.4735 ±0.043
2	300	0.0281	1.0110	0.0608	0.7126	50.830	0.4121 ±0.024
3	300	0.0248	0.7995	0.0508	0.5963	51.002	0.2883 ±0.056

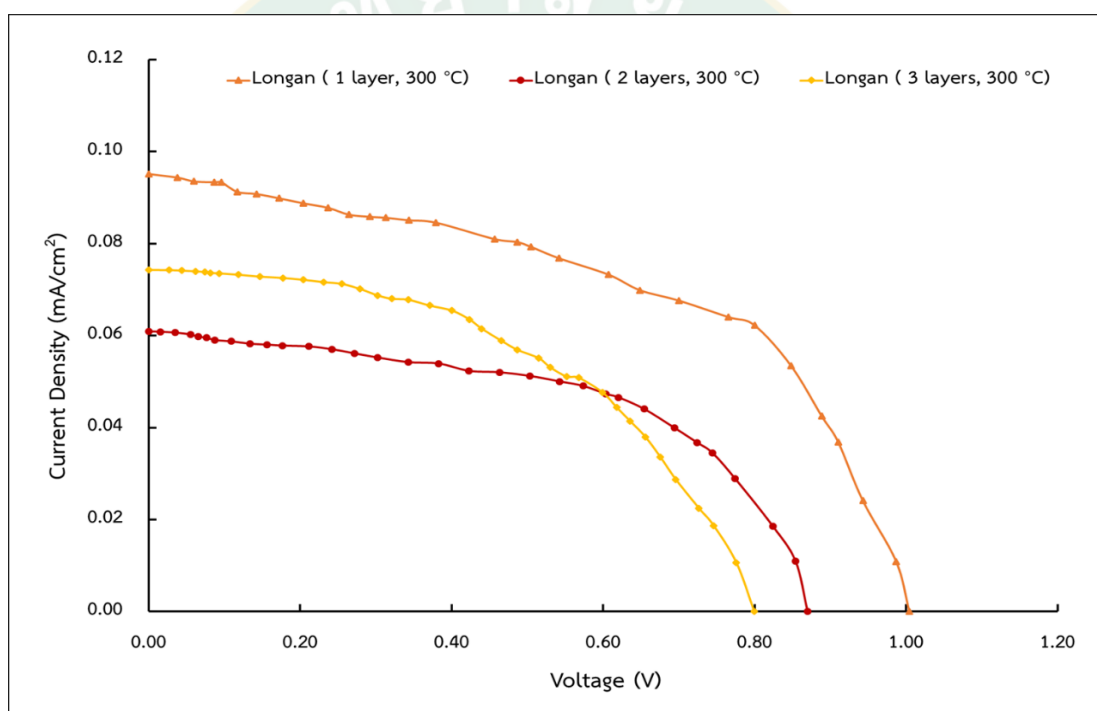


Figure 30 The photocurrent–voltage characteristics curve for the DSSC extraction natural pigment (Longan leaves)

#### 4.4 The effect of different temperature of photoanode

One of the most foreshadowing semiconductor materials is Titanium dioxide ( $\text{TiO}_2$ ). Owing to its characteristic properties for example a wide bandgap, exuberance in nature, and high physical and chemical stability (Archaapinun et al., 2013; Hossain et al., 2008; Richards, 2002).  $\text{TiO}_2$  has been wide examined for potential application in photocatalysts and photovoltaic devices. Normally,  $\text{TiO}_2$  has three crystalline phases which is anatase, rutile, and brookite. Anatase phase of  $\text{TiO}_2$  has better photocatalytic and photovoltaic activity when compared with other phases of  $\text{TiO}_2$  Due to, its larger bandgap and higher surface energy. However, anatase is the metastable phase and can easily transform to rutile phase which reported research has shown that the anatase to rutile transformation occurs at temperatures between 450 and 850 °C, depending on fabrication method and precursors (Archaapinun et al., 2013; Farrell, 2001; Hanaor and Sorrell, 2011).

This research's different temperature affects the pores of  $\text{TiO}_2$  nanoparticles and the absorption of natural dyes that result in the performance of DSSC as shown in table 3 and photocurrent–voltage characteristics curve for the DSSC extraction natural pigment (Longan leaves) shown in figure 31. The result shows that the condition of 300 °C has the highest efficiency with  $0.4735 \pm 0.043$  %, followed by  $0.3803 \pm 0.044$  % of 200 °C and  $0.1202 \pm 0.013$ % of 100 °C respectively. There examined by using the laser scanning microscope to analyzed the surface and morphology of longan dyes coated on  $\text{TiO}_2$  layers (1 layer and 100 °C) and (1 layer and 300 °C) to the comparison of the low and the highest efficiency of DSSC as shown in figure 32 and 33. Also, the area under a curve of the surface of the low and high efficiency of DSSC was presented in table 4.

In general, for annealing used, the low temperature for the fabrication DSSCs should override two main problems for improving photovoltaic performance: the first problem is the defective connection of  $\text{TiO}_2$  particles (Miyasaka et al., 2007) and the

second issue is the residuals of the organic binder within the TiO<sub>2</sub> film. Due to during the preparation of TiO<sub>2</sub> paste usually added organic binder thus the residuals of the binder would become an insulating core in an annealing process using the low temperature and would block the transportation path of electrons that result in the electron transport rate and electron lifetime would decrease (Lin et al., 2012; Longo et al., 2002). It can be seen that figure 33 (c) the surface area and morphology of longan dyes coated on TiO<sub>2</sub> layers (1 layer and 300 °C) using the laser scanning microscope has a roughness than the surface area and morphology of longan dyes coated on TiO<sub>2</sub> layers (1 layer and 100 °C) in figure 32 (c), due to the difference in temperatures during the annealing process.

The results of the area under a graph of the natural pigments extracted from longan leaves were found that the condition of the thickness of TiO<sub>2</sub> layer; 1 layer and annealing at 300 °C has the higher result than the TiO<sub>2</sub> layer; 1 layer and annealing at 100 °C as shown in table 4. This recommends that the binder's residuals within the TiO<sub>2</sub> paste will decompose during the annealing process at high temperature. There could be correlated with increasing the layer's surface area, increasing the dye adsorption and then high photocurrent generation (Karasovec et al., 2009)

Table 3 The DSSC parameters of the devices obtained with different thicknesses (1,2 and 3 layers) with natural dyes extracted from Longan leaves

Thickness (layers)	Temperature (°C)	I <sub>sc</sub> (mA/cm <sup>2</sup> )	V <sub>oc</sub> (V)	I <sub>max</sub> (mA)	V <sub>max</sub> (V)	FF (%)	η (%)
1	100	0.0135	0.6780	0.0326	0.3877	46.070	0.1202 ± 0.013
1	200	0.0271	0.9790	0.0590	0.6774	50.198	0.3803 ± 0.044
1	300	0.0317	1.0045	0.0622	0.8002	52.086	0.4735 ± 0.043

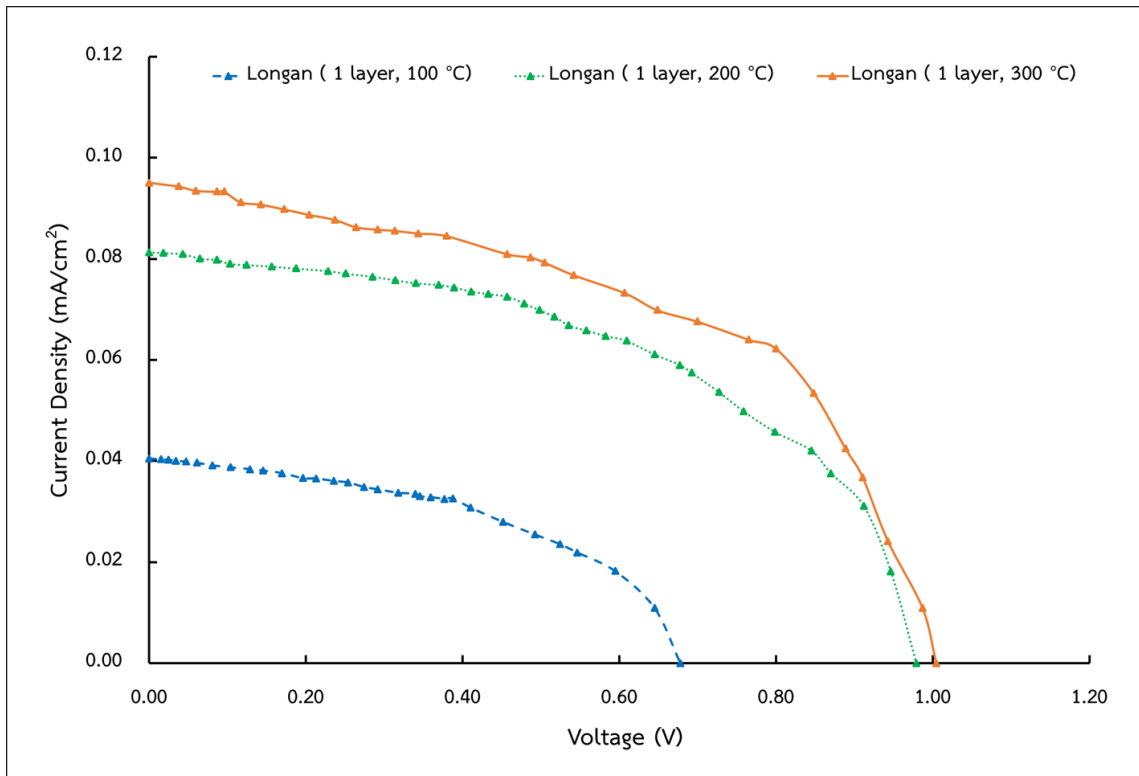


Figure 31 The photocurrent-voltage characteristics curve for the DSSC extraction natural pigment (Longan leaves)

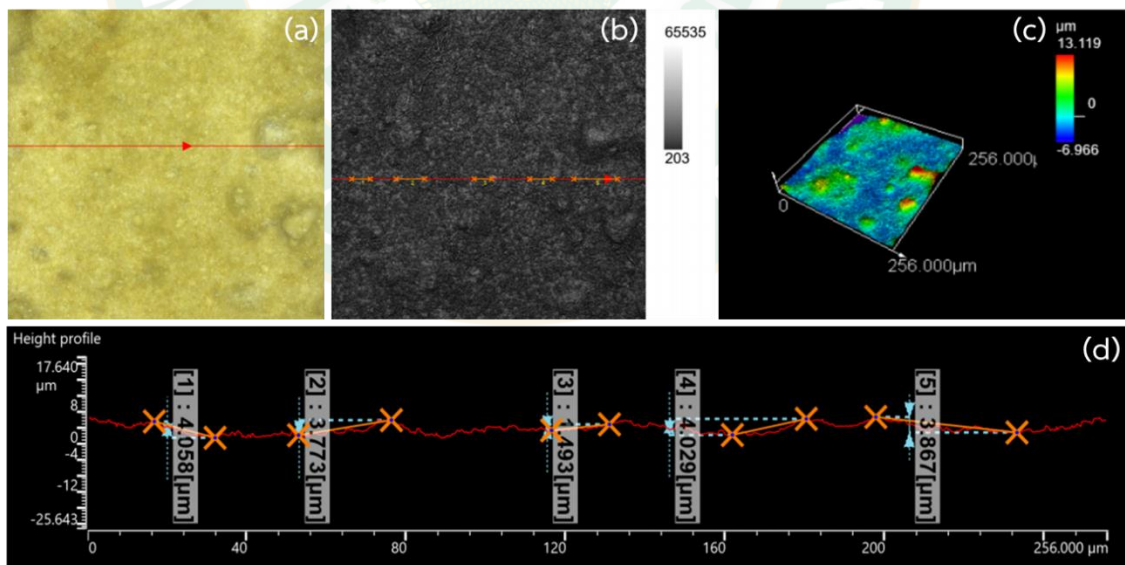


Figure 32 The laser scanning microscope analyzed the surface and morphology of longan dyes coated on  $\text{TiO}_2$  layers (1 layer and 100 °C )



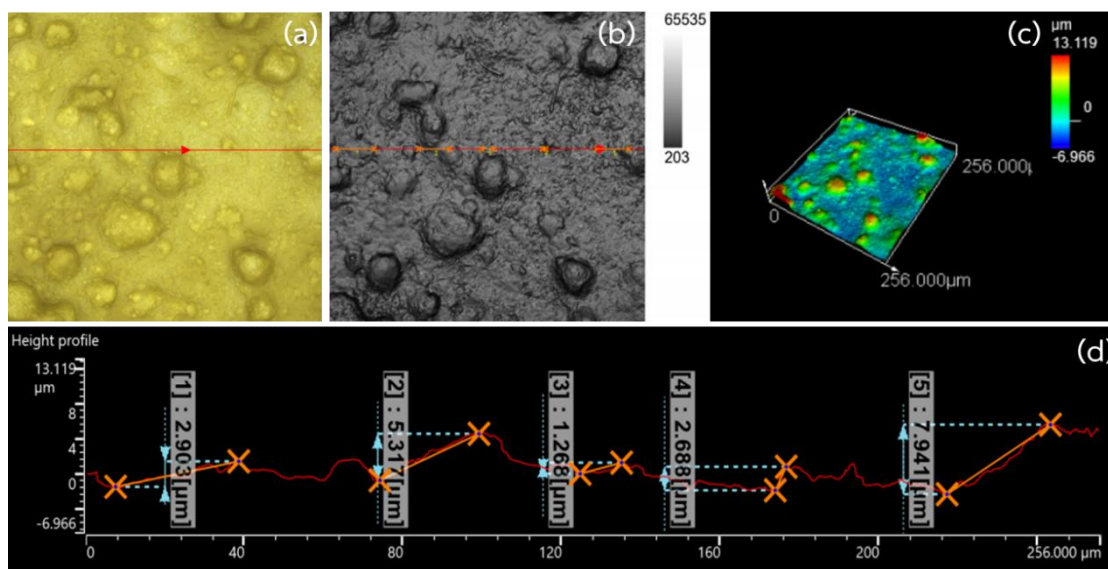


Figure 33 The laser scanning microscope analyzed the surface and morphology of longan dyes coated on  $\text{TiO}_2$  layers (1 layer and  $300\text{ }^\circ\text{C}$ )

Table 4 The area under a graph ( $\mu\text{m}^2$ ) of longan dyes coated on  $\text{TiO}_2$  layers

Methods	The area under a graph ( $\mu\text{m}^2$ )
Longan (1 layer, $100\text{ }^\circ\text{C}$ )	38.303
Longan (1 layer, $300\text{ }^\circ\text{C}$ )	45.033

#### 4.5 The surface and morphology analysis of TiO<sub>2</sub> nanoparticles with natural dyes

The scanning electron micrographs (SEM) of surface morphology characteristics of TiO<sub>2</sub> nanoparticles pure show in figure 34 and with natural dye extracted from (a) Indian almond, (b) Yellow cotton, (c) Longan and (d) Inthanin bok annealed at 300 °C was shown in figure 35. The spherical TiO<sub>2</sub> nanoparticles pure were observed to be homogeneously distributed and porous. No cracks have been identified and stuck on the FTO glass substrate very well, as shown in figure 34 (a) and (b). The agglomeration of small particles brings about to formation of porous structure (Ruhane et al., 2017). The advantages of mesoporous holes of the TiO<sub>2</sub> is to provide the surface of a large hole for higher adsorption of dye molecules and facilitate the penetration of electrolyte within their pores (Jin et al., 2010). Usually, the highest pigment performance consists of the smallest molecule, the highest refractive index, brightness, and scattering coefficient. The chemical adsorption of natural dyes becomes possible because of the condensation of hydroxyl and methoxy protons with the hydroxyl groups on the surface of nanostructured TiO<sub>2</sub> (Kushwaha et al., 2013). Therefore, figure 35. Shows that their pores and surface of the TiO<sub>2</sub> layer were covered with natural dyes extracted from (a) Indian almond, (b) Yellow cotton, (c) Longan and (d) Inthanin bok. The spherical, agglomerate grain morphology can predicted; it is the natural pigment. Therefore, the spherical, agglomerate grain morphology and cover on their pores and surface of TiO<sub>2</sub> layer in figure 35. can forecast; it is a natural pigment extracted from (a) Indian almond, (b) Yellow cotton, (c) Longan and (d) Inthanin bok leaves.

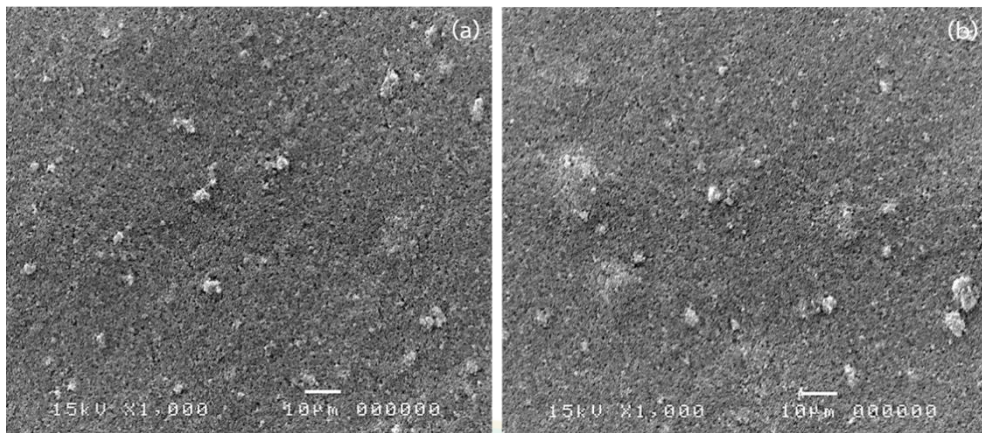


Figure 34 Scanning electron microscope of morphological characteristics of  $\text{TiO}_2$  thin films annealed at 300 °C

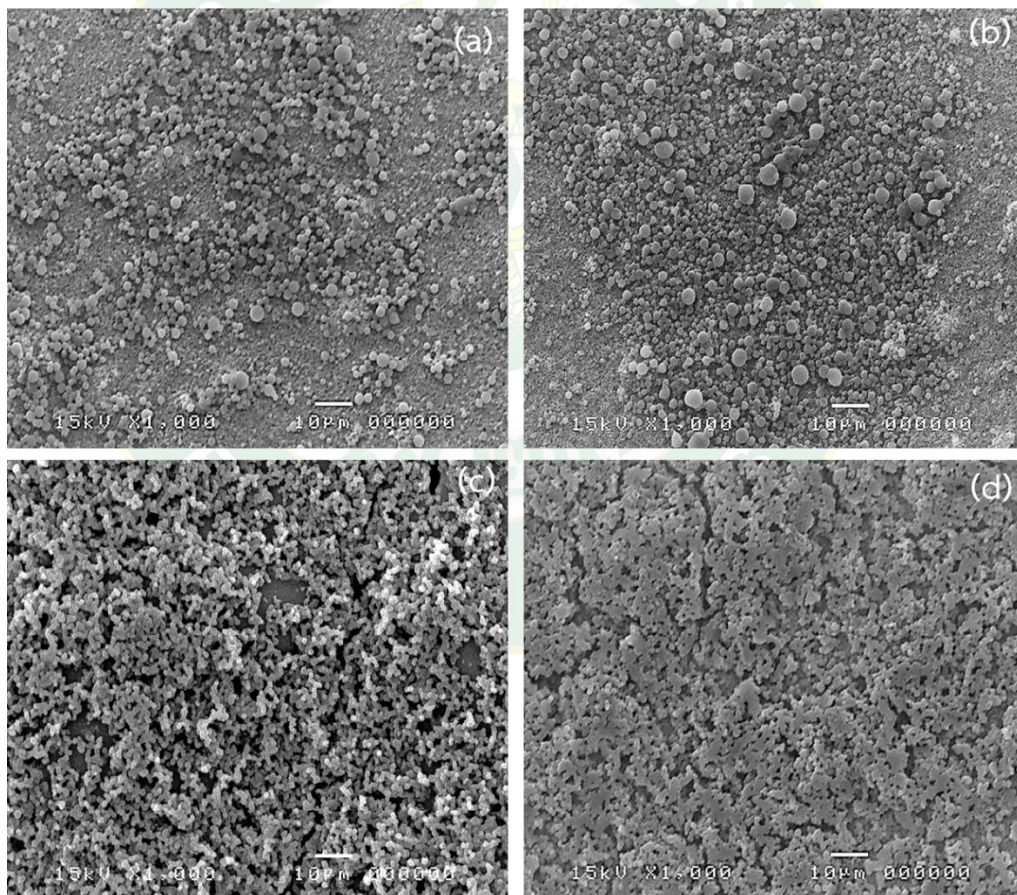


Figure 35 Scanning electron microscope of morphological characteristics of  $\text{TiO}_2$  thin films with natural dye extraction from (a) Indian almond, (b) Yellow cotton, (c) Longan and (d) Inthanin bok leaves dye annealed at 300 °C



The energy-dispersive X-ray spectroscopy (EDX) was used to analyze the elemental contents of  $\text{TiO}_2$  nanoparticles pure as shown in figure 36 and with natural dye extracted as shown in figure 37 (a1,2) Indian almond, (b1,2) Yellow cotton, (c1,2) Longan and (d1,2) Inthanin bok leaves. The data of elemental contents were presented in Table 5 indicates that the  $\text{TiO}_2$  nanoparticles were coated on FTO glass due to elemental contents of oxygen (O), and titanium (Ti). The atomic ratios were 80.33 and 19.67%, respectively. Follow by the natural pigments from Indian almond, Yellow cotton, Longan and Inthanin bok leaves immersion on  $\text{TiO}_2$  nanoparticles. The results show that the highest elemental contents were carbon (C) with 77.53, 85.96, 72.28 and 82.29%. This indicated that attendance of natural pigments of functional groups coated on the surfaces of  $\text{TiO}_2$  particles. The adsorption of natural dyes on the  $\text{TiO}_2$  layer can be enhanced electron transfer rates (Al-Alwani et al., 2018).

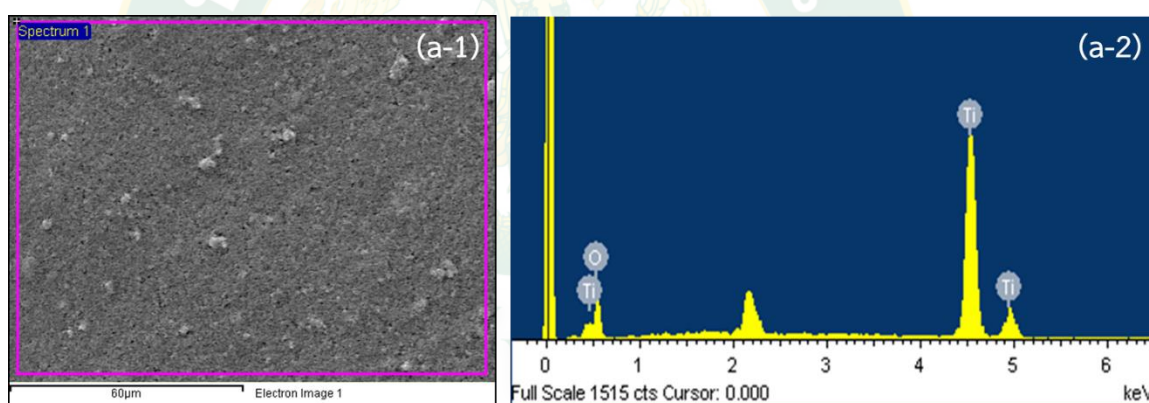


Figure 36 The energy-dispersive X-ray spectroscopy (EDX) analysis of  $\text{TiO}_2$  coated on FTO glass substrate (a1,2)

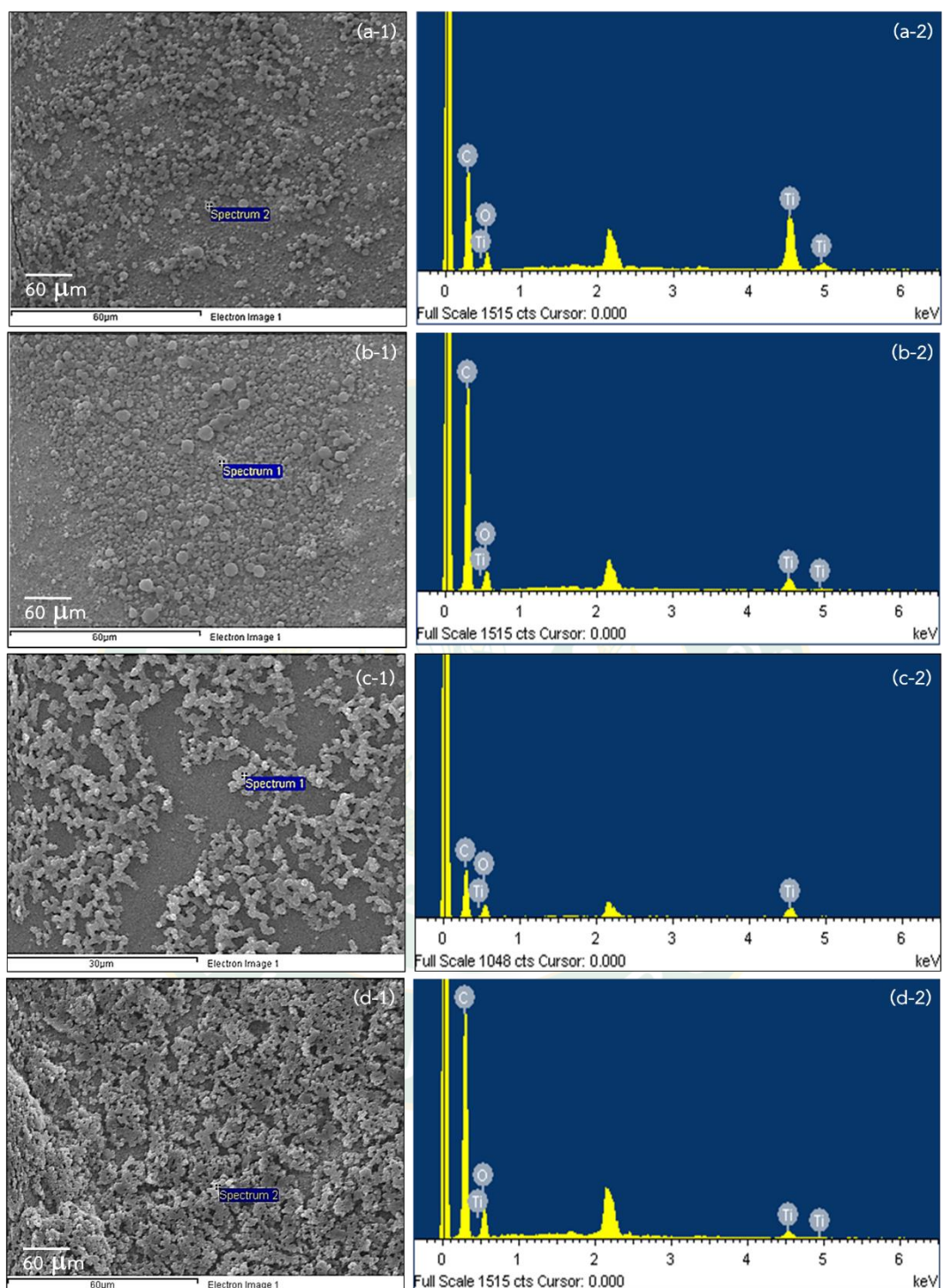


Figure 37 The energy-dispersive X-ray spectroscopy (EDX) analysis of  $\text{TiO}_2$  coated on FTO glass substrates with natural dyes immersion (a1,2) Indian almond, (b1,2) Yellow cotton, (c1,2) Longan and (d1,2) Inthanin bok leaves.



Table 5 The elemental composition of TiO<sub>2</sub> coated on FTO glass substrate with natural dyes immersion of Indian almond, Yellow cotton, Longan and Inthanin bok leaves.

Methods	Element	Weight %	Atomic %
Blank TiO <sub>2</sub> (spectrum 1) (a-1,2)	O, K	57.70	80.33
	Ti, K	42.30	19.67
Indian almond (spectrum 2) (a-1,2)	C, K	67.46	77.53
	O, K	22.80	19.67
	Ti, K	9.74	2.81
Yellow cotton (spectrum 1) (b-1,2)	C, K	81.30	85.96
	O, K	17.17	13.63
	Ti, K	1.53	0.40
Longan (spectrum 1) (c-1,2)	C, K	64.60	72.28
	O, K	31.80	26.71
	Ti, K	3.60	1.01
Inthanin bok (spectrum 1) (d-1,2)	C, K	77.41	82.29
	O, K	21.98	17.54
	Ti, K	0.61	0.16

The laser scanning microscope was analyzed the surface and morphology of natural dyes including of Indian almond, Yellow cotton, Longan and Inthanin bok coated on TiO<sub>2</sub> layers (1 layer and 100 °C) and (1 layer and 300 °C) as shown in figure 38, 39, 40 and 41. Moreover, the result of the area under a graph ( $\mu\text{m}^2$ ) of natural dyes coated on TiO<sub>2</sub> layers was shown in table 6. The result of the area under a graph of natural dyes coated on TiO<sub>2</sub> layers, which, the condition of 1 layer and 300 °C has the higher value than the condition of 1 layer and 300 °C of Indian almond, Yellow cotton, Longan and Inthanin bok. Due to, the binder's residuals within the TiO<sub>2</sub> paste will decompose during the annealing process at high temperature. There could be correlated with increasing the layer's surface area, which can increase the dye adsorption and then high photocurrent generation (Karasovec et al., 2009). The rough surface of the photoanodes means the increasing surface area of the film, which enabled much more natural dye to be adsorbed. Moreover, this increasing surface area increases the absorption of the incident light with much more adsorbed natural dyes. Thus the more electrons excited in CB of natural dyes increase, the more  $J_{sc}$  of DSCC increases (Kutlu, 2020; Snaith and Grätzel, 2006).

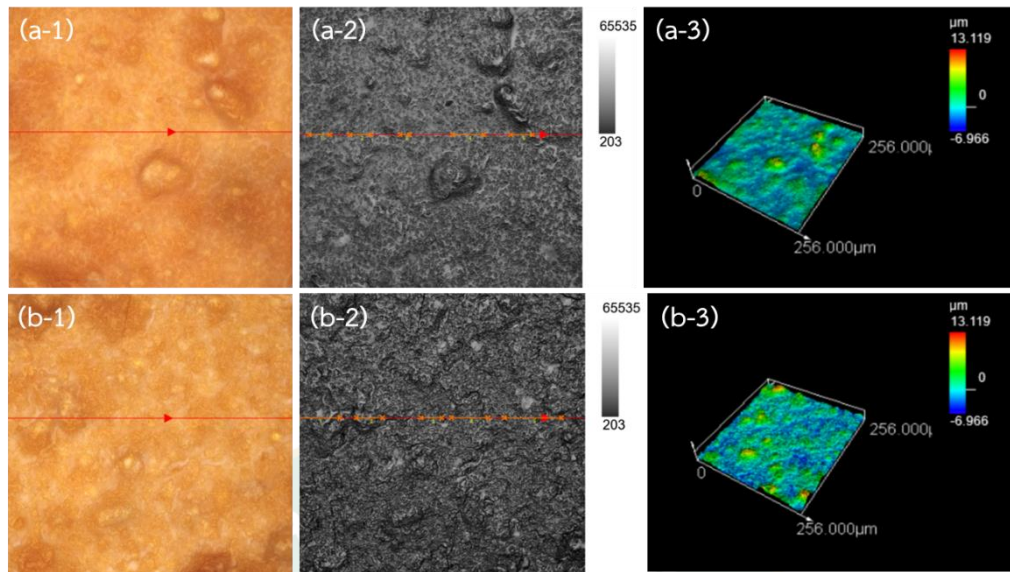


Figure 38 The laser scanning microscope analyzed the surface and morphology of Indian almond dyes coated on  $\text{TiO}_2$  layers; (a1-3) 1 layer and 100 °C and (b1-3) 1 layer and 300 °C

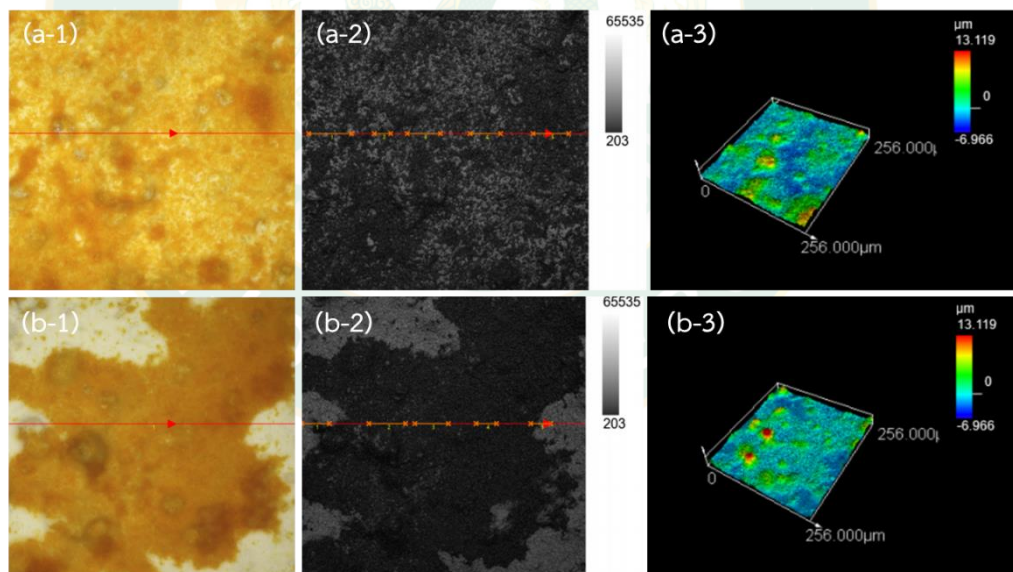


Figure 39 The laser scanning microscope analyzed the surface and morphology of yellow cotton dyes coated on  $\text{TiO}_2$  layers; (a1-3) 1 layer and 100 °C and (b1-3) 1 layer and 300 °C

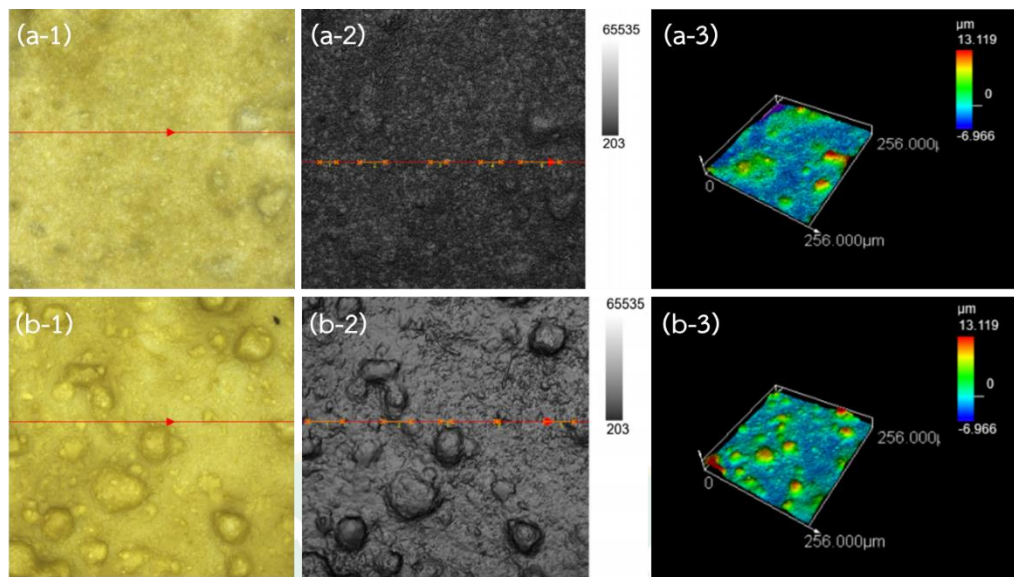


Figure 40 The laser scanning microscope analyzed the surface and morphology of longan dyes coated on  $\text{TiO}_2$  layers; (a1-3) 1 layer and 100 °C and (b1-3) 1 layer and 300 °C

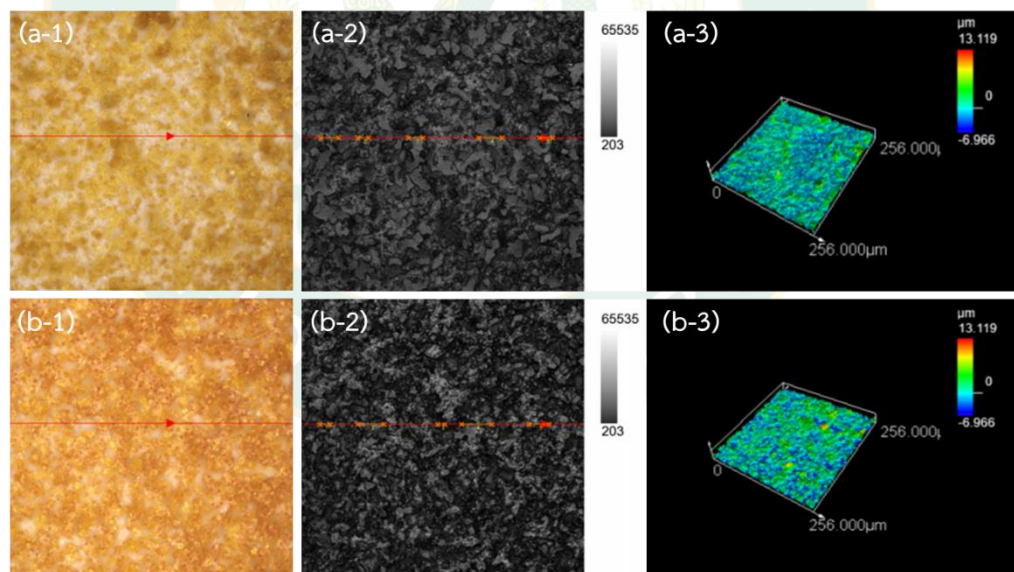


Figure 41 The laser scanning microscope analyzed the surface and morphology of inthanin bok dyes coated on  $\text{TiO}_2$  layers; (a1-3) 1 layer and 100 °C and (b1-3) 1 layer and 300 °C



Table 6 The area under a graph ( $\mu\text{m}^2$ ) of natural dyes coated on  $\text{TiO}_2$  layers

Methods	The area under a graph ( $\mu\text{m}^2$ )
Indian almond (1 layer, 100 °C)	20.044
Indian almond (1 layer, 300 °C)	88.974
Yellow cotton (1 layer, 100 °C)	35.048
Yellow cotton (1 layer, 300 °C)	69.848
Longan (1 layer, 100 °C)	38.303
Longan (1 layer, 300 °C)	45.033
Inthanin bok (1 layer, 100 °C)	31.110
Inthanin bok (1 layer, 300 °C)	61.426



#### 4.6 Performance of DSSC with the natural dyes

The photovoltaic characteristics of the natural dye extracted from Indian almond, yellow cotton, longan and inthanin bok were tested the current density–voltage (J–V) by using a digital multimeter (UNI-T UT61E) with variable resistance (10 k $\Omega$ ) under illuminated with the yellow light of 24000 LUX (0.03504 W/cm<sup>2</sup>) in the ambient atmosphere. The output result of photovoltaic performance and different parameters of DSSCs including short circuit current density ( $I_{sc}$ ), open-circuit voltage ( $V_{oc}$ ), maximum current ( $I_{max}$ ), maximum voltage ( $V_{max}$ ), fill factor (FF), efficiency ( $\eta$ ) were given in Table 7. Furthermore, the photocurrent–voltage characteristics curve for the DSSC extraction from Indian almond, yellow cotton, longan and inthanin bok was shown in figures 42, 43, 44 and 45 respectively. The highest efficiency is achieved by the cell fabricated with the condition of 1 layer at 300 °C of inthanin bok dye, with short circuit current density ( $I_{sc}$ ) of 0.092 mA/cm<sup>2</sup>, open-circuit voltage ( $V_{oc}$ ) of 0.807 V, fill factor (FF) of 53.709%, and efficiency ( $\eta$ ) of 1.1383  $\pm$  0.018%. The results was shown that natural dye extracted from Yellow cotton and Indian almond has the efficiency higher than natural dye extracted from longan. Due to, chlorophyll-a, chlorophyll-b and the pheophytins do not make strong bonds with the TiO<sub>2</sub> surface, due to the weak interaction of the phytylester group and keto carbonyl groups (Kay and Graetzel, 1993; Kumara et al., 2017). It was known that the photon-to-current efficiency depends on the intensity and range of the light absorption of the dye on TiO<sub>2</sub>, and the interaction between TiO<sub>2</sub> and the dye. Moreover, a distance between the dye skeleton and the point connected to TiO<sub>2</sub> surface facilitate an electron transfer. During chlorophylls was deteriorate and melt covered on TiO<sub>2</sub> was an impediment to electron exchange as shown in figures 46 due to the amount of pigments extracted from longan leaves has the highest concentration pigments of chlorophyll a and b compare with other plants. Thus, illustrates that the time, temperature affects the quality and stability of the pigment. The morphology of the pigment was changed with clustering and forming a homogeneous mass while the pigments were completely homogeneous by coating

the surface of  $\text{TiO}_2$  (Khammee et al., 2020; Wongcharee et al., 2007). Thus, the efficiency of longan leaves which has the highest pigments content got the low efficiency than Indian almond, yellow cotton, and inthanin bok.

Table 7 The DSSC parameters of the devices obtained with different thicknesses and temperature with natural dyes extracted from Indian almond, yellow cotton, longan and inthanin bok

Dye	Thickness (layers)	Temp. ( $^{\circ}\text{C}$ )	$I_{sc}$ ( $\text{mA}/\text{cm}^2$ )	$V_{oc}$ (V)	$I_{max}$ (mA)	$V_{max}$ (V)	FF (%)	$\eta$ (%)
Indian almond	1	100	0.0254	0.6535	0.0585	0.4322	50.768	$0.2405 \pm 0.057$
	2	100	0.0183	0.7020	0.0398	0.4905	50.726	$0.1859 \pm 0.018$
	3	100	0.0167	0.6160	0.0355	0.4148	47.551	$0.1399 \pm 0.014$
	1	200	0.0287	0.9450	0.0616	0.6978	52.810	$0.4089 \pm 0.023$
	2	200	0.0224	0.7800	0.0413	0.6426	50.637	$0.2525 \pm 0.049$
	3	200	0.0208	0.8100	0.0448	0.5685	50.508	$0.2425 \pm 0.009$
	1	300	0.0335	0.9900	0.0688	0.7489	51.743	$0.4898 \pm 0.081$
	2	300	0.0262	0.9360	0.0544	0.6905	51.019	$0.3573 \pm 0.001$
	3	300	0.0263	0.7300	0.0468	0.6058	49.241	$0.2695 \pm 0.024$
Yellow cotton	1	100	0.0319	1.0436	0.0664	0.7717	51.229	$0.4874 \pm 0.059$
	2	100	0.0295	0.7450	0.0534	0.6196	50.185	$0.3149 \pm 0.052$
	3	100	0.0324	1.0800	0.0705	0.8216	55.159	$0.5509 \pm 0.098$
	1	200	0.0330	1.4046	0.0817	0.9547	56.154	$0.4089 \pm 0.023$
	2	200	0.0259	1.1278	0.0618	0.7221	50.883	$0.2525 \pm 0.049$
	3	200	0.0340	1.1701	0.0734	0.8234	50.658	$0.2425 \pm 0.009$

Dye	Thickness (layers)	Temp. (°C)	$I_{sc}$ (mA/cm <sup>2</sup> )	$V_{oc}$ (V)	$I_{max}$ (mA)	$V_{max}$ (V)	FF (%)	$\eta$ (%)
Longan	1	300	0.0336	1.4178	0.0814	0.9504	54.082	0.7362 ± 0.033
	2	300	0.0339	1.1264	0.0719	0.7975	50.057	0.5452 ± 0.044
	3	300	0.0309	1.1820	0.0724	0.8153	53.837	0.5618 ± 0.038
	1	100	0.0135	0.6780	0.0326	0.3877	46.070	0.1202 ± 0.013
	2	100	0.0172	0.6850	0.0380	0.4367	46.845	0.1579 ± 0.053
	3	100	0.0228	0.7800	0.0467	0.5646	49.456	0.2510 ± 0.025
	1	200	0.0271	0.9790	0.0590	0.6774	50.198	0.3803 ± 0.044
	2	200	0.0319	1.0265	0.0645	0.8116	53.336	0.4977 ± 0.030
	3	200	0.0203	0.8700	0.0441	0.6202	51.632	0.2602 ± 0.035
Inthanin bok	1	300	0.0317	1.0045	0.0622	0.8002	52.086	0.4735 ± 0.043
	2	300	0.0281	1.0110	0.0608	0.7126	50.830	0.4121 ± 0.024
	3	300	0.0248	0.7995	0.0508	0.5963	51.002	0.2883 ± 0.056
	1	100	0.082	0.759	0.0326	0.3877	53.203	0.9475 ± 0.031
	2	100	0.079	0.788	0.0380	0.4367	52.600	0.9319 ± 0.127
	3	100	0.088	0.760	0.0467	0.5646	53.269	1.0144 ± 0.033
	1	200	0.063	0.763	0.0590	0.6774	46.414	0.6334 ± 0.065
	2	200	0.065	0.816	0.0645	0.8116	48.505	0.7376 ± 0.157
	3	200	0.066	0.710	0.0441	0.6202	53.801	0.7205 ± 0.018
Inthanin bok	1	300	0.092	0.807	0.0622	0.8002	53.709	1.1383 ± 0.018
	2	300	0.111	0.785	0.0608	0.7126	45.458	1.1344 ± 0.160
	3	300	0.096	0.754	0.0508	0.5963	52.333	1.0801 ± 0.086

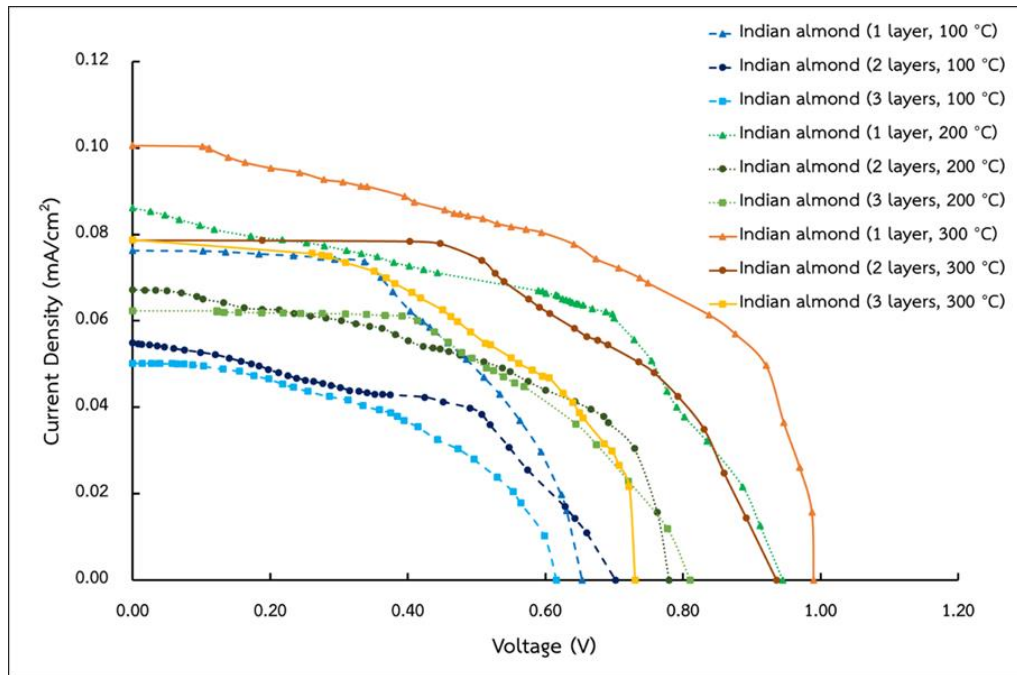


Figure 42 The photocurrent–voltage characteristics curve for the DSSC extraction from Indian almond

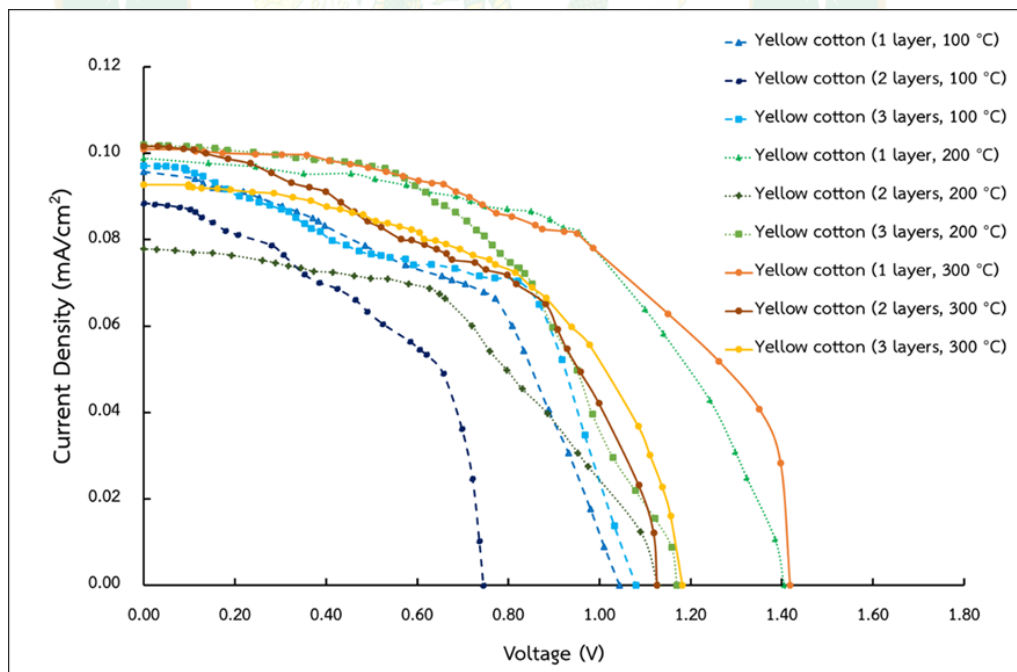


Figure 43 The photocurrent–voltage characteristics curve for the DSSC extraction from yellow cotton

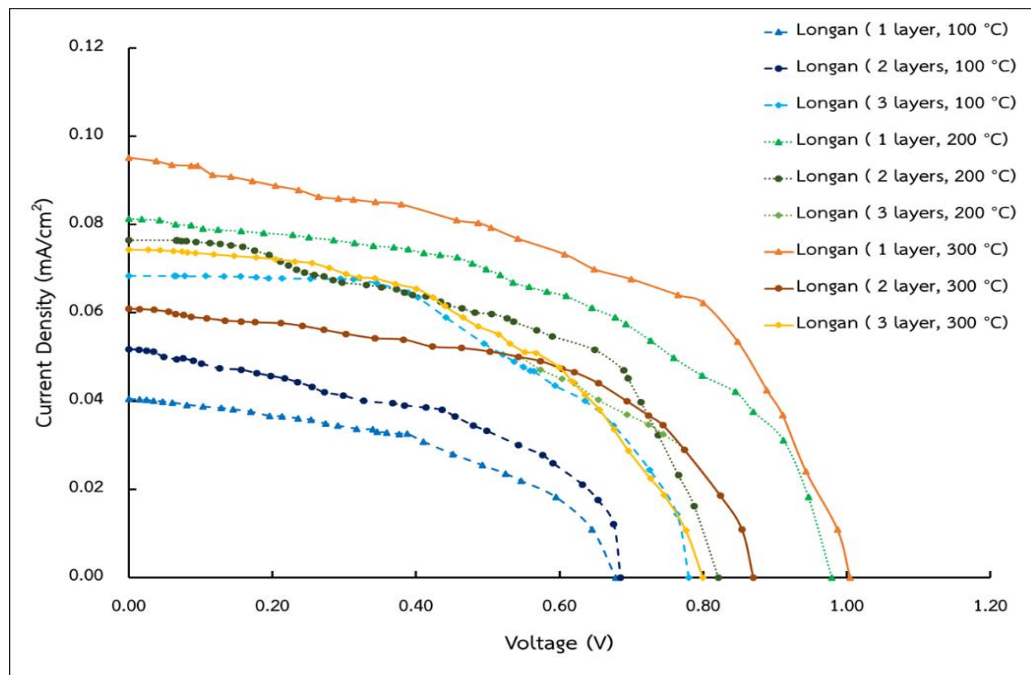


Figure 44 The photocurrent–voltage characteristics curve for the DSSC extraction from longan

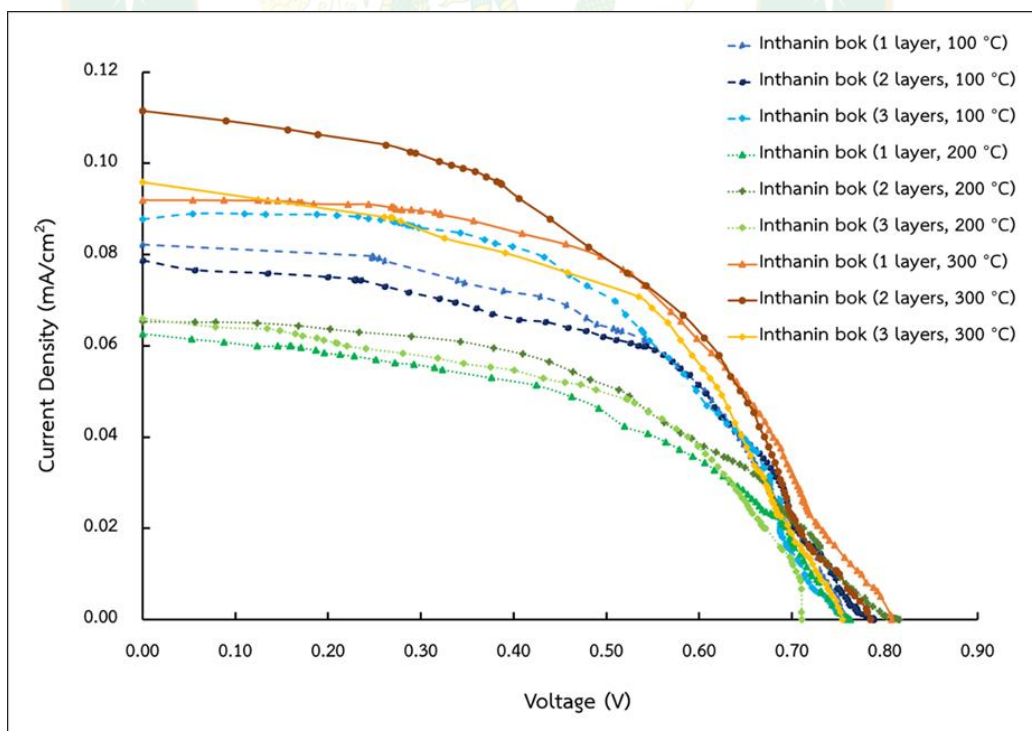


Figure 45 The photocurrent–voltage characteristics curve for the DSSC extraction from inthanin bok



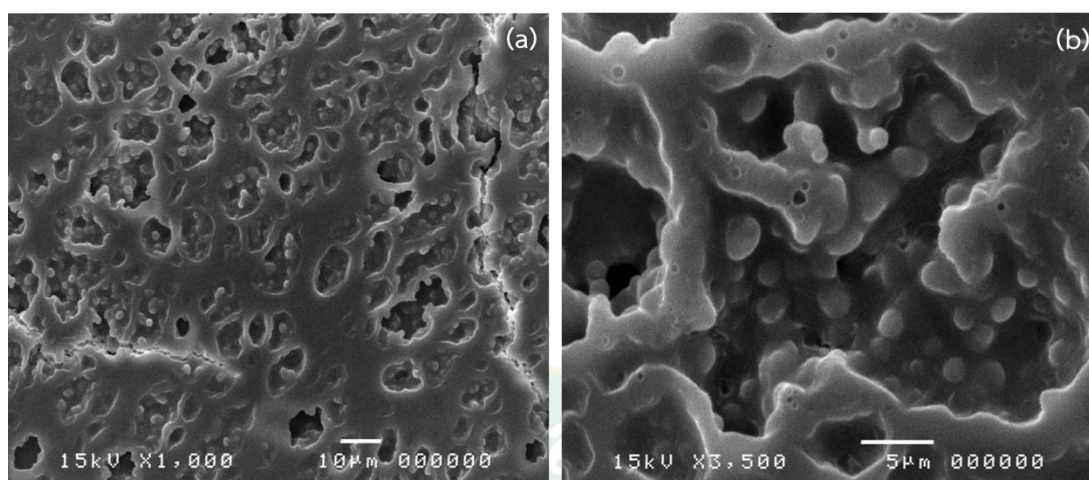












Figure 46 Scanning electron microscope of morphological characteristics of  $\text{TiO}_2$  thin films with natural dye extraction from longan (stored pigment)

Table 8 indicates the values of  $I_{sc}$ ,  $V_{oc}$ , FF and  $\eta$  obtained from the photovoltaic device (DSSCs) employing photoanodes with sensitizer from natural dye extracts. Obviously, our best device, which is one layer of  $\text{TiO}_2$  and annealing at  $300^\circ\text{C}$  has the highest performance compared with other dye pigments extracted from different plants.

Table 8 The DSSC parameters of the devices obtained with different natural dyes extraction

Dyes	Dye pigments	$I_{sc}$ ( $\text{mA}/\text{cm}^2$ )	$V_{oc}$ (V)	FF (%)	$\eta$ (%)	Reference
	Perilla Chlorophylls	1.36	0.522	69.9	0.50	(Shalini et al., 2015)
	Bitterleaf Chlorophylls	0.07	0.34	81	0.69	(Tributsch, 1972)

	Dyes	Dye pigments	$I_{sc}$ (mA/cm <sup>2</sup> )	$V_{oc}$ (V)	FF (%)	$\eta$ (%)	Reference
	Spinach	Chlorophylls	0.470	0.550	51	0.13	(Chang et al., 2010)
	Parsley	Chlorophylls	0.530	0.440	34	0.07	(Shalini et al., 2015)
	Arugula	Chlorophylls	0.780	0.590	42.0	0.20	(Shalini et al., 2015)
	Achiote	Carotenoids	1.100	0.57	59	0.37	(Gómez-Ortíz et al., 2010)
	Alkanet	Carotenoids	0.268	0.372	46	0.03	(Shalini et al., 2015)
	Turmeric	Carotenoids	0.200	0.280	65	0.36	(Shalini et al., 2015)
	Golden trumpet	Carotenoids	0.878	0.405	54	0.40	(Shalini et al., 2015)
	Inthanin bok	Carotenoids and Chlorophylls	0.092	0.807	53.71	1.138	This research

## CHAPTER 5

### SUMMARY AND CONCLUSION

Dye-sensitized solar cells have become a topic of valuable research because of their scientific prominence in the area of energy utilization and conversion. Typically, the dyes extracted from plant materials contained anthocyanins, betalains and chlorophyll. In this study, I carried out three aspects of experimental design: natural dye preparations, DSSC fabrications, and material characterizations. The pigment extractions were conducted with tropical plants including *Terminalia catappa*, *Cochlospermum regium*, *Dimocarpus longan* and *Lagerstroemia macrocarpa* to produce natural dyes by using the solvent extraction method. The quantity of pigments (Chlorophylls and Carotenoids) was higher in the longan plant leaves than Indian almond, yellow cotton flowers and inthanin bok leaves.

Subsequently, these natural dyes were applied in the fabrication process. Natural dye consists of natural pigments and these pigments are used as natural dyes sensitizers for solar cells. For an efficient approach, pigments and  $\text{TiO}_2$  were used with different layers and different temperatures were used with DSSC. That's the main progress of the research with introducing natural dyes extracted instead of  $\text{TiO}_2$  itself but also using different nanostructure layers (1,2 and 3 layers) and temperatures (100, 200 and 300 °C) to increase the absorption capacity and efficiency of DSSC. My experimental study results were expressed that one layer with 300 °C of fabricated DSSC contain higher efficiency on inthanin bok compared to other plants.

The DSSC material characterizations were studied with SEM, energy-dispersive X-ray spectroscopy (EDX) and confocal layer microscope. This equipment was used to confirm the elemental of the  $\text{TiO}_2$  nanoparticles and natural dyes from Indian almonds, yellow cotton flowers, longan leaves, and inthanin bok leaves. Thus, this study recommends that chlorophylls and carotenoids have good potential to be photosensitizers in DSSC. In addition, natural pigments are cheap, safe, environmentally friendly, easily found, and easy extraction process. For the recommendation of this research was provide in below:

1. Selection of raw materials for extraction plant pigments, it is advisable to extract the pigment and calculate the amount of pigment before selecting and starting research. Due to, can choose the raw material with the highest amount of pigment to be used as a dye sensitizer for DSSC. In addition, use pH meter measure the pH of the pigments due to low pH will have effect of photoanode. This this study Indian almond has the low pH that break the TiO<sub>2</sub> nanoparticle that coated on FTO glass that made the DSSC has low efficiency.
2. The graphs obtained by measuring spectrophotometers. The wavelength should use in the range that the pigment could absorb. Because it is easy to calculate and analyze results in the range of 380-700 nm.
3. Develop an electrolyte with highly efficient to increase the open circuit voltage, so that value close to the theory.
4. Develop microstructures of metal oxide semiconductors. In order to have an increased distance of electron diffusion by changing the shape of the metal oxide used from nanoparticle particles to nanowire.

## REFERENCES

- Adedokun, O., Titilope, K. & Awodugba, A. O. 2016. Review on natural dye-sensitized solar cells (DSSCs). **International journal of engineering technologies**, 2(34-41).
- Ahmad, M. S., Pandey, A. K. & Rahim, N. A. 2017. Advancements in the development of TiO<sub>2</sub> photoanodes and its fabrication methods for dye sensitized solar cell (DSSC) applications. A review. **Renewable and Sustainable Energy Reviews**, 77(89-108).
- Al-Alwani, M. A., Ludin, N. A., Mohamad, A. B., Kadhum, A. A. H. & Mukhlus, A. 2018. Application of dyes extracted from *Alternanthera dentata* leaves and *Musa acuminata* bracts as natural sensitizers for dye-sensitized solar cells. **Spectrochimica acta part A: molecular and biomolecular spectroscopy**, 192(487-498).
- Albrecht, S., Saliba, M., Baena, J. P. C., Lang, F., Kegelmann, L., Mews, M., Steier, L., Abate, A., Rappich, J. & Korte, L. 2016. Monolithic perovskite/silicon-heterojunction tandem solar cells processed at low temperature. **Energy & Environmental Science**, 9(1), 81-88.
- Alhamed, M., Issa, A. S. & Doubal, A. W. 2012. Studying of natural dyes properties as photo-sensitizer for dye sensitized solar cells (DSSC). **Journal of electron Devices**, 16(11), 1370-1383.
- Anandan, S. 2007. Recent improvements and arising challenges in dye-sensitized solar cells. **Solar energy materials and solar cells**, 91(9), 843-846.
- Ananthakumar, S., Kumar, J. R. & Babu, S. M. 2019. Third-Generation Solar Cells: Concept, Materials and Performance-An Overview. In **Emerging Nanostructured Materials for Energy and Environmental Science**, (305-339).
- Andersen, O. M. & Markham, K. R. 2005. **Flavonoids: chemistry, biochemistry and applications**. CRC press.
- Apriyanto, D. R., Aoki, C., Hartati, S., Hanafi, M., Kardono, L. B. S., Arsianti, A., Louisa, M., Sudiro, T. M., Dewi, B. E. & Sudarmono, P. 2015. Anti-hepatitis C virus activity of



- a crude extract from longan (*Dimocarpus longan* Lour.) leaves. **Japanese journal of infectious diseases**, JJID. 2015.2107.
- Archaapinun, K., Witit-Anun, N. & Visuttipitukul, P. 2013. Effect of heat treatment on phase transformation of TiO<sub>2</sub> and its reflectance properties. **Journal of Metals, Materials and Minerals**, 23(2).
- Arulraj, A., Senguttuvan, G., Veeramani, S., Sivakumar, V. & Subramanian, B. 2019. Photovoltaic performance of natural metal free photo-sensitizer for TiO<sub>2</sub> based dye-sensitized solar cells. **Optik**, 181(619-626).
- Bauer, C., Boschloo, G., Mukhtar, E. & Hagfeldt, A. 2002. Interfacial electron-transfer dynamics in Ru (tcterpy)(NCS) 3-sensitized TiO<sub>2</sub> nanocrystalline solar cells. **The Journal of Physical Chemistry B**, 106(49), 12693-12704.
- Boschloo, G., Mukhtar, E. & Hagfeldt, A. 2002b. Ultrafast studies of electron injection in Ru dye sensitized SnO<sub>2</sub> nanocrystalline thin film. **International Journal of Photoenergy**, 4(1), 17-20.
- Birnie, D. (2004). Spin coating technique. In **Sol-gel technologies for glass producers and users**, 49-55.
- Boyo, A., Shitta, M., Oluwa, T. & Adeola, S. 2012. Bitter leaf (*Vernonia amygdalin*) for dye sensitized solar cell. **Trends in Applied Sciences Research**, 7(7), 558-564.
- Britt, J. & Ferekides, C. 1993. Thin-film CdS/CdTe solar cell with 15.8% efficiency. **Applied physics letters**, 62(22), 2851-2852.
- Britton, G. 1992. Natural food colorants. **Carotenoids**, 5(141-182).
- Calogero, G. & Di Marco, G. 2008. Red Sicilian orange and purple eggplant fruits as natural sensitizers for dye-sensitized solar cells. **Solar Energy Materials and Solar Cells**, 92(11), 1341-1346.
- Carvalho, R. F., Takaki, M. & Azevedo, R. A. 2011. Plant pigments: the many faces of light perception. **Acta Physiologiae Plantarum**, 33(2), 241-248.
- Chang, H., Kao, M.-J., Chen, T.-L., Kuo, C.-G., Cho, K.-C. & Lin, X.-P. 2011. Natural sensitizer for dye-sensitized solar cells using three layers of photoelectrode thin films with a Schottky barrier. **American Journal of Engineering and Applied Sciences**, 4(2).

- Chang, H. & Lo, Y.-J. 2010. Pomegranate leaves and mulberry fruit as natural sensitizers for dye-sensitized solar cells. **Solar Energy**, 84(10), 1833-1837.
- Chang, H., Wu, H., Chen, T., Huang, K., Jwo, C. & Lo, Y. 2010. Dye-sensitized solar cell using natural dyes extracted from spinach and ipomoea. **Journal of Alloys and Compounds**, 495(2), 606-610.
- Chitnis, K. 2013. Extraction, Characterization and Application as Natural Dyes of extracts from Terminalia catappa leaf and seed pericarp. **Research Journal of Chemistry and Environment**, 10(1)
- Correa de Oliveira, C., de Siqueira, J., BORGES DE SOUZA, K. & Rezende, U. 1996. Antibacterial activity of rhizomes from Cochlospermum regium: preliminary results. **Fitoterapia (Milano)**, 67(2), 176-177.
- Davies, K. 2004. **Plant pigments and their manipulation**. Blackwell Publishing.
- Dawoud, A. M. 2016. naturl pigments extracted from plant leaves as photosensitizers for dye-sensitized solar cells. **naturl pigments extracted from plant leaves as photosensitizers for dye-sensitized solar cells**.
- Desilvestro, J., Graetzel, M., Kavan, L., Moser, J. & Augustynski, J. 1985. Highly efficient sensitization of titanium dioxide. **Journal of the American Chemical Society**, 107(10), 2988-2990.
- Eshaghi, A. & Aghaei, A. A. 2015. Effect of TiO<sub>2</sub>-graphene nanocomposite photoanode on dye-sensitized solar cell performance. **Bulletin of Materials Science**, 38(5), 1177-1182.
- Fakharuddin, A., Jose, R., Brown, T. M., Fabregat-Santiago, F. & Bisquert, J. 2014. A perspective on the production of dye-sensitized solar modules. **Energy & Environmental Science**, 7(12), 3952-3981.
- Farrell, K. A. 2001. **Synthesis effects on grain size and phase content in the anatase-rutile TiO<sub>2</sub> system**. Worcester Polytechnic Institute Worcester.
- Frank, H. A. & Cogdell, R. J. 1996. Carotenoids in photosynthesis. **Photochemistry and photobiology**, 63(3), 257-264.
- Gómez-Ortíz, N., Vázquez-Maldonado, I., Pérez-Espadas, A., Mena-Rejón, G., Azamar-Barrios, J. & Oskam, G. 2010. Dye-sensitized solar cells with natural dyes

- extracted from achiote seeds. **Solar Energy Materials and Solar Cells**, 94(1), 40-44.
- Gong, J., Sumathy, K., Qiao, Q. & Zhou, Z. 2017. Review on dye-sensitized solar cells (DSSCs): Advanced techniques and research trends. **Renewable and Sustainable Energy Reviews**, 68(234-246).
- Grant, F. 1959. Properties of rutile (titanium dioxide). **Reviews of Modern Physics**, 31(3), 646.
- Grätzel, M. 2003. J Photochem Photobiol C **Photochem Rev** 4: 145 doi: 10.1016. S1389-5567 (03), 00026-00021.
- Grätzel, M. 2005. Solar energy conversion by dye-sensitized photovoltaic cells. **Inorganic chemistry**, 44(20), 6841-6851.
- Green, B. & Parson, W. W. 2003. **Light-harvesting antennas in photosynthesis**. Springer Science & Business Media.
- Green, M. A. 2006. Third generation photovoltaics.
- Green, M. A., Emery, K., Hishikawa, Y. & Warta, W. 2010. Solar cell efficiency tables (version 37). **Progress in photovoltaics: research and applications**, 1(19), 84-92.
- Grotewold, E. 2006. **The science of flavonoids**. Springer.
- Gu, C., Tembrock, L. R., Li, Y., Lu, X. & Wu, Z. 2016. The complete chloroplast genome of queen's crape-myrtle (*Lagerstroemia macrocarpa*). **Mitochondrial DNA Part B**, 1(1), 408-409.
- Gu, P., Yang, D., Zhu, X., Sun, H., Wangyang, P., Li, J. & Tian, H. 2017. Influence of electrolyte proportion on the performance of dye-sensitized solar cells. **AIP Advances**, 7(10), 105219.
- Guerin, V., Magne, C., Pauporté, T., Le Bahers, T. & Rathousky, J. 2010. Electrodeposited nanoporous versus nanoparticulate ZnO films of similar roughness for Dye-Sensitized Solar Cell applications. **ACS applied materials & interfaces**, 2(12), 3677-3685.
- Gupta, M., Makda, S. & Senthil, R. 2018. **The latest trends in synthesis of dye-sensitized solar cells**. IOP Publishing.

- Hadi, A. 2018. **Laser Processing of TiO<sub>2</sub> Films on ITO-glass for Dye-sensitized Solar Cells**. University of Manchester.
- Hanaor, D. A. & Sorrell, C. C. 2011. Review of the anatase to rutile phase transformation. **Journal of Materials science**, 46(4), 855-874.
- He, Y., Du, Z., Ma, S., Cheng, S., Jiang, S., Liu, Y., Li, D., Huang, H., Zhang, K. & Zheng, X. 2016. Biosynthesis, antibacterial activity and anticancer effects against prostate cancer (PC-3) cells of silver nanoparticles using Dimocarpus Longan Lour. peel extract. **Nanoscale research letters**, 11(1), 300.
- Higashino, T. & Imahori, H. 2015. Porphyrins as excellent dyes for dye-sensitized solar cells: recent developments and insights. **Dalton Transactions**, 44(2), 448-463.
- Hossain, M., Biswas, S., Takahashi, T., Kubota, Y. & Fujishima, A. 2008. Influence of direct current power on the photocatalytic activity of facing target sputtered TiO<sub>2</sub> thin films. **Thin Solid Films**, 517(3), 1091-1095.
- Hubka, V. 2015. **Principles of engineering design**. Elsevier.
- Hug, H., Bader, M., Mair, P. & Glatzel, T. 2014. Biophotovoltaics: natural pigments in dye-sensitized solar cells. **Applied Energy**, 115(216-225).
- Ito, S., Murakami, T., Comte, P., Liska, P. & Grätzel, M. 2008. C.; Nazeeruddin, K.; Grätzel, M. **Thin Solid Films**, 516(4613-4619).
- Ito, S., Murakami, T. N., Comte, P., Liska, P., Grätzel, C., Nazeeruddin, M. K. & Grätzel, M. 2008. Fabrication of thin film dye sensitized solar cells with solar to electric power conversion efficiency over 10%. **Thin solid films**, 516(14), 4613-4619.
- Jamalullail, N., Smohamad, I., Nnorizan, M. & Mahmed, N. 2018. **Enhancement of energy conversion efficiency for dye sensitized solar cell using zinc oxide photoanode**. IOP Publishing.
- Jasim, K. E. 2011. Dye sensitized solar cells-working principles, challenges and opportunities. **Solar Cells-Dye-Sensitized Devices**, 8(172-210).
- Jeng, M.-J., Wung, Y.-L., Chang, L.-B. & Chow, L. 2013. Dye-sensitized solar cells with anatase TiO<sub>2</sub> nanorods prepared by hydrothermal method. **International Journal of Photoenergy**, 2013(1)

- Jin, E. M., Park, K.-H., Jin, B., Yun, J.-J. & Gu, H.-B. 2010. Photosensitization of nanoporous TiO<sub>2</sub> films with natural dye. **Physica Scripta**, 2010(T139), 014006.
- Karasovec, U., Berginc, M. & Hocevar, M. 2009. Topic M 2009. **Solar Energy Materials & Solar Cell**, 93(379-381).
- Kay, A. & Graetzel, M. 1993. Artificial photosynthesis. 1. Photosensitization of titania solar cells with chlorophyll derivatives and related natural porphyrins. **The Journal of Physical Chemistry**, 97(23), 6272-6277.
- Khammee, P., Unpaprom, Y., Subhasaen, U. & Ramaraj, R. 2020. Potential evaluation of yellow cotton (*Cochlospermum regium*) pigments for dye sensitized solar cells application. **GJSE**, 2(16-21).
- Khammee, P., Unpaprom, Y., Whangchai, K. & Ramaraj, R. 2020. Comparative studies of the longan leaf pigment extraction as a photosensitizer for dye-sensitized solar cells' purpose. **Biomass Conversion and Biorefinery**, 1-8.
- Kishimoto, S., Maoka, T., Sumitomo, K. & Ohmiya, A. 2005. Analysis of carotenoid composition in petals of calendula (*Calendula officinalis* L.). **Bioscience, biotechnology, and biochemistry**, 69(11), 2122-2128.
- Kong, F.-T., Dai, S.-Y. & Wang, K.-J. 2007. Review of recent progress in dye-sensitized solar cells. **Advances in OptoElectronics**, 2007(1)
- Koyama, Y. & Fujii, R. (1999). Cis-trans carotenoids in photosynthesis: configurations, excited-state properties and physiological functions. In **The photochemistry of carotenoids** (pp. 161-188): Springer.
- Krebs, F. C. 2009. Fabrication and processing of polymer solar cells: A review of printing and coating techniques. **Solar energy materials and solar cells**, 93(4), 394-412.
- Kuang, D., Ito, S., Wenger, B., Klein, C., Moser, J.-E., Humphry-Baker, R., Zakeeruddin, S. M. & Grätzel, M. 2006. High molar extinction coefficient heteroleptic ruthenium complexes for thin film dye-sensitized solar cells. **Journal of the American Chemical Society**, 128(12), 4146-4154.
- Kumara, N., Ekanayake, P., Lim, A., Liew, L. Y. C., Iskandar, M., Ming, L. C. & Senadeera, G. 2013. Layered co-sensitization for enhancement of conversion efficiency of natural dye sensitized solar cells. **Journal of alloys and compounds**, 581(186-191).



- Kumara, N., Lim, A., Lim, C. M., Petra, M. I. & Ekanayake, P. 2017. Recent progress and utilization of natural pigments in dye sensitized solar cells: A review. **Renewable and Sustainable Energy Reviews**, 78(301-317).
- Kushwaha, R., Srivastava, P. & Bahadur, L. 2013. Natural pigments from plants used as sensitizers for TiO<sub>2</sub> based dye-sensitized solar cells. **Journal of Energy**, 2013(1).
- Kutlu, N. 2020. Investigation of electrical values of low-efficiency dye-sensitized solar cells (DSSCs). **Energy**, 199(117222).
- Lee, C.-P., Lin, C.-A., Wei, T.-C., Tsai, M.-L., Meng, Y., Li, C.-T., Ho, K.-C., Wu, C.-I., Lau, S.-P. & He, J.-H. 2015. Economical low-light photovoltaics by using the Pt-free dye-sensitized solar cell with graphene dot/PEDOT: PSS counter electrodes. **Nano Energy**, 18(109-117).
- Lichtenthaler, H. K. 1987. Chlorophylls and carotenoids: pigments of photosynthetic biomembranes. **Methods in enzymology**, 148(350-382).
- Lin, L. Y., Lee, C. P., Tsai, K. W., Yeh, M. H., Chen, C. Y., Vittal, R., Wu, C. G. & Ho, K. C. 2012. Low-temperature flexible Ti/TiO<sub>2</sub> photoanode for dye-sensitized solar cells with binder-free TiO<sub>2</sub> paste. **Progress in Photovoltaics: Research and Applications**, 20(2), 181-190.
- Longo, C., Nogueira, A., De Paoli, M.-A. & Cachet, H. 2002. Solid-state and flexible dye-sensitized TiO<sub>2</sub> solar cells: a study by electrochemical impedance spectroscopy. **The Journal of Physical Chemistry B**, 106(23), 5925-5930.
- Ludin, N. A., Mahmoud, A. A.-A., Mohamad, A. B., Kadhum, A. A. H., Sopian, K. & Karim, N. S. A. 2014. Review on the development of natural dye photosensitizer for dye-sensitized solar cells. **Renewable and Sustainable Energy Reviews**, 31(386-396).
- Luque, A. & Hegedus, S. 2011. **Handbook of photovoltaic science and engineering**. John Wiley & Sons.
- Martí, A. & Luque, A. 2003. **Next generation photovoltaics: High efficiency through full spectrum utilization**. CRC Press.
- Mathew, S., Yella, A., Gao, P., Humphry-Baker, R., Curchod, B. F., Ashari-Astani, N., Tavernelli, I., Rothlisberger, U., Nazeeruddin, M. K. & Grätzel, M. 2014. Dye-

- sensitized solar cells with 13% efficiency achieved through the molecular engineering of porphyrin sensitizers. **Nature chemistry**, 6(3), 242-247.
- Matthews, D., Infelta, P. & Grätzel, M. 1996. Calculation of the photocurrent-potential characteristic for regenerative, sensitized semiconductor electrodes. **Solar Energy Materials and Solar Cells**, 44(2), 119-155.
- Maurya, I. C., Singh, S., Srivastava, P., Maiti, B. & Bahadur, L. 2019. Natural dye extract from *Cassia fistula* and its application in dye-sensitized solar cell: Experimental and density functional theory studies. **Optical Materials**, 90(273-280).
- Mehmood, U., Rahman, S.-u., Harrabi, K., Hussein, I. A. & Reddy, B. 2014. Recent advances in dye sensitized solar cells. **Advances in Materials Science and Engineering**, 2014(1).
- Menning, M. & Aegerter, M. A. 2004. **Sol-Gel Technologies for Glass Producers and Users**. Kluwer Academic Publishers.
- Merzlyak, M., Chivkunova, O., Lehimena, L. & Belevich, N. 1996. Some limitations and potentialities of the spectrophotometric assay of pigments extracted from leaves of higher plants. **Russian Journal of Plant Physiology**, 43(6), 800-809.
- Merzlyak, M., Gitelson, A., Chivkunova, O., Solovchenko, A. & Pogosyan, S. 2003. Application of reflectance spectroscopy for analysis of higher plant pigments. **Russian journal of plant physiology**, 50(5), 704-710.
- Miyasaka, T., Ikegami, M. & Kijitori, Y. 2007. Photovoltaic performance of plastic dye-sensitized electrodes prepared by low-temperature binder-free coating of mesoscopic titania. **Journal of the Electrochemical Society**, 154(5), A455.
- Morton, J. F. & Dowling, C. F. 1987. **Fruits of warm climates**. JF Morton Miami, FL.
- Mubarak, Z., Nursam, N. M., Shobih, S., Hidayat, J. & Tahir, D. 2018. A Comparison of the Utilization of Carbon Nanopowder and Activated Carbon as Counter Electrode for Monolithic Dye-Sensitized Solar Cells (DSSC). **Jurnal Elektronika dan Telekomunikasi**, 18(1), 15-20.
- Narayan, M. & Raturi, A. 2011. Investigation of some common Fijian flower dyes as photosensitizers for dye sensitized solar cells abstract. **Applied Solar Energy**, 47(2), 112.

- Narayan, M. R. 2012. Dye sensitized solar cells based on natural photosensitizers. **Renewable and Sustainable Energy Reviews**, 16(1), 208-215.
- Nazeeruddin, M. K., Kay, A., Rodicio, I., Humphry-Baker, R., Müller, E., Liska, P., Vlachopoulos, N. & Grätzel, M. 1993. Conversion of light to electricity by cis-X2bis (2, 2'-bipyridyl-4, 4'-dicarboxylate) ruthenium (II) charge-transfer sensitizers (X= Cl-, Br-, I-, CN-, and SCN-) on nanocrystalline titanium dioxide electrodes. **Journal of the American Chemical Society**, 115(14), 6382-6390.
- Nishantha, M., Yapa, Y. & Perera, V. 2012. Sensitization of photoelectrochemical solar cells with a natural dye extracted from *Kopsia flavida* fruit. **Proceed Tech Sess**, 28(54-58).
- Nunes, G., Da Silva, M., Resende, U. d. & De Siqueira, J. 2003. Plantas medicinais comercializadas por raizeiros no Centro de Campo Grande, Mato Grosso do Sul. **Revista Brasileira de Farmacognosia**, 13(2), 83-92.
- O'regan, B. & Grätzel, M. 1991. A low-cost, high-efficiency solar cell based on dye-sensitized colloidal TiO<sub>2</sub> films. **nature**, 353(6346), 737-740.
- Padinger, F., Brabec, C., Fromherz, T., Hummelen, J. & Sariciftci, N. S. 2000. Fabrication of large area photovoltaic devices containing various blends of polymer and fullerene derivatives by using the doctor blade technique. **Optoelectronics Review**, 4), 280-283.
- Parida, B., Iniyar, S. & Goic, R. 2011. A review of solar photovoltaic technologies. **Renewable and sustainable energy reviews**, 15(3), 1625-1636.
- Patrocinio, A., Mizoguchi, S., Paterno, L., Garcia, C. & Iha, N. M. 2009. Efficient and low cost devices for solar energy conversion: efficiency and stability of some natural-dye-sensitized solar cells. **Synthetic Metals**, 159(21-22), 2342-2344.
- Perez, M. & Perez, R. 2015. Update 2015--A Fundamental Look at Supply Side Energy Reserves for the Planet. **Natural Gas**, 2(9), 215.
- Pinsly, J. B. (2001). **Dip coating process**: Google Patents.
- Prakash, T. 2012. Review on nanostructured semiconductors for dye sensitized solar cells. **Electronic materials letters**, 8(3), 231-243.
- Puspitasari, N., Adawiyah, S. R., Fajar, M. N., Yudoyono, G., Rubiyanto, A. & Endarko, E. 2017. Pengaruh jenis katalis pada elektroda pembanding terhadap efisiensi dye

- sensitized solar cells dengan klorofil sebagai dye sensitizer. **Jurnal Fisika dan Aplikasinya**, 13(1), 30-33.
- Radwan, I. M. 2015. Dye sensitized solar cells based on natural dyes extracted from plant roots. **Dye Sensitized Solar Cells Based on Natural Dyes Extracted from Plant Roots**.
- Rajan, A. K. & Cindrella, L. 2019. Studies on new natural dye sensitizers from Indigofera tinctoria in dye-sensitized solar cells. **Optical Materials**, 88(39-47).
- Rekha, M., Kowsalya, M., Ananth, S., Vivek, P. & Jauhar, R. M. 2019. Current–voltage characteristics of new organic natural dye extracted from Terminalia chebula for dye-sensitized solar cell applications. **Journal of Optics**, 48(1), 104-112.
- Richards, B. S. 2002. **Novel uses of titanium dioxide for silicon solar cells**. Center for Photovoltaic Engineering.
- Ritchie, R. J. 2006. Consistent sets of spectrophotometric chlorophyll equations for acetone, methanol and ethanol solvents. **Photosynthesis research**, 89(1), 27-41.
- Ruhane, T., Islam, M. T., Rahaman, M. S., Bhuiyan, M., Islam, J. M., Newaz, M., Khan, K. & Khan, M. A. 2017. Photo current enhancement of natural dye sensitized solar cell by optimizing dye extraction and its loading period. **Optik**, 149(174-183).
- Ruiz-Anchondo, T., Flores-Holguín, N. & Glossman-Mitnik, D. 2010. Natural carotenoids as nanomaterial precursors for molecular photovoltaics: a computational DFT study. **Molecules**, 15(7), 4490-4510.
- Ruiz-Anchondo, T. & Glossman-Mitnik, D. 2009. Computational characterization of the  $\beta$ ,  $\beta$ -carotene molecule. **Journal of Molecular Structure: THEOCHEM**, 913(1-3), 215-220.
- Saelim, N.-o., Magaraphan, R. & Sreethawong, T. 2011. Preparation of sol–gel TiO<sub>2</sub>/purified Na-bentonite composites and their photovoltaic application for natural dye-sensitized solar cells. **Energy conversion and management**, 52(8-9), 2815-2818.
- Saravanan, R. 2019. **Emerging nanostructured materials for energy and environmental science**. Springer.

- Sato, M. & Fujii, I. (1978). **Spin coating process**: Google Patents.
- Sayama, K., Sugihara, H. & Arakawa, H. 1998. Photoelectrochemical properties of a porous Nb<sub>2</sub>O<sub>5</sub> electrode sensitized by a ruthenium dye. **Chemistry of Materials**, 10(12), 3825-3832.
- Selopal, G. S., Memarian, N., Milan, R., Concina, I., Sberveglieri, G. & Vomiero, A. 2014. Effect of blocking layer to boost photoconversion efficiency in ZnO dye-sensitized solar cells. **ACS applied materials & interfaces**, 6(14), 11236-11244.
- Semalti, P. & Sharma, S. N. 2020. Dye Sensitized Solar Cells (DSSCs) Electrolytes and Natural Photo-Sensitizers: A Review. **Journal of nanoscience and nanotechnology**, 20(6), 3647-3658.
- Shalini, S., Prasanna, S., Mallick, T. K. & Senthilarasu, S. 2015. Review on natural dye sensitized solar cells: operation, materials and methods. **Renewable and Sustainable Energy Reviews**, 51(1306-1325).
- Sharma, K., Sharma, V. & Sharma, S. 2018. Dye-sensitized solar cells: fundamentals and current status. **Nanoscale research letters**, 13(1), 381.
- Siddiquee, S., Melvin, G. J. H. & Rahman, M. 2019. **Nanotechnology: Applications in Energy, Drug and Food**. Springer.
- Sinha, K., Saha, P. D. & Datta, S. 2012. Extraction of natural dye from petals of Flame of forest (*Butea monosperma*) flower: Process optimization using response surface methodology (RSM). **Dyes and Pigments**, 94(2), 212-216.
- Smestad, G. P. 1998. Education and solar conversion:: demonstrating electron transfer. **Solar Energy Materials and Solar Cells**, 55(1-2), 157-178.
- Snaith, H. J. & Grätzel, M. 2006. The role of a “Schottky Barrier” at an electron-collection electrode in solid-state dye-sensitized solar cells. **Advanced Materials**, 18(14), 1910-1914.
- Sokolský, M. & Cirák, J. 2010. Dye-sensitized solar cells: materials and processes. **Acta Electrotechnica et Informatica**, 10(3), 78-81.
- Solon, S., Carollo, C. A., Brandão, L. F. G., Macedo, C. d. S. d., Klein, A., Dias-Junior, C. A. & Siqueira, J. M. d. 2012. Phenolic derivatives and other chemical compounds from *Cochlospermum regium*. **Química Nova**, 35(6), 1169-1172.



- Solovchenko, A., Chivkunova, O., Merzlyak, M. & Reshetnikova, I. 2001. A spectrophotometric analysis of pigments in apples. **Russian Journal of Plant Physiology**, 48(5), 693-700.
- Spath, M., Sommeling, P., van Roosmalen, J. & Smit, H. 2003. JP; van der Burg, NPG; Mahieu, DR; Bakker, NJ; Kroon, JM. **Prog. PhotoVoltaics**, 11(3), 207-220.
- Şükran, D., GÜNEŞ, T. & Sivaci, R. 1998. Spectrophotometric determination of chlorophyll-A, B and total carotenoid contents of some algae species using different solvents. **Turkish Journal of Botany**, 22(1), 13-18.
- Sumanta, N., Haque, C. I., Nishika, J. & Suprakash, R. 2014. Spectrophotometric analysis of chlorophylls and carotenoids from commonly grown fern species by using various extracting solvents. **Res J Chem Sci**, 2231(606X).
- Tennakone, K., Kumara, G. R., Kottegoda, I. R. & Perera, V. P. 1999. An efficient dye-sensitized photoelectrochemical solar cell made from oxides of tin and zinc. **Chemical Communications**, 1), 15-16.
- Tributsch, H. 1972. Reaction of excited chlorophyll molecules at electrodes and in photosynthesis. **Photochemistry and Photobiology**, 16(4), 261-269.
- Vachali, P. P., Li, B., Besch, B. M. & Bernstein, P. S. 2016. Protein-flavonoid interaction studies by a Taylor dispersion surface plasmon resonance (SPR) Technique: A novel method to assess biomolecular interactions. **Biosensors**, 6(1), 6.
- Veerappan, G., Bojan, K. & Rhee, S.-W. 2012. Amorphous carbon as a flexible counter electrode for low cost and efficient dye sensitized solar cell. **Renewable Energy**, 41(383-388).
- Wang, X.-F., Kitao, O., Hosono, E., Zhou, H., Sasaki, S.-i. & Tamiaki, H. 2010. TiO<sub>2</sub>-and ZnO-based solar cells using a chlorophyll a derivative sensitizer for light-harvesting and energy conversion. **Journal of Photochemistry and Photobiology A: Chemistry**, 210(2-3), 145-152.
- Wang, X.-F., Xiang, J., Wang, P., Koyama, Y., Yanagida, S., Wada, Y., Hamada, K., Sasaki, S.-i. & Tamiaki, H. 2005. Dye-sensitized solar cells using a chlorophyll a derivative as the sensitizer and carotenoids having different conjugation lengths as redox spacers. **Chemical physics letters**, 408(4-6), 409-414.

- Watson, T., Mabbett, I., Wang, H., Peter, L. & Worsley, D. 2011. Ultrafast near infrared sintering of TiO<sub>2</sub> layers on metal substrates for dye-sensitized solar cells. **Progress in Photovoltaics: Research and Applications**, 19(4), 482-486.
- Wongcharee, K., Meeyoo, V. & Chavadej, S. 2007. Dye-sensitized solar cell using natural dyes extracted from rosella and blue pea flowers. **Solar Energy Materials and Solar Cells**, 91(7), 566-571.
- Yildiz, Z., Atilgan, A., Atli, A., Özel, K., Altinkaya, C. & Yildiz, A. 2019. Enhancement of efficiency of natural and organic dye sensitized solar cells using thin film TiO<sub>2</sub> photoanodes fabricated by spin-coating. **Journal of Photochemistry and Photobiology A: Chemistry**, 368(23-29).
- Yue, G., Wu, J., Xiao, Y., Huang, M., Lin, J., Fan, L. & Lan, Z. 2013. Platinum/graphene hybrid film as a counter electrode for dye-sensitized solar cells. **Electrochimica Acta**, 92(64-70).
- Yun, S., Qin, Y., Uhl, A. R., Vlachopoulos, N., Yin, M., Li, D., Han, X. & Hagfeldt, A. 2018. New-generation integrated devices based on dye-sensitized and perovskite solar cells. **Energy & Environmental Science**, 11(3), 476-526.
- Zainudin, S. N. F., Markom, M., Abdullah, H., Adami, R. & Tasirin, S. M. 2011. Supercritical anti-solvent process for the enhancement of dye-sensitized solar cell efficiency: A review. **Asian J Appl Sci**, 4(331-342).
- Zhang, Q. & Cao, G. 2011. Nanostructured photoelectrodes for dye-sensitized solar cells. **Nano Today**, 6(1), 91-109.
- Zhang, Q., Dandeneau, C. S., Zhou, X. & Cao, G. 2009. ZnO nanostructures for dye-sensitized solar cells. **Advanced Materials**, 21(41), 4087-4108.
- Zhao, J., Wang, A. & Green, M. A. 1999. 24. 5% Efficiency silicon PERT cells on MCZ substrates and 24. 7% efficiency PERL cells on FZ substrates. **Progress in Photovoltaics: Research and Applications**, 7(6), 471-474.
- Zulkifli, A., Kento, T., Daiki, M. & Fujiki, A. (2015). The basic research on the dye-sensitized solar cells (DSSC). **J Clean Energy Technol** 3: 382–387.

# APPENDIX A

## PUBLICATIONS

Biomass Conversion and Biorefinery  
<https://doi.org/10.1007/s13399-020-01060-x>

ORIGINAL ARTICLE



### Comparative studies of the longan leaf pigment extraction as a photosensitizer for dye-sensitized solar cells' purpose

Phitchaphorn Khammee<sup>1,2</sup> · Yuwalee Unpaprom<sup>2,3</sup> · Kanda Whangchai<sup>4</sup> · Rameshprabu Ramaraj<sup>1,2</sup>

Received: 10 August 2020 / Revised: 24 September 2020 / Accepted: 2 October 2020  
© Springer-Verlag GmbH Germany, part of Springer Nature 2020

#### Abstract

Renewable energy is the main key to production, long-term environmental sustainability, and safe and inexhaustible energy source. One of the interesting devices of renewable energy that has received considerable attention as an alternative technology is dye-sensitized solar cells (DSSCs), which is considered the third generation of solar cells. These solar cells can convert solar radiation into electric current by using natural pigments as sensitizers by using natural pigments in the regulation of solar energy, which is similar to the photosynthesis process of the plant. Thus, this study results recommend that the fresh longan extraction method (original) has the highest pigment extraction yields of chlorophyll-a, chlorophyll-b, and carotenoids that were  $88.055 \pm 0.424$   $\mu\text{g/ml}$ ,  $26.178 \pm 0.343$   $\mu\text{g/ml}$ , and  $16.307 \pm 0.564$   $\mu\text{g/ml}$ , respectively, and suitable for preparation as a photosensitizer for the DSSC production. Dye addition to semiconductor improves the basicity of titanium dioxide ( $\text{TiO}_2$ ), leading to enhanced dye adsorption and UV-vis spectroscopy measurements confirmed. Dye absorption range is 400–700 nm visible on a solar spectrum and significant adsorption onto the semiconductor surface. The scanning electron microscope (SEM) and X-ray spectroscopy (EDX) analysis described that the extract encourages the formation of large crystals of the dye into the layers of  $\text{TiO}_2$ . Therefore, the use of these extracts would increase efficiency and reduce production costs for the manufacture of DSSC.

**Keywords** Longan leaves · Pigment extraction · Chlorophylls · Carotenoid · DSSC preparation

#### 1 Introduction

Photosynthetic pigments in plants, algae, and some bacteria are vital to the survival of the plant, animal, and other kingdoms in nature [1–3]. The flowers, leaves, and fruits show different types and comprise of various pigments that can be promptly extricated and utilized for dye sensitizer solar cell (DSSC) establishment. These pigments function as dye sensitizers, and they play a significant role in DSSC by absorbing light and supplying electrons to the semiconductor matrixes in

the cell. Thus, dye sensitizers fill in as the solar energy absorber in DSSC, whose attribute will have much impact on the light collecting efficiency and the general photoelectric change effectiveness. The common choices of dyes are metal complexes and organic or natural dyes [4, 5]. Natural pigments have been consulted as promising elective sensitizer colors for DSSC due to their straightforward readiness system, low cost, complete biodegradation, simple accessibility, virtue grade, ecological neighborliness, etc., a high decrease of noble metal and substance amalgamation cost [6, 7].

Plant pigmentation produces from the electronic structure of colors, responding with daylight to change the wavelengths. The particular shading depends on the limits of the watcher. The pigment can be depicted by the most extreme assimilation wavelength ( $\lambda$  max) [8]. Several critical subjects of research have been a study on many pigment (natural dyes) use sensitizers in DSSC, such as pigments, flavonoids, cyanine, and tannin. Recently, the DSSCs are receiving widespread attention because it can replace the use of silicon-based solar cells. Also, it is easy to produce. There are no complicated steps and can produce the panel with flexibility solar cell type uses light-sensitive dye molecules as the light

✉ Rameshprabu Ramaraj  
rrameshprabu@gmail.com; rameshprabu@mju.ac.th

<sup>1</sup> School of Renewable Energy, Maejo University, Chiang Mai 50290, Thailand

<sup>2</sup> Sustainable Resources and Sustainable Engineering Research Lab, Maejo University, Chiang Mai 50290, Thailand

<sup>3</sup> Program in Biotechnology, Faculty of Science, Maejo University, Chiang Mai 50290, Thailand

<sup>4</sup> Center of Excellence in Bioresources for Agriculture, Industry and Medicine, Chiang Mai University, Chiang Mai 50200, Thailand

Published online: 16 October 2020

Springer

Content courtesy of Springer Nature, terms of use apply. Rights reserved.



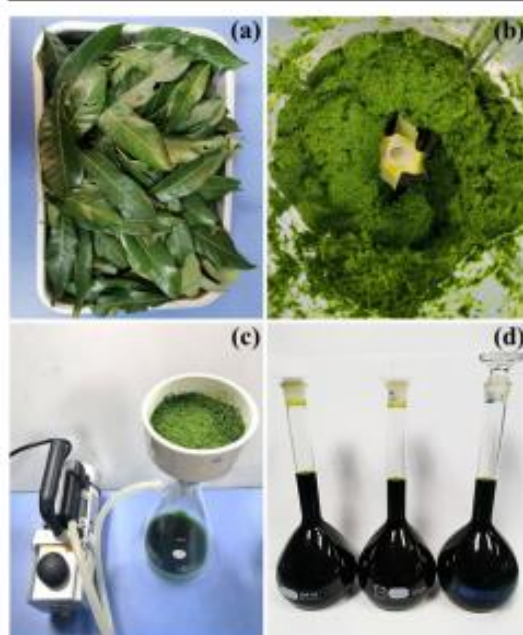


**Fig. 1** The pigment extraction processes (a–d)

absorption and free charging medium which can conduct electricity. The structure of the dye-sensitized solar cell consists of the layers of titanium dioxide; the dye and the electrolyte layers are between two electrical sections. The fabrication of DSSC consists of two layers of fluorine-doped tin oxide (FTO)-coated glass that sandwich a photoanode, a counter platinum electrode, and a liquid electrolyte containing an iodide/tri-iodide redox couple [9].

The photoanode is made of layers of dye-sensitized full-band semiconductor oxides. These sensitizers are photoactive molecules from natural and organic dyes. Also, it has low production cost, ease of fabrication, and reasonable energy

conversion efficiencies; the enhancement of dye-sensitized solar cells has been broadly studied in the past decades [10]. That provides more economic benefits and uses materials that are more environmentally friendly than traditional solar cells. It has efficient energy diversion 11% and is being developed to be more efficient in designing cells to have high efficiency that depends on the suitability and stability and durability of the solution. Electrolyte (I<sup>-</sup>/I<sub>3</sub><sup>-</sup>) mixed with organic substances is another option, and the ability to achieve success is acetonitrile, propylene carbonate, and ethylene carbonate.

On the other hand, the organic solution is volatile and can work in DSSC. Additionally, the DSSCs also have the advantage of producing more energy in diffuse light conditions for transportation systems and architecture [4, 5]. Natural dyes are colors that are extracted from raw materials from different parts of plants. Therefore, the extraction process was significant to lead the further dye production stage. As required, with different production methods, one of the most popular products is DSSC dyes. A source of raw materials for DSSC dyes that are commonly used is plant pigments, mainly chlorophylls and carotenoids which make use of local resources to benefit and the highest and transferring local wisdom.

The use of several natural dyes and different coating techniques for the semiconductor oxides has been in the focus of the research. Natural pigments, such as anthocyanin, carotenoid, chlorophyll, and flavonoid, from various plants, have been tested [4, 5, 11]. The pigments were used separately or as mixtures and have shown promising results, both inefficiency and broad light absorbance properties [4, 5]. The objective of this study is to utilize tropical plants as *Dimocarpus longan* to produce natural dyes. To produce environmentally friendly, easy to produce, and long-lasting, renewable energy sources, the enhancement of DSSCs is a crucial factor.

## 2 Materials and methods

### 2.1 Material collection

Longan (*Dimocarpus longan*) was collected from Energy Research Center, Maejo University, Chiang Mai, Thailand. The longan leaves were transferred to Saowaran Nittayawattana Building, Faculty of Science, Maejo University, Chiang Mai, Thailand. After that, longan leaves were washed with tap water and then blotted dry with paper toweling. Then, the leaves were removed from the middle parts to prepare for the pigment extraction process.

### 2.2 Pigment extraction and evaporation processes

The extraction process was adopted by Sumanta et al. [12] and modified. For the extraction, 100 g of longan leaves was used and methanol was used as a solvent for the extraction

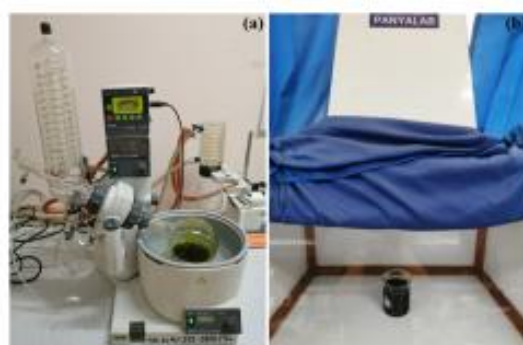
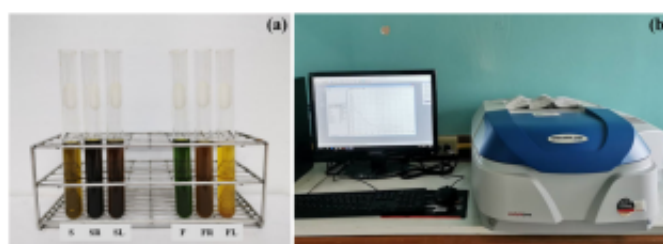


**Fig. 2** The evaporation processes: a rotary evaporator and b laminar airflow

**Fig. 3** **a** Longan leaf pigment extracted and evaporated. **b** Longan leaf pigment measures the absorbance wavelength by using a UV-visible spectrophotometer



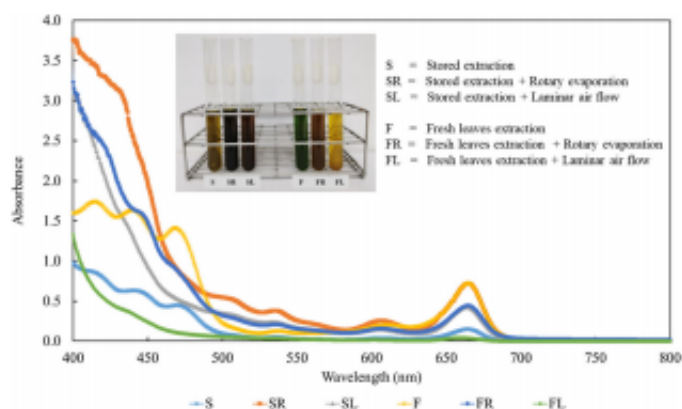
procedure. After that, the 100 g of longan leaves is mixed with methanol 250 ml by using a blender and set the time for 10 min for this process. Subsequently, the vacuum filter was applying for separated solid and liquid. Afterward, the pigment extraction was adjusted the volume to 500 ml in a volumetric flask. The experiment was operated with triplications, and the experiment processes are shown in Fig. 1. Furthermore, prepared extracts were stored in the refrigerator at 4 °C for 4 months to avoid light exposure.

This research has evaporated the pigment extraction from longan leaves from two methods: using a rotary evaporator and laminar airflow and then using the fresh pigment and pigment extracted, which is stored for 4 months. For the evaporation processes, 200 ml of pigment extracted (fresh and stored) was used for evaporation from the rotary evaporator and laminar airflow, which is evaporated until the volume of natural pigment is 40 ml. By the rotary evaporator, the temperature was established around 40–45 °C and in the dark at room temperature for laminar airflow. The evaporation processes are shown in Fig. 2.

### 2.3 Pigment analysis and characterization

The pigment extracted and evaporated from longan leaves was measured using the absorbance wavelength by using

**Fig. 4** UV-Vis analysis of longan leaves with difference condition, which is stored extraction (S), stored extraction + rotary evaporation (SR), stored extraction + laminar airflow (SL), fresh leaf extraction (F), fresh leaf extraction + rotary evaporation (FR), and fresh leaf extraction + laminar airflow (FL)



a UV-visible spectrophotometer (SPECORD 200 PLUS, Analytik Jena, Germany), as shown in Fig. 3. Analysis of the determination of chlorophylls (chlorophyll a (Chl-a) and chlorophyll b (Chl-b)) and carotenoid content by using Eqs. 1–3. The characterization of the samples (TiO<sub>2</sub> dye/FTO composite films with dye immersion methods consists of fresh leaves extraction, stored extraction and stored extraction + laminar airflow) was examined under the scanning electron microscope (SEM) for the determination of the morphology. Moreover, the energy-dispersive X-ray spectroscopy (EDX) analyzed the elemental composite of the samples.

The amount of chlorophyll a

$$= (12.25 \times A_{663} - 2.79 \times A_{645}) \times DF \quad (1)$$

The amount of chlorophyll b

$$= (21.50 \times A_{645} - 5.10 \times A_{663}) \times DF \quad (2)$$

The amount of carotenoids

$$= \frac{(1000 \times A_{470} - 1.43 \times C_a - 35.87 \times C_b) \times DF}{205} \quad (3)$$



**Table 1** The amount of pigment extract from longan leaves

Methods	The amount of pigments ( $\mu\text{g/ml}$ )		
	Chlorophyll-a	Chlorophyll-b	Carotenoids
S	15.500 $\pm$ 0.519	8.285 $\pm$ 0.126	8.440 $\pm$ 0.225
SR	85.778 $\pm$ 0.287	19.202 $\pm$ 0.494	13.601 $\pm$ 0.845
SL	50.138 $\pm$ 0.198	12.257 $\pm$ 0.202	10.420 $\pm$ 0.327
F	88.055 $\pm$ 0.424	26.178 $\pm$ 0.343	16.307 $\pm$ 0.564
FR	47.571 $\pm$ 0.592	14.461 $\pm$ 0.356	13.184 $\pm$ 0.563
FL	4.766 $\pm$ 0.197	2.271 $\pm$ 0.127	6.133 $\pm$ 0.300

## 2.4 Statistical analysis

Data are reported as mean  $\pm$  SE from triplicate observations. Significant differences between means were analyzed. All statistical analyses were performed using SPSS Version 20.0. A correlation was assumed significant when  $P < 0.05$ .

## 3 Results and discussion

### 3.1 Analysis of the absorption wavelength of pigment extraction

In this study, the absorption qualification of the pigment extraction from longan leaves were examined with different conditions. An aliquot of the natural dye extract was diluted by

**Fig. 5** The amount of pigment extract from longan leaves with different methods, which is stored extraction (S), stored extraction + rotary evaporation (SR), stored extraction + laminar airflow (SL), fresh leaf extraction (F), fresh leaf extraction + rotary evaporation (FR), and fresh leaf extraction + laminar airflow (FL)

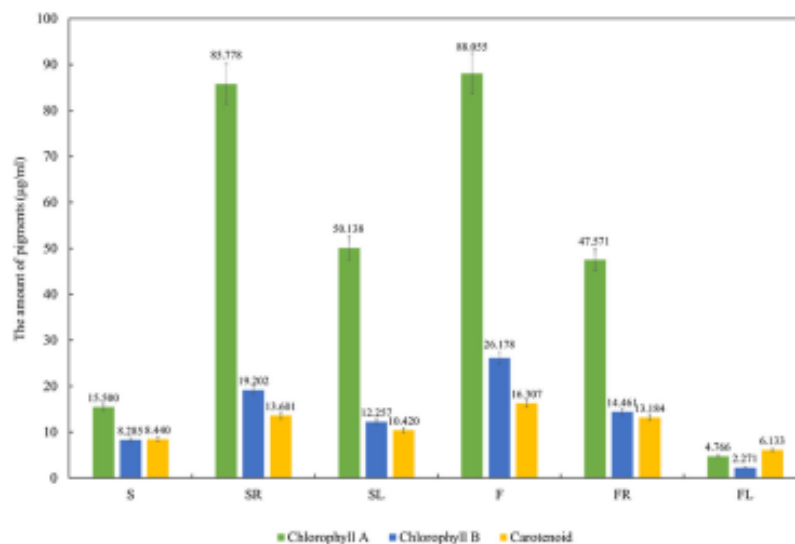


**Fig. 6** Scanning electron micrographs of morphological characteristics of  $\text{TiO}_2$  dye/FTO composite films with dye immersion method consists of (a-1) fresh leaf extraction (F), (b-1) stored extraction (S), and (c-1) stored extraction + laminar airflow (SL) and (a-2) fresh leaf extraction (F), (b-2) stored extraction (S), and (c-2) stored extraction + laminar airflow (SL)

methanol and was examined by the UV-Vis spectrophotometer that has wavelength between 400 and 800 nm, as shown in Fig. 4. The results show that the fresh leaf extraction (F) had the highest absorbance in the visible light wavelength of  $\sim$  640–680 nm, with a wide peak at 664 nm, followed by stored extraction + rotary evaporation (SR), fresh leaf extraction rotary evaporation (FR), stored extraction laminar airflow (SL), stored extraction (S), and fresh leaf extraction laminar airflow (FL), respectively. The result matches the standard absorption wavelength of chlorophyll, the main peak at 662–666 nm and chlorophyll b the shoulder near 650 nm; both were present in the red band of the absorption wavelength. In the blue region, visible absorption wavelength between 430 and 440 nm and 470 and 480 nm is the light absorption by chlorophyll and carotenoids [13–15].

Moreover, the consideration of the absorption wavelength of carotenoid pigments in the blue region of the spectrum is considerably sophisticated due to an overlapping absorption of chlorophyll appear in most plant tissues [16]. However, the absorption wavelength peak of carotenoids is present at 420, 450, and 480 nm [13]. The fresh leaf extraction had three absorption peaks at 415 nm, 440 nm, and 470 nm, which is similar to the functional group of carotenoids. Consequently, the pigment extraction from longan leaves that consist of Chl-a, Chl-b, and carotenoids can be considering as investigation dye sensitizer material for the fabrication DSSC.

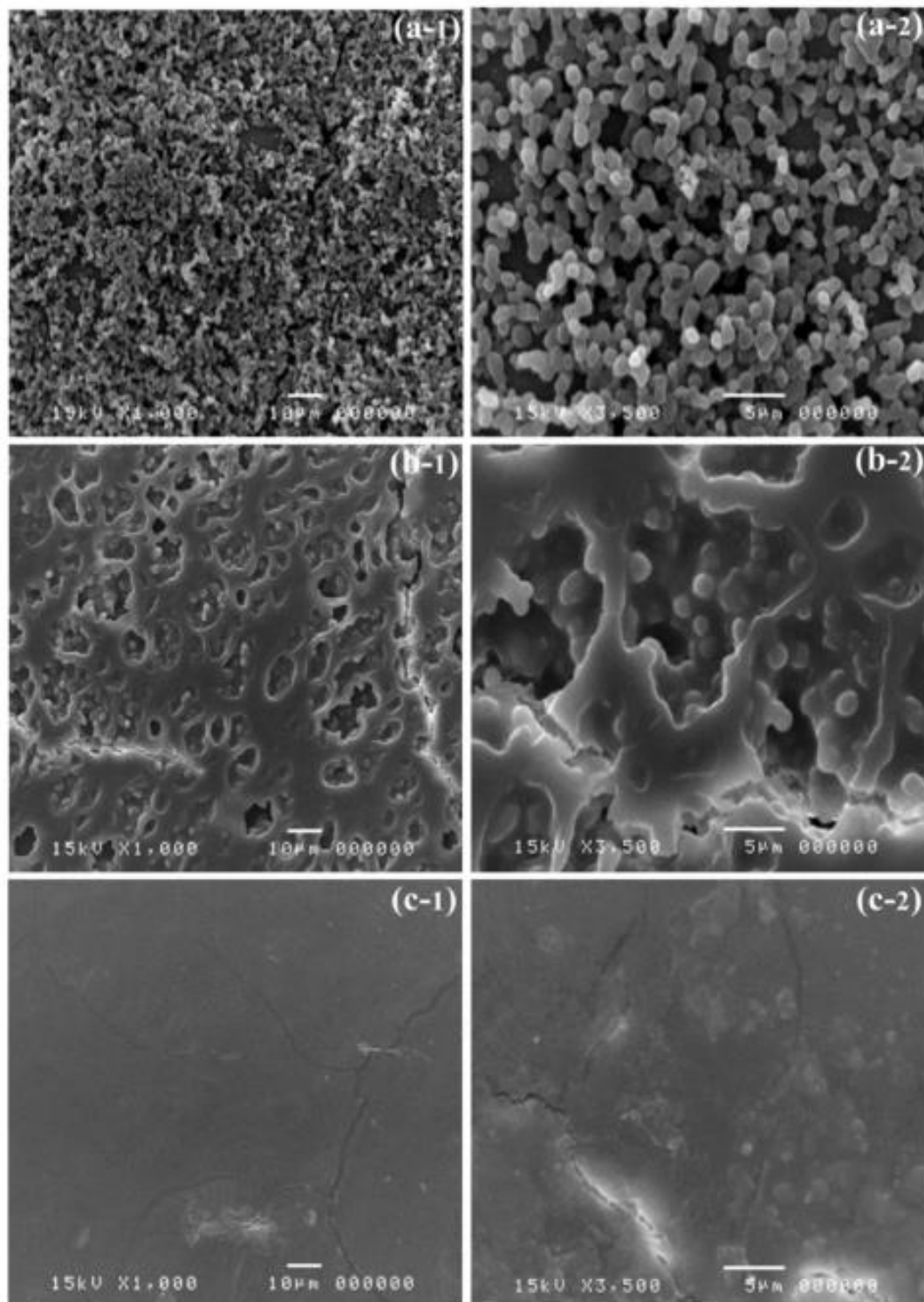


**Table 2** The elemental composition of TiO<sub>2</sub> dye/FTO composite films with dye immersion methods consists of fresh leaf extraction and stored extraction + laminar airflow (SL)

Methods	Element	Weight %	Atomic %
F (spectrum 1) (a-1,2)	C, K	64.60	72.28
	O, K	31.80	26.71
	Ti, K	3.60	1.01
F (spectrum 2) (b-1,2)	C, K	28.56	41.97
	O, K	43.15	47.61
	Ti, K	28.29	10.42
SL (spectrum 1) (a-1,2)	C, K	52.59	59.64
	O, K	47.41	40.36

### 3.2 The pigment extraction content and estimation of longan leaves

For the extraction process, methanol is an excellent solvent extracting for chlorophylls, especially from recalcitrant vascular plants and algae [17]. The amount of pigment extract from longan leaves with different methods of testing is shown in Fig. 5 and Table 1, and it was observed that the pigment extract is mostly composed of Chl-a. The amount of Chl-a from fresh leaf extraction (F) has the highest Chl-a with  $88.055 \pm 0.424 \mu\text{g/ml}$ , which is similar to the stored extraction + rotary evaporation (SR) with  $85.778 \pm 0.287 \mu\text{g/ml}$ . However, the amount of Chl-b and carotenoids of fresh leaf extraction (F) has the highest content

than another method, with is  $26.178 \pm 0.343 \mu\text{g/ml}$  and  $16.307 \pm 0.564 \mu\text{g/ml}$ , respectively. Usually, the most reliable results of the extraction process were to examine extraction. If stored pigment extraction is inevitable, it must be stored under normal condition, incapable stored for a very long time [18]. The result of the experimental of Negi et al. [18] has shown that the amaranth and fenugreek leaves had losses  $\beta$ -carotene ranged from 46.5 to 85.0% and 24.0 to 73.0%, respectively, depending on period time and conditions of stored. Moreover, increased temperatures and reduced humidity in the storage room have an effect that is able to reduce the total chlorophyll content [18].

Wasmund et al. [19] was an experiment for two combinations of essence which is (1) instant extraction and measurement compared with storage and (2) stored extract comparison with the storage of filters for the same time periods (3 months) and at the same temperature ( $-20^\circ\text{C}$ ). The result has shown that the natural phytoplankton sample, the Chl-a yield, was inconsequentially reduced after stored extracts, but stored filters were stalwartly reduced compared with instantly measured data. Therefore, fresh leaf extraction is a more reliable method for the extraction process [17].

### 3.3 Morphological analysis

The chemical adsorption of natural dyes becomes possible because of the condensation of hydroxyl and methoxy protons with the hydroxyl groups on nanostructured TiO<sub>2</sub>. The

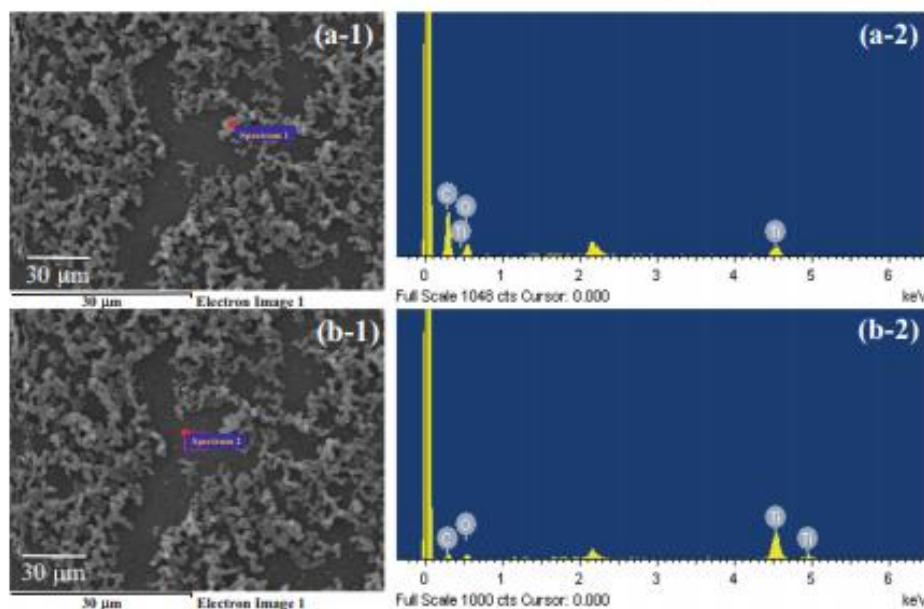
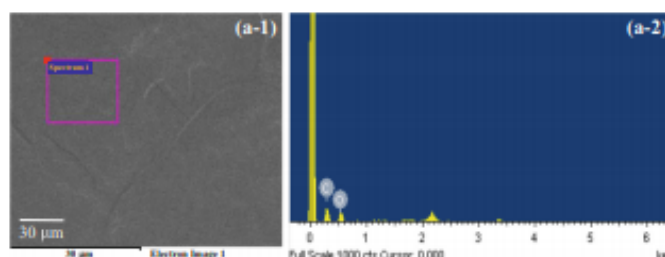


**Fig. 7** The energy-dispersive X-ray spectroscopy (EDX) analysis of TiO<sub>2</sub> dye/FTO composite films with dye immersion method of (a-1,2) and (b-1,2) fresh leaf extraction (F)



**Fig. 8** The energy-dispersive X-ray spectroscopy (EDX) analysis of TiO<sub>2</sub> dye/FTO composite films with dye immersion method of (a-1,2) stored extraction + laminar airflow (SL)



morphological features of prepared pigments of the longan leaves and TiO<sub>2</sub> powders were examined using field emission scanning electron microscopy (SEM). The morphology of TiO<sub>2</sub> dye/FTO composite films is presented in Fig. 6. SEM images were shown in a variety of particle morphologies, including cubic, acicular, and scalenohedral. These morphologies are chosen to impart specific end-use properties such as smoothness, bulk, and enhanced opacity. The morphology of composite films with dye consists of fresh leaf extraction (a-1), stored extraction (b-1), and stored extraction + laminar airflow at a total magnification of  $\times 1000$ . Furthermore, the fresh leaf extraction (a-2), stored extraction (b-2), and stored extraction + laminar airflow (c-2) at a total magnification of  $\times 3500$  were shown in the same figure with spherical, coagulate grain morphology which can be predicted; it is the pigment of the longan leaves.

The most important characteristics of natural pigments on a renewable energy perspective are cost, color, brightness, and opacifying power, as suggested by the size of their scattering coefficient [4, 5]. Usually, the highest optically performing pigments have the smallest particle size, and highest refractive index, brightness, and scattering coefficient. The chemical adsorption of natural dyes becomes possible because of the condensation of hydroxyl and methoxy protons with the hydroxyl groups on the surface of nanostructured titanium dioxide (TiO<sub>2</sub>) [20]. The results of the SEM image show that composites of TiO<sub>2</sub> dye (F)/FTO films (a-1,2) have a spherical, coagulate grain morphology which can be predicted; it is pigment of the longan leaves.

EDX analyzed for determining dye, and TiO<sub>2</sub> was measured. EDS was used to test elemental contents. The results are shown in Fig. 7 (a-1,2; b-1,2), and feature details are presented in Table 2. EDX confirmed the elemental analysis of the TiO<sub>2</sub> nanoparticles and natural dyes. This can be proven from the EDX results, which show an increase in the number of molecules deposited in TiO<sub>2</sub> molecules. The atomic ratio for the prepared TiO<sub>2</sub> and dyes (Fig. 7, a-1,2), the mass carbon (C), oxygen (O), and titanium (Ti), were 72.28, 26.71, and 1.01%, respectively. Also, in Fig. 7, b-1,2 mass (%) of C, O, and Ti was 41.97, 47.61, and 10.42%, respectively.

Furthermore, only in Fig. 8, a-1,2 mass of C and O, and Ti was 59.64 and 40.36%. From the detailed observation in Fig.

6, it is found that the time (stored pigment extracted) and temperature affects the quality and stability of the pigment. Figure 7 illustrates that over time, the morphology of the pigment was changed with clustering and forming a homogeneous mass while the pigments were completely homogeneous by coating the surface of TiO<sub>2</sub>.

On the other hand, Fig. 8 shows that elemental composition only has carbon and oxygen. Usually, TiO<sub>2</sub> shows the characteristic spectrum with its fundamental absorption of Ti–O bond in the UV region between 320 and 400 nm, with the characteristic peak around 350 nm (band edge) for TiO<sub>2</sub>. These depend on the generation of highly reactive free radicals, such as the hydroxyl radical (HO•), useful in degrading organic contaminants. The HO• can be produced by different processes, photocatalysis with semiconductor and light [21]. Also, the signal characteristic bands of C=O (carbonyl) and C–O and stretching vibration can be observed. Whereas naturally prepared pigment dye exhibits maximum absorption at 413 and 665 nm in the visible region. Chlorophylls and carotenoids, which act as an effective photosensitizer in photosynthesis of green plant, have an absorption maximum at 670 nm; thus, it is an attractive potential compound as a photosensitizer in the visible region.

Finally, the spectrophotometric measurements of the pigments of the longan leaf dyes in solution and on a TiO<sub>2</sub> substrate were carried out in order to assess changes in the status of the dyes. It may be summed up from this study presented that longan leaf is one of the prominent fibers used mostly. The reactive dye is mostly used for the dyeing of cotton, which can be bonded. The longan leaves can be dyed by both exhaust and continuous methods. Movahedi et al. [22] stated that sensitizers were quickly regenerated and the redox mediator efficiently captures the dye cations. Furthermore, organic dyes are suitable for DSSC. To increase the power conversion efficiency, many efforts, such as the synthesis of new materials and structure optimization, have been devoted to further commercialization. Dye-sensitized solar cells have engrossed a great deal of interest, as they offer high energy conversion efficiencies due to low cost, ease of assembling with the flexibility of renewable energy preparation, and environmentally friendly.

## 4 Conclusion

In this study, total pigments were extracted from longan leaves. The extractions contain chlorophyll and carotenoid pigments. These extracted photosynthetic pigments as natural dyes were evaluated for solar cells. The elemental analysis of the TiO<sub>2</sub> nanoparticles and natural dyes was confirmed by using the energy-dispersive X-ray spectroscopy. The SEM results clearly illustrated surface characteristics of natural dye and TiO<sub>2</sub>, and it was observed that the samples were almost the granular particles and porous. Moreover, this study suggested that chlorophylls and carotenoids have good potential to serve as photosensitizers in dye-sensitized solar cells. Additionally, they are inexpensive, non-toxic, environmentally sustainable, easily found, and easy to use as sensitizers.

**Acknowledgments** The authors gratefully acknowledged the School of Renewable Energy, Program in Biotechnology, Energy Research Center and the Department of Graduate Studies, Office of Academic Administration and Development, Maejo University, Chiang Mai, Thailand, for the research fund and facilities to accomplish this experimental study. The authors also thank Center of Excellence in Bioresources for Agriculture, Industry and Medicine, Chiang Mai University, Chiang Mai, Thailand for additional experimental support.

## Compliance with ethical standards

**Conflict of interest** The authors declare that they have no conflict of interest.

## References

1. Tipnee S, Ramaraj R, Unpaprom Y (2015) Nutritional evaluation of edible freshwater green macroalgae *Spirogyra varians*. *Emerg Life Sci Res* 1(2):1–7
2. Ramaraj R, Dussadee N, Whangchai N, Unpaprom Y (2016) Microalgae biomass as an alternative substrate in biogas production. *IJSGE* 4:13–19
3. Ramaraj R, Tsai DD, Chen PH (2013) Chlorophyll is not accurate measurement for algal biomass. *Chiang Mai J Sci* 40(4):547–545
4. Mejica GFC, Unpaprom Y, Khonkaen P, Ramaraj R (2020) Extraction of anthocyanin pigments from malabar spinach fruits as a potential photosensitizer for dye-sensitized solar cell. *GJSE* 2:5–9
5. Khammee P, Unpaprom Y, Subhasaen U, Ramaraj R (2020) Potential evaluation of yellow cotton (*Cochlospermum regium*) pigments for dye sensitized solar cells application. *GJSE* 2:16–21
6. Ramar A, Saraswathi R, Rajkumar M, Chen SM (2016) TiO<sub>2</sub>/polyisothianaphthene—a novel hybrid nanocomposite as highly efficient photoanode in dye sensitized solar cell. *J Photochem Photobiol A* 329:96–104
7. Ramar A, Soundappan T, Chen SM, Rajkumar M, Ramiah S (2012) Incorporation of multi-walled carbon nanotubes in ZnO for dye sensitized solar cells. *Int J Electrochem Sci* 7:11734–11744
8. Schwinn KE, Davies KM (2004) Flavonoids. In: Davies K (ed) *Plant pigments and their manipulation*. Blackwell, Oxford, pp 92–149
9. Yildiz Z, Atilgan A, Atli A, Özel K, Altinkaya C, Yildiz A (2019) Enhancement of efficiency of natural and organic dye sensitized solar cells using thin film TiO<sub>2</sub> photoanodes fabricated by spin-coating. *J Photochem Photobiol A* 368:23–29
10. Maurya IC, Singh S, Srivastava P, Maiti B, Bahadur L (2019) Natural dye extract from *Cassia fistula* and its application in dye-sensitized solar cell: experimental and density functional theory studies. *Opt Mater* 90:273–280
11. Unpaprom Y, Whangchai N, Prasongpol P (2020) Antibacterial, antifungal properties and chemical composition of freshwater macroalgae, *Cladophora glomerata*. *J Bio Med Open Access* 1(1):107
12. Sumanta N, Haque CI, Nishika J, Suprakash R (2014) Spectrophotometric analysis of chlorophylls and carotenoids from commonly grown fern species by using various extracting solvents. *Res J Chem Sci* 2231:606X
13. Solovchenko AE, Chivkunova OB, Merzlyak MN, Reshetnikova IV (2001) A spectrophotometric analysis of pigments in apples. *Russ J Plant Physiol* 48(5):693–700
14. Lichtenthaler HK (1987) Chlorophyll and carotenoids: pigments of photosynthetic biomembranes. *Methods Enzymol* 148:331–382
15. Merzlyak MN, Chivkunova OB, Lekhimena L, Belevich NP (1996) Some limitation and potentialities of the spectrophotometric assay of pigment extracted from leaves of higher plants. *Russ J Plant Physiol* 43:926–936
16. Merzlyak MN, Gitelson AA, Chivkunova OB, Solovchenko AE, Pogosyan SI (2003) Application of reflectance spectroscopy for analysis of higher plant pigments. *Russ J Plant Physiol* 50(5):704–710
17. Ritchie RJ (2006) Consistent sets of spectrophotometric chlorophyll equations for acetone, methanol and ethanol solvents. *Photosynth Res* 89:27–41
18. Wasmund N, Topp I, Schories D (2006) Optimising the storage and extraction of chlorophyll samples. *Oceanologia* 48(1):125–144
19. Negi PS, Roy SK (2003) Changes in  $\beta$ -carotene and ascorbic acid content of fresh amaranth and fenugreek leaves during storage by low cost technique. *Plant Foods Hum Nutr* 58:225–230
20. Kushwaha R, Srivastava P, Bahadur L (2013) Natural pigments from plants used as sensitizers for TiO<sub>2</sub> based dye-sensitized solar cells. *J Energy* 2013:654953
21. Pawar KS, Baviskar PK, Nadaf AB, Salunke-Gawali S, Pathan HM (2019) Layer-by-layer deposition of TiO<sub>2</sub>-ZrO<sub>2</sub> electrode sensitized with pandan leaves: natural dye-sensitized solar cell. *Mater Renew Sustain Energy* 8:12
22. Movahedi J, Hosseinezhad M, Haratizadeh H, Falah N (2019) Synthesis and investigation of photovoltaic properties of new organic dye in solar cells device. *Prog Color Color Coat* 12(1):33–38

**Publisher's Note** Springer Nature remains neutral with regard to jurisdictional claims in published maps and institutional affiliations.





**Original Research Article**

# POTENTIAL EVALUATION OF YELLOW COTTON (COCHLOSPERMUM REGIUM) PIGMENTS FOR DYE SENSITIZED SOLAR CELLS APPLICATION

**PHITCHAPHORN KHAMMEE <sup>1</sup>, YUWALEE UNPAPROM <sup>2</sup>, UBONWAN SUBHASAEN <sup>3</sup>, RAMESHPRABU RAMARAJ <sup>1</sup>**

## ABSTRACT

Recently, dye-sensitized solar cells (DSSC) have concerned significant attention attributable to their material preparation process, architectural and environmental compatibility, also low cost and effective photoelectric conversion efficiency. Therefore, this study aimed to use potential plant materials for DSSC. This research presents the extraction of natural pigments from yellow cotton flowers (*Cochlospermum regium*). In addition, the natural pigments were revealed that outstanding advantages, including a wide absorption range (visible light), easy extraction method, safe, innocuous pigments, inexpensive, complete biodegradation and ecofriendly. Methanol was used as a solvent extraction for the yellow cotton flower. The chlorophylls and carotenoid pigments extractions were estimated by a UV-visible spectrometer. The chlorophyll-a, chlorophyll-b, and carotenoid yield were  $0.719 \pm 0.061$   $\mu\text{g/ml}$ ,  $1.484 \pm 0.107$   $\mu\text{g/ml}$  and  $7.743 \pm 0.141$   $\mu\text{g/ml}$ , respectively. Thus, this study results suggested that yellow cotton flowers containing reasonable amounts appealable in the DSSC production.

**Keywords:** Yellow cotton flower, pigments extraction, chlorophylls, carotenoid, DSSC application

## AUTHOR AFFILIATION

<sup>1</sup>School of Renewable Energy, Maejo University, Chiang Mai 50290, Thailand

<sup>2</sup>Program in Biotechnology, Faculty of Science, Maejo University, Chiang Mai 50290, Thailand

<sup>3</sup>Program of Political Science, Maejo University Phrae campus, Phrae 54140, Thailand

## CORRESPONDENCE

Rameshprabu Ramaraj, School of Renewable Energy, Maejo University, Chiang Mai 50290, Thailand  
Email: rameshprabu@gmail.com  
rameshprabu@mju.ac.th

## PUBLICATION HISTORY

Received: June 30, 2020  
Accepted: July 01, 2020

**ARTICLE ID:** GJSE-CP-08

## 1. INTRODUCTION

Energy may be our most valuable resource, and all societies require energy services to meet basic human needs. Abundant energy makes it easy to be sustainable because it can be used to produce essential resources such as lighting, food, communication and potable water where they are scarce [1-3]. The energy crisis is the main worldwide concern since fossil fuels are facing rapid depletion and its consumption contributes to the rise in the average global temperature. Among the challenges to be embedded lately with agricultural activities is to explore clean and renewable energy resources [4-6]. Renewable energy is generated from sources that are derived from and quickly replenished by the natural movements and mechanisms of the Earth.

For decades now, the perception of dwindling fossil fuels has motivated the government, economists, and scientists to find an alternative energy source that is not only endless in supply but also inexpensive and comparable in terms of storage density and capacity to fossil fuels [7, 8]. There are five major renewable energy resources: wind energy, hydropower, geothermal energy, biomass energy and solar energy. Accordingly, the development of renewable energy technologies provides a significant solution to deal with the energy crisis, along with

resolving the environment-related issues [9, 10]. Solar energy is one of the emerging technologies, which has been established as an effective alternative to fossil fuels and is an eco-friendly source for the sustainable development of society throughout the globe. Photovoltaic is a promising renewable energy technology that converts sunlight to electricity, with broad potential to contribute significantly to solving the future energy problem that humanity faces.

A low-cost and environmentally friendly alternative to conventional Si solid-state devices is the dye-sensitized solar cell (DSSC). It is considered to be one of the most promising technological developments in the field of solar cells. DSSCs are a class of photoelectrochemical cells, which converts solar light to electric energy. It is inexpensive to prepare, and the light-weight thin-film structures are compatible with automated manufacturing and thus potentially have easy scaling possibilities. Its immediate advantages are low production cost, easy scale-up, admirable performance under weak or diffuse light, and compatibility with building window glass and on flexible substrates [11]. Therefore, DSSCs has been placed as one of the promising alternatives to the bulk silicon-based solar cell. It is basically a cell that imitates the process seen in plant cells to produce energy. It is a photoelectrochemical cell, considering the electron

moments caused by the combined effect of the photon energy and the chemical reactions.

The DSSC being transparent to some extent and comparatively cheaper than conventional solar photovoltaic can be a potential energy source for the future. However, many aspects need to be worked upon before declaring it as an available commercial product. The use of synthetic dyes as sensitizers in DSSC provides better efficiency and high durability, but they suffer from several limitations such as higher cost, tendency to undergo degradation, and usage of toxic materials [12]. These limitations have opened up for alternate sensitizers that are biocompatible natural sensitizers. Natural sensitizers contain plant pigments such as anthocyanin, carotenoid, flavonoid, and chlorophyll that are responsible for chemical reactions such as absorption of light as well as injection of charges to the conduction band of TiO<sub>2</sub> by the sensitizer.

Naturally available fruits, flowers, leave, bacteria etc. exhibit various colors and contain several pigments that can be easily extracted and employed in DSSC. Chlorophylls and carotenoid based-dyes obtained from plants, seaweeds, or algae represent attractive alternatives to the expensive and polluting pyridyl based Ru complexes because of their abundance in nature [13]. One of the main targets of contemporary scientific research is finding a solution to the urgent need for a clean and cheap energy source. The performance of the dye-sensitized solar cell mainly depends on the dye used as a sensitizer. Therefore, in this study, we aim to focus on pigments extraction from the yellow cotton (*Cochlospermum regium*) flower pigments for dye-sensitized solar cells application.

## 2. MATERIALS & METHODS

### 2.1. Material Collection

Yellow cotton (*Cochlospermum regium*) was collected from Maejo University Farm, Chiang Mai, Thailand. The plant and collecting process was displayed in Figure 1. After flower collection, the materials were transferred to Energy Research Center, Maejo University, within 1-2 hours. The flower washed by tap water to get rid of dust. After that, blow the wind to dry the petals.



**Figure 1.** Material collection from Maejo University's Farm, Chiang Mai, Thailand

### 2.2. Pigments Extraction and Estimation

The extraction process was Sumanta et al. [14] adopted and modified to this study. The twenty (20) grams of flowers were used for extraction (i.e., Methanol solvent extraction procedure). After that, the weighed flowers are mixed with methanol 50 ml using a blender and timer for 10 minutes. Then, the flower was separated solid and liquid by applying the vacuum filter. Subsequently, the pigments extraction was poured in a volumetric flask and adjust to 100 ml. The experiment was carried with a triplication method, and the experiment step by step process, as shown in Figure 2. Finally, measure the absorbance wavelength by using a UV-visible spectrophotometer and analyzed the determination of chlorophylls (Ch-a and Ch-b) and carotenoids content by using the following equations;

$$\text{The amount of chlorophyll A} = (12.25 \times A_{663} - 2.79 \times A_{645}) \times \text{DF} \quad (1)$$

$$\text{The amount of chlorophyll B} = (21.50 \times A_{645} - 5.10 \times A_{663}) \times \text{DF} \quad (2)$$

$$\text{The amount of carotenoid} = \frac{(1000 \times A_{430} - 1.43 \times C_1 - 25.87 \times C_2) \times \text{DF}}{205} \quad (3)$$

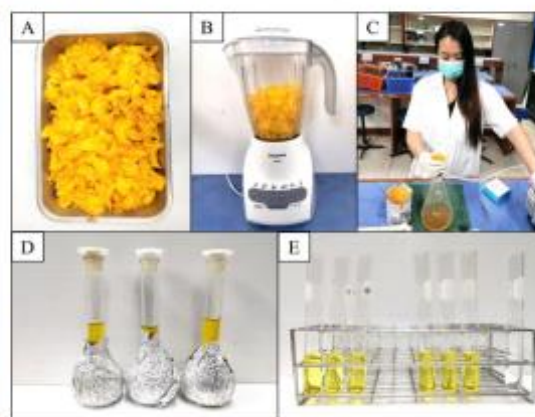


**Figure 2.** Pigments extraction step by step procedure (A-E)

### 2.3. Statistical Analysis

Data are reported as mean  $\pm$  SE from triplicate observations. Significant differences between means were analyzed. All statistical analyses were performed using SPSS Version 20.0. A correlation was assumed significant when  $P < 0.05$ .

## 3. RESULTS & DISCUSSION

### 3.1 Natural Pigments

Pigments are colorful compounds. Pigments are chemical compounds that reflect only specific wavelengths of visible light. Photosynthetic plant pigments can absorb specific wavelengths (colors) of light and change the light energy to chemical energy [13]. More important than their reflection of light is the ability of pigments to absorb certain wavelengths. This makes them appear "colorful". The plant pigments are found in chloroplasts on the membranes of the thylakoids. Because they interact with light to absorb only specific wavelengths, pigments are useful to plants and other autotrophs organisms that make their own food using photosynthesis. In plants, algae, and cyanobacteria, pigments are how the energy of sunlight is captured for photosynthesis [15, 16]. However, since each pigment reacts with only a narrow range



of the spectrum, there is usually a need to produce several kinds of pigments, each of a different color, to capture more of the sun's energy. There are five basic classes of pigments: 1. chlorophyll, 2. carotenoids, 3. xanthophylls, 4. anthocyanins and 5. betalains. In flowers, there are two major classes of flower pigments: carotenoids and flavonoids. Carotenoids include carotene pigments, which produce yellow, orange and red colors). Flavonoids include anthocyanin pigments, which produce red, purple, magenta and blue colors.

Chlorophyll, being the most abundant pigment that commonly found in plants, bacteria, bryophytes, and algae, plays a vital role in photosynthesis. Chlorophylls are natural pigments and, therefore, safe, environmentally friendly, readily available, and cheap. Chlorophyll has been experimented to function as a photosensitizer in dye-sensitized solar cells (DSSCs) as DSSCs mimic the photosynthesis process in green plants [17]. The structure of chlorophyll a and chlorophyll b was displayed in Figure 3. Chlorophyll has been experimented to function as a photosensitizer in dye-sensitized solar cells as DSSCs mimic the photosynthesis process in green plants. The natural dye, chlorophyll, can be extracted from the plants and used as the photosensitizer in DSSC.

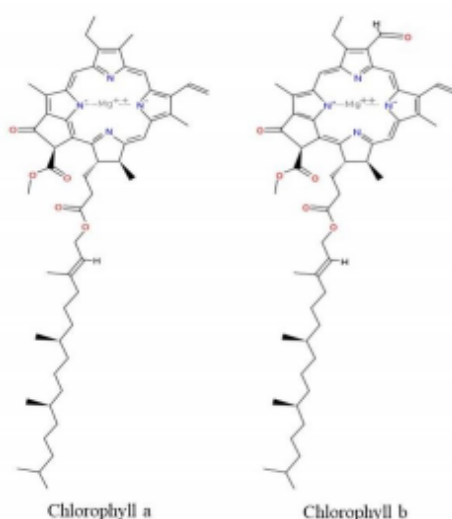


**Figure 3.** Structure of chlorophylls

Carotenoids are general isoprenoids that intervene in actions ranging from the collection of light and photoprotection to the regulation of gene expression and communication within or between species. They are versatile compounds that are eliciting increasing interest in different disciplines, such as plant science, agriculture, food science and technology, nutrition and health, among others. Plant carotenoids with 8–10 conjugated double bonds, having higher singlet energies than those of bacterial carotenoids with 9–13 conjugated double bonds, were added as redox spacers to a titania-based Grätzel-type solar cell using a chlorophyll derivative as the sensitizer [18]. Carotenoid pigments do make provisions for many flowers and fruits with typically red, yellow and orange colors, and numbers of carotenoid derived aromas. There are over 600 carotenoids known and are divided into two categories; carotenes (pure hydrocarbons) and xanthophylls (which contain oxygen). Generally, carotenoids absorb wavelengths ranging from 400–550 nanometers (violet to green light). The general

structure of plant carotenoids presented in Figure 4. The DSSCs were assembled by using natural carotenoids, crocetin (8,8'-diapocarotenedioic acid) and crocin (crocetin-di-gentiobioside), as sensitizers and their photoelectrochemical properties were investigated taking a presence or absence of carboxylic group in the dye molecule into consideration.

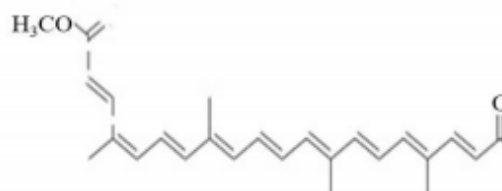


**Figure 4.** Structure of carotenoids

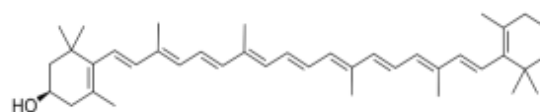


**Figure 5.** Structure of xanthophylls

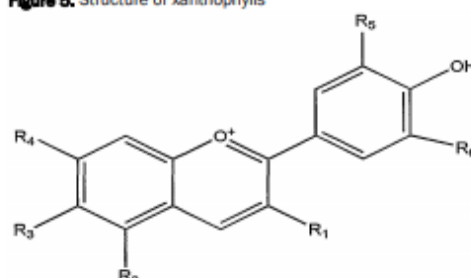


**Figure 6.** Structure of anthocyanins

Xanthophyll is one of the carotenoids present naturally in the thylakoid membrane. The general structure of the xanthophyll displayed in figure 5. Xanthophylls are efficient quenchers of chlorophyll triplets that can originate on chlorophyll-a molecules. This natural system provides an attractive solution to the drawback of natural DSSC [19]. Anthocyanins are glycoside salts of phenyl-2-benzopyrylium based on a C15 skeleton with a chromane ring bearing a second aromatic ring B in position 2 (C6-C3-C6). The basic chemical structure of anthocyanin is shown in Figure 6. Anthocyanins are responsible for the existence of attractive colors, from scarlet to blue, of flowers, fruits, leaves etc., and are also identified in mosses and ferns. Anthocyanins are also responsible for modifying the quantity and quality of light that is incident on the chloroplasts [20]. Anthocyanin molecules have carbonyl and hydroxyl groups bound to the surface of titanium dioxide (TiO<sub>2</sub>) semiconductor, which helps in excitation and transfer of electrons from the anthocyanin molecules to the conduction band of porous TiO<sub>2</sub> system.

Betalains are plant-derived natural pigments that are presently gaining popularity for use as natural colorants in the food industry. The betalains' chemical structure was exhibited in figure 7. Although betalains from red beet are one of the most widely used food colorants, betalains are not as well studied as compared to other natural

pigments such as anthocyanins, carotenoids, and chlorophylls. Betalain is another interesting class of pigments, whose purified extracts from commercial sources have been subjected to photoelectrochemical study [21]. Generally, betalains consisting of the yellow betaxanthins and red-violet betacyanins are a group of water-soluble nitrogen-containing alkaloid pigments characteristic of individual members of the plant sub-order Chenopodiaceae within Caryophyllales and some higher fungi. They absorb visible radiation over the range 476–600 nm, they are immonium derivatives of betalamic acid (the chromophore of all betalains).

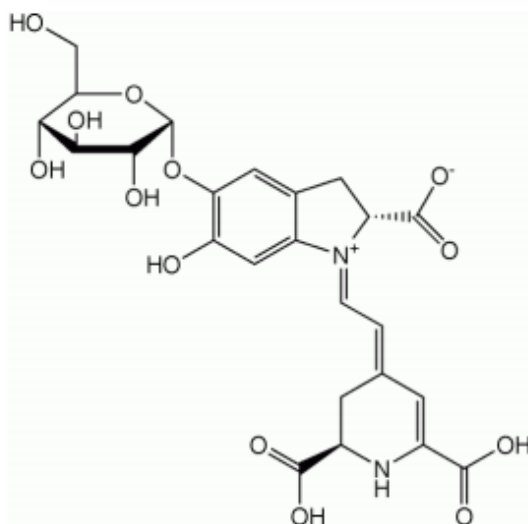


**Figure 7.** Structure of betalains

### 3.2. Yellow Cotton (*Cochlospermum Regium*)

*Cochlospermum regium* was known as the yellow cotton tree. It is a shrub or small tree—a yellow cotton tree in flower. The tree is native to the Cerrado tropical savanna of South America but is now common in Southeast Asia and some Pacific islands. New Caledonia. The yellow cotton tree has been introduced to Northern Thailand about 60 years ago, where it became a popular ornamental plant. While the up to about 8 meters high tree starts blooming in late winter, it drops all its leaves. The yellow cotton tree has much simpler flowers. The impressive orange-yellow flowers get a size of about 15 cm in diameter and are widely used for floral decorations and as offerings and temple activities. The tree reaches up to 15 meters in height at maturity and when the tree blossoms, the leaves fall [22].

The yellow cotton tree behaves like a weed and is often found in habitats severely influenced by man besides is often to be found along roadsides, railroad right-of-ways, in dump areas, forest clearings, and secondary grow etc. The branches are not straight but grow in unusual twisted forms. The leaves are heart-shaped with five smooth serrated edges [23]. Bunches of thin petaled yellow blossoms grow at the end of the branches, flowering one after the other. The fragrance is particularly sweet and pleasant. After blossoming, the flower turns into a brown fruit. The tree blossoms almost all year round but is particularly beautiful in February and April. The tree is very versatile and has a fantastic number of uses. The blossoms are used, of course, as decoration—all in all, the most beautiful, interesting and wonderful tree.

### 3.3. UV-Vis Analysis of Dye

The light absorption spectrum of the mixed extract contained peaks corresponding to the contributions from the individual extracts. The result of absorbance spectra by using UV-Vis Spectrophotometer of the extraction of the dye from the yellow cotton flower by use methanol as a solvent that is wavelength between 350 to 800 nm as shown in figure 8. Yellow cotton had three peaks with wavelengths of 374.5 nm, 396.5 nm and 420.5 nm in the absorbance rate of 0.768, 0.881 and 0.734 [24]. The wavelengths 374.5 nm and 396.5 nm presume that is the functional group of flavonoids. Due to comprised absorption bands of flavonoids are near 350 to 400 nm [25].

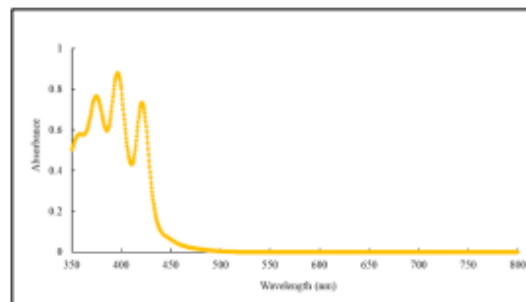


**Figure 8.** UV-Vis analysis of yellow cotton dye

Therefore, the yellow cotton flower is a possibility that had the functional group of flavonoids as the pigments. While the wavelengths of 420.5 nm are feasibility, that is the chlorophylls and carotenoids. Owing to the characteristic absorption maximum of chlorophyll a is 420 nm, 490 nm and 660 nm. The wavelength range of carotenoids is 420 nm, 440 nm and 470 nm [13]. Thus, the peaks at 420 nm, which correspond to the absorption bands of chlorophylls and carotenoids [26, 27]. The structure of the pigments extraction from yellow cotton flower containing chlorophylls, flavonoids and carotenoids can be considered as an investigation dyes sensitizer material for fabrication DSSC.

### 3.4. Pigments Extraction and Estimation of Yellow Cotton Flower

The yellow cotton flower is composed of three major pigments, namely, chlorophyll A (Chl-a), chlorophyll B (Chl-b) and carotenoids. Among the stated pigments, it was observed that the flower is mostly composed of carotenoid, as shown in figure 9. The carotenoids content of the yellow cotton flower was  $7.743 \pm 0.141$   $\mu\text{g}/\text{mL}$ . Followed by chlorophyll-b with  $1.484 \pm 0.107$   $\mu\text{g}/\text{mL}$  and lastly, by chlorophyll-a with  $0.719 \pm 0.061$   $\mu\text{g}/\text{mL}$ .

Results concerning chlorophylls (Chl-a, b) and carotenoids pigments present yellow cotton tree flowers analyzed by using UV-Vis spectrometry, are included. These natural colorants have been of interest in different fields and applications. Most useful is the use of natural dyes as sensitizers in DSSCs, their key benefits being a simple extraction procedure, low cost, wide availability, and their environmentally friendly nature.

### 3.5. Pigments Roles in DSSC

Various types of solar cells convert sunlight into electrical energy. The commercially obtainable solar cells are currently based on inorganic silicon semiconductors. The demand for silicon will climb sharply within the next decade, and its price possible to increase intensely. Organic solar cells, therefore, appear to be a much favorable and economically

alternative for the photovoltaic energy sector [26]. Currently, in this perspective, DSSC has attracted significant attention. A dye-sensitized solar cell converts the visible light into electricity using the sensitization of the cell. Performances of DSSCs were basically based on dye used as a sensitizer. At the moment, the study of dyes extracted from natural resources is a vital concern for researchers. The application of natural dyes is a promising development in the field of this technology.

Natural dyes are cutting down the high cost of metal complex sensitizers and also replacing the expensive chemical synthesis process through a simple extraction process. Natural dyes are abundant, easily extractable, and safe material causes no environmental threat. These can be extracted from flower petals, leaves, roots besides barks in the form of anthocyanin, carotenoid, flavonoid, and chlorophyll pigments. In this study, yellow cotton flower extraction processes have revealed that flowers were containing a high yield of carotenoid and chlorophylls. This amount could generate a significant amount of dyes and it is applicable in the DSSC fabrication. Commonly, photovoltaic tests of DSSCs using these natural dyes as sensitizers were performed by measuring the current density-voltage ( $J-V$ ) curves under irradiation with white light ( $100 \text{ mW cm}^{-2}$ ). The performance of natural dyes as sensitizers in DSSCs was evaluated by short circuit current density (JSC), open-circuit voltage ( $V_{oc}$ ), fill factor (FF), and power conversion efficiency ( $\eta$ ) [12]. These parameters illustrated that carotenoids, chlorophylls and anthocyanins are more suitable pigments than flavonoid pigment in addition to the estimated open-circuit photo-voltage values ( $eV_{oc}$ ) showed that flavonoids are the desirable pigment. Therefore, this study suggested that the development of yellow cotton flower dyes and pigments effect on various performance parameters of DSSC in further studies.

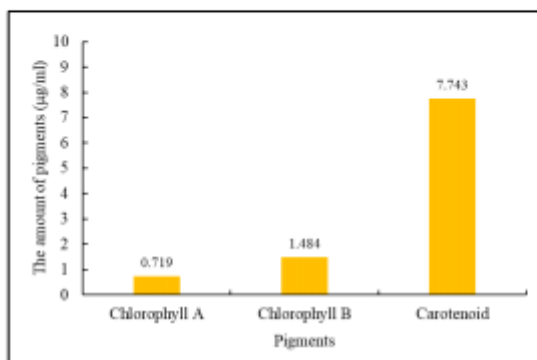


**Figure 9.** Extraction yield of the pigments

#### 4. CONCLUSIONS

Dye-sensitized solar cells have become a topic of valuable research because of their scientific prominence in the area of energy utilization and conversion. Typically, the dyes extracted from plant materials contained anthocyanins, betalains and chlorophyll. This study results detailed that yellow cotton flowers contain a high amount of carotenoids (7.743 µg/ml) compared to chlorophyll-a (0.719 µg/ml) chlorophyll-b (1.484 µg/ml) pigments. These are highly suitable to produce natural dyes that were obtained from flower yellow cotton plants. These natural dyes are directly applicable as sensitizers for DSSC. Therefore, the methanol extract of yellow cotton flowers should be an alternative pigment source for DSSC preparation. This study performance could be helpful for DSSC producers to choose highly efficient natural dyes according to their optical and electronic properties. Overall, natural dyes as sensitizers of DSSCs are favorable

because of their environmentally friendly, low-cost production and efficient manufacturing processes.

#### ACKNOWLEDGEMENTS

The authors gratefully acknowledged the Program in Biotechnology, Energy Research Center, School of Renewable Energy, Maejo University, Chiang Mai, Thailand, for the research facilities to accomplish this experimental study.

#### CONFLICT OF INTERESTS

The authors declare that there is no conflict of interest related to the publication of this article.

#### REFERENCES

- [1] K. Khunchit, S. Nitayavardhana, R. Ramaraj, V. K. Ponnusamy, and Y. Unpaprom, "Liquid hot water extraction as a chemical-free pretreatment approach for biobutanol production from *Cassia fistula* pods," *Fuel*, vol. 279, 2020.
- [2] B. Saengsawang, P. Bhuyar, N. Manmai, V. K. Ponnusamy, R. Ramaraj, and Y. Unpaprom, "The optimization of oil extraction from macroalgae, *Rhizoclonium* sp. by chemical methods for efficient conversion into biodiesel," *Fuel*, vol. 274, 2020.
- [3] N. Manmai, Y. Unpaprom, V. K. Ponnusamy, and R. Ramaraj, "Bioethanol production from the comparison between optimization of sorghum stalk and sugarcane leaf for sugar production by chemical pretreatment and enzymatic degradation," *Fuel*, vol. 278, 2020.
- [4] N. Manmai, Y. Unpaprom, and R. Ramaraj, "Bioethanol production from sunflower stalk: application of chemical and biological pretreatments by response surface methodology (RSM)," *Biomass Convers. Biorefinery*, 2020.
- [5] G. Van Tran, Y. Unpaprom, and R. Ramaraj, "Methane productivity evaluation of an invasive wetland plant, common reed," *Biomass Convers. Biorefinery*, 2019.
- [6] J. Kaewdiew, R. Ramaraj, S. Koonaphapdeelert, N. Dussadee, "Assessment of the biogas potential from agricultural waste in northern Thailand," *Maejo International Journal of Energy and Environmental Communication*, vol. 1, no. 1, pp. 40-47, 2019.
- [7] A. Chuanchai, S. Tipnee, Y. Unpaprom, and K. T. Wu, "Green biomass to biogas - A study on anaerobic monodigestion of para grass," *Maejo International Journal of Energy and Environmental Communication*, vol. 1, 32-38, 2019.
- [8] A. Chuanchai and R. Ramaraj, "Sustainability assessment of biogas production from buffalo grass and dung: biogas purification and bio-fertilizer," *3 Biotech*, vol. 8, no. 3, 2018.
- [9] N. Dussadee, K. Reansuwan, and R. Ramaraj, "Potential development of compressed bio-methane gas production from pig farms and elephant grass silage for transportation in Thailand," *Bioresour. Technol.*, vol. 155, pp. 438-441, 2014.
- [10] R. Ramaraj, N. Dussadee, N. Whangchai, and Y. Unpaprom, "Microalgae Biomass as an Alternative Substrate in Biogas Production," *Int. J. Sustain. Green Energy. Spec. Issue Renew. Energy Appl. Agric. F. Nat. Resour. Technol.*, vol. 4, no. 1, pp. 13-19, 2015.



- [11] S. Shalini, R. Balasundara Prabhu, S. Prasanna, T. K. Mallick, and S. Senthilarasu, "Review on natural dye sensitized solar cells: Operation, materials and methods," *Renewable and Sustainable Energy Reviews*, vol. 51, pp. 1306–1325, 2015.
- [12] D. J. Godibo, S. T. Anshebo, and T. Y. Anshebo, "Dye sensitized solar cells using natural pigments from five plants and Quasi-solid state electrolyte," *J. Braz. Chem. Soc.*, vol. 26, no. 1, pp. 92–101, 2015.
- [13] R. Ramaraj, D. D. W. Tsai, and P. H. Chen, "Chlorophyll is not accurate measurement for Algal Biomass," *Chiang Mai J. Sci.*, vol. 40, no. 4, pp. 547–555, 2013.
- [14] N. Sumanta, C. I. Haque, J. Nishika, and R. Suprakash, "Spectrophotometric Analysis of Chlorophylls and Carotenoids from Commonly Grown Fern Species by Using Various Extracting Solvents," *Res. J. Chem. Sci. Res. J. Chem. Sci.*, vol. 4, no. 9, pp. 2231–606, 2014.
- [15] R. Ramaraj, D. David, and P. Chen, "Algae Growth in Natural Water Resources," *J. Soil Water Conserv.*, vol. 42, no. 4, pp. 439–450, 2010.
- [16] R. Ramaraj, D. D. W. Tsai, and P. H. Chen, "Freshwater microalgae niche of air carbon dioxide mitigation," *Ecol. Eng.*, vol. 68, pp. 47–52, 2014.
- [17] A. K. Arof and T. L. Ping, "Chlorophyll as Photosensitizer in Dye-Sensitized Solar Cells," in *Chlorophyll*, 2017.
- [18] F. Zanjanchi and J. Beheshtian, "Natural pigments in dye-sensitized solar cell (DSSC): a DFT-TDDFT study," *J. Iran. Chem. Soc.*, vol. 16, no. 4, pp. 795–805, 2019.
- [19] I. Kartini, L. Dwitarsari, T. D. Wahyuningsih, C. Chotimah, L. Wang, "Sensitization of Xanthophylls-Chlorophyllin Mixtures on Titania Solar Cells," *International Journal of Science and Engineering*, vol. 8, no. 2, pp. 109–114, 2015.
- [20] C. Y. Chien and B. D. Hsu, "Optimization of the dye-sensitized solar cell with anthocyanin as photosensitizer," *Sol. Energy*, vol. 98, no. PC, pp. 203–211, 2013.
- [21] A. R. Obasuyi, D. Glossman-Mitnik, and N. Flores-Holguin, "Electron injection in anthocyanidin and betalain dyes for dye-sensitized solar cells: a DFT approach," *J. Comput. Electron.*, vol. 18, no. 2, pp. 396–406, 2019.
- [22] H. H. Poppendieck, "Cochlospermeaceae," *Flora Neotropica*, vol. 27, pp. 1-33, 1981.
- [23] M. C. Inácio, T. A. Paz, B. W. Bertoni, M. A. R. Vieira, M. O. M. Marques, and A. M. S. Pereira, "Histochemical investigation of *Cochlospermum regium* (Schrank) Pilg. leaves and chemical composition of its essential oil," *Nat. Prod. Res.*, vol. 28, no. 10, pp. 727–731, 2014.
- [24] F. Van Der Meer and S. M. de Jong, *Imaging spectrometry: basic principles and prospective applications*, vol. 1, no. C, 2002.
- [25] P. P. Vachell, B. Li, B. M. Besch, and P. S. Bernstein, "Protein-flavonoid interaction studies by a Taylor dispersion surface plasmon resonance (SPR) technique: A novel method to assess biomolecular interactions," *Biosensors*, vol. 6, no. 1, 2016.
- [26] G. Britton, *Carotenoids*. In *Natural food colorants* (pp. 197-243). Springer, Boston, MA, 1996.
- [27] A. E. Solovchenko, O. B. Chivkunova, M. N. Merzlyak, and I. V. Reshetnikova, "A spectrophotometric analysis of pigments in apples," *Russ. J. Plant Physiol.*, vol. 48, no. 5, pp. 693–700, 2001.
- [28] A. Wadsworth, M. Moser, A. Marks, M. S. Little, N. Gasparini, C. J. Brabec, D. Baran, and I. McCulloch, "Critical review of the molecular design progress in non-fullerene electron acceptors towards commercially viable organic solar cells," *Chemical Society Reviews*, vol. 48, no. 6, pp. 1596–1625, 2019.



## Natural dyes extracted from Inthanin bok leaves as light-harvesting units for dye-sensitized solar cells

Phitchaphorn Khammee<sup>1,2</sup> · Yuwalee Unpaprom<sup>2,3</sup> · Theerapol Thurakitserree<sup>4</sup> · Natthawud Dussadee<sup>1</sup> · Suchanya Kojinok<sup>5</sup> · Rameshprabu Ramaraj<sup>1</sup>

Received: 16 January 2021 / Accepted: 3 March 2021  
 © King Abdulaziz City for Science and Technology 2021

### Abstract

The dye-sensitized solar cells (DSSC) deliver a low-cost and dependable alternative for various photovoltaic devices. The extraction process of natural pigments is simple and inexpensive compared with synthetic dyes. Natural plant pigments were extracted from flowers, leaves, roots, and fruits. Thus, this research focuses on the potential of natural dye using cold extraction with methanol. A UV–visible spectrometer was used for analyzing the Inthanin bok (*Lagerstroemia macrocarpa*) pigments absorption wavelength for the DSSC application. Carotenoids have the highest content, which is  $10.666 \pm 0.324 \mu\text{g}/\text{ml}$ ; followed by chlorophyll-a with  $2.708 \pm 0.251 \mu\text{g}/\text{ml}$  and lastly chlorophyll-b with  $2.500 \pm 0.102 \mu\text{g}/\text{ml}$ . Elemental of the  $\text{TiO}_2$  nanoparticles and natural dyes was confirmed by energy-dispersive X-ray spectroscopy (EDX). The scanning electron microscope (SEM) and the laser scanning microscope used for analyzed morphological characteristics of  $\text{TiO}_2$  nanoparticles and natural dyes. Moreover, the highest efficiency of the pigments extracted from Inthanin bok leaves is  $1.138\% \pm 0.018$ , which the condition of 1 layer of  $\text{TiO}_2$  nanoparticles and the temperature;  $300^\circ\text{C}$ .

**Keywords** Inthanin bok leaves · Pigments extraction · Chlorophylls · Carotenoids · Natural dye · Dye-sensitized solar cells

### Introduction

Natural gas, petroleum, and coal are various statuses (gaseous, liquid, and solid) of fossil fuels. Fossil fuels are considered non-renewable resources, and their probable reserves are depleted faster than the natural process of fresh fossil fuels was created (Unpaprom et al. 2020; Whangchai et al. 2021). Also, severe environmental issues, for example, global warming and  $\text{CO}_2$  emission, are the effect of used fossil fuels (Nguyen et al. 2020). Due to global energy

situations such as the energy crisis, they decrease fossil fuels, environmental issues, and climate change. Humanity realizes that is a very significant issue. Therefore, it essentials to find clean and sustainable energy. This alternative energy source is vast and cheap, and environmentally friendly (Khammee et al. 2020a, b; Nong et al. 2020).

The alternative energy resources have five primaries: wind energy, hydropower, geothermal energy, biomass energy, and solar energy (Vu et al. 2018; Sophanodorn et al. 2020a, b). The highest potential energy in electricity generation was reachable by solar energy, about 6.5 EJ compared to all other energy sources. Therefore, the solar cell's enormous potential was attended to provides an effective solution to handle the problem related to the energy crisis and environmental issues (Alami et al. 2019).

Nowadays, researchers, academia, and governments worldwide have attention to solar energy conversion (Rajkumar et al. 2019). Various solar photovoltaic approaches have been developed and prove using enhanced overall performance. One of the most promising technological developments in the solar cells field is dye-sensitized solar cell (DSSC), the third generation of solar cells. Moreover, a potential alternative has come with the long-term target

Rameshprabu Ramaraj  
 rrameshprabu@gmail.com; rameshprabu@mju.ac.th

<sup>1</sup> School of Renewable Energy, Maejo University, Chiang Mai 50290, Thailand

<sup>2</sup> Sustainable Resources and Sustainable Engineering Research Lab, Maejo University, Chiang Mai 50290, Thailand

<sup>3</sup> Program in Biotechnology, Faculty of Science, Maejo University, Chiang Mai 50290, Thailand

<sup>4</sup> Program in Applied Physics, Maejo University, Chiang Mai 50290, Thailand

<sup>5</sup> Institute of Product Quality and Standardization (IQS), Maejo University, Chiang Mai 50290, Thailand



of reach efficiency comparative with first-generation technology (silicon-based photovoltaics) at the economics of second-generation (thin-film solar cell) manufacturing. Its simple fabrication process, low manufacturing cost, high cell performance on the widespread light condition, and eco-friendly (Bashar et al. 2019).

Dye-sensitized solar cells also can operate in low light circumstances that virtually feasible during cloudy days. It has been recommended that it be used indoors to operate from various lights such as illuminate the indoors (Ananthi et al. 2020). In DSSCs, a sensitized dye adsorbed the lights and transmission an electron to the semiconductor, which is usually used nanostructured  $\text{TiO}_2$ , followed by dye regeneration. Most traditional DSSCs used the transition metal coordination compounds (ruthenium and osmium complexes mostly) as a sensitizer due to their remarkable efficiency. However, the large-scale fabrication when using this kind of metal complexes as a sensitizer often a big problem because of its complex synthesis and purification process (Arulraj et al. 2019; Ocakoglu et al. 2012; Cerda et al. 2016; Argazzi et al. 2004).

Thus, natural dyes were becoming popular and attracted most of the research. Due to its easy extraction process, the abundance of material, cheap, innocuous, etc. Accordingly, much research was investigated and took advantage of natural pigments to convert photons into electrons with a cost-beneficial approach and environmentally friendly (Arulraj et al. 2019, 2017; Richhariya et al. 2017; Wongcharee et al. 2007). Natural pigments can be easily extracted from fruits, flowers, leaves, bacteria, etc. By exhibiting various colors from pigments. The major pigments for natural dyes consist of chlorophylls, carotenoids, flavonoids, and anthocyanin (Shalini et al. 2015). Besides, the dye-sensitized solar cell performance essentially depends on the dye sensitizer. This is the first novel investigation of using natural dyes extracted from Inthanin bok leaves as light-harvesting units for dye-sensitized solar cells. This study aimed to focus on pigments' extraction from Inthanin bok leaves (*Lagerstroemia macrocarpa*), which is waste material (red or orange colors) that fall from the trees to become a light harvester for DSSC. The dyes and the manufactured DSSC cells were analyzed

for their optical and structural properties. In addition, laser scanning microscopy explored the interface between the natural dye and nano- $\text{TiO}_2$ ; in addition, using various nanostructure layers (1, 2, and 3 layers) and temperatures (100, 200, and 300 °C) to figure out the best DSSC condition to obtain high efficiency.

## Materials and methods

### Materials collection

The materials are Inthanin bok (*Lagerstroemia macrocarpa*), collected from the Inthanin field of Maejo University, Chiang Mai, Thailand. The leaves of those plants are shown in Fig. 1. After collecting the leaves, the dust was removed with tap water and scrape dry with a towel. Then, the middle parts of the leaves were removed for the next process, the pigment extraction process.

### Pigments extraction and analysis

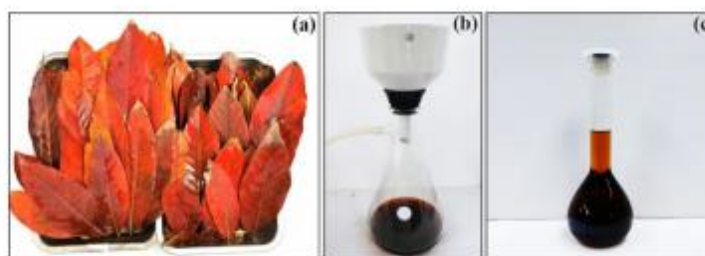
This research was modified by the extraction method from Sumanta et al. (2014). The extraction process was used the solvent extraction method in the ratio (20 g of Inthanin bok leaves: 100 ml of methanol). The leaves were mixed with the solvent using a blender and set the time for 10 min. After that, separated residue and pigments by used a vacuum filter. The experiment was operated with triplications, and the experiment processes are shown in Fig. 1.

For preparation for the next process was measure the absorption wavelength of natural dyes (Inthanin bok leaves) by using a UV-visible spectrophotometer and analyzed the determination of chlorophylls (Chl-a and Chl-b) and carotenoids content by using the following equations:

$$\text{The amount of chlorophyll-a} = (12.25 \times A_{665} - 2.79 \times A_{645}) \times \text{DF}, \quad (1)$$

$$\text{The amount of chlorophyll-b} = (21.50 \times A_{645} - 5.10 \times A_{665}) \times \text{DF}, \quad (2)$$

**Fig. 1** Material collection of Inthanin bok (a), and pigments' extraction (b) and (c)



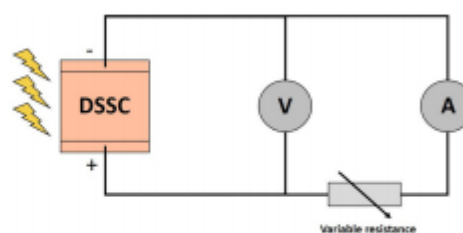
126 The amount of carotenoids  
 127 
$$= \frac{(1000 \times A_{470} - 1.43 \times C_a - 35.87 \times C_b) \times DF}{205} \quad (3)$$

### 128 Preparation of TiO<sub>2</sub> electrode

129 The first step was to clean the FTO glass for photoanode  
 130 and counter electrode by ultrasonic with soap solution dis-  
 131 tilled water and methanol for 10 min each consecutively.  
 132 Meanwhile, TiO<sub>2</sub> powder reduced the particle size using  
 133 a magnetic mixer set the time for 1 h to prepare the TiO<sub>2</sub>  
 134 paste. A ratio of TiO<sub>2</sub> paste is 5 g of TiO<sub>2</sub> powder, 10 ml  
 135 of 5% acetic acid, and 0.5 ml of surfactant (Tween 20)  
 136 was utterly mix using a magnetic stirrer for 1 h. After that,  
 137 to avoid evaporation of the TiO<sub>2</sub> paste must be kept in a  
 138 sealed receptacle. Eventually, the TiO<sub>2</sub> paste was depos-  
 139 ited on the conduction electrode fluorine-doped SnO<sub>2</sub> on  
 140 the glass substrate (FTO) using the doctor blading tech-  
 141 nique. This experiment's layers are 1, 2, and 3 layers using  
 142 the adhesive tape to determine the layers and the active  
 143 area is 3 cm<sup>2</sup>. After that, wait until the active area of the  
 144 FTO glass dried and remove the tape. The film was gradu-  
 145 ally sintered at 100, 200, and 300 °C for 1 h. The TiO<sub>2</sub> film  
 146 was then cooled at room temperature and subsequently  
 147 immerse in 30 drops of natural dye sensitizer (Inthanin  
 148 bok) solution at room temperature for 1 h under a dark  
 149 condition.

### 150 Assembling and testing the DSSC

151 The natural dyes (Inthanin bok leaves) coated on an  
 152 active layer of photoanode and the counter electrode  
 153 coated on FTO glass by platinum paste (Sigma Aldrich)  
 154 annealed at 200 °C for 1 h. These were assembled like  
 155 a sandwich by the gap between photoanode and coun-  
 156 ter electrode was injected the electrolyte, consisting of  
 157 0.6 mol/l of KI, 0.075 mol/l of I<sub>2</sub>, 20 ml of acetonitrile,  
 158 and 5 ml of ethylene glycol (Gu et al. 2017). Finally, the  
 159 DSSC is sealed entirely in order as sealed completely to  
 160 avoid leakage of the DSSC cell's electrolyte. A digital  
 161 multimeter (UNI-T UT61E) was used to measure the cur-  
 162 rent–voltage characteristics of DSSC with variable resist-  
 163 ance (10 kΩ) under illuminated with the tungsten light of  
 164 24,000 lx (0.03504 W/cm<sup>2</sup>) in the ambient atmosphere and



165 Fig. 2 Schematic circuit diagram of the experimental setup  
 166 used to measure the current–voltage characteristics of DSSC with variable  
 167 resistance (10 kΩ)

168 the schematic circuit diagram of the experimental setup  
 169 displayed in Fig. 2.

170 The fill factor, all the more ordinarily known by its  
 171 acronym “FF”, is essentially a proportion of solar cells.  
 172 The FF is comparing by the  $I_{\max}$  and  $V_{\max}$  at maximum  
 173 power point ( $P_{\max}$ ) of the  $I$ – $V$  curve and the open-circuit  
 174 voltage ( $V_{oc}$ ) is the maximum voltage accessible from a  
 175 solar cell, and this happens at zero current. The short cir-  
 176 cuit current ( $I_{sc}$ ) is the current through the solar cell per  
 177 unit area when the voltage across the solar cell is zero  
 178 (Sharma et al. 2018) The FF is generally determined as:

$$176 \text{ FF} = (I_{\max} \times V_{\max}) / (I_{sc} \times V_{oc}). \quad (4)$$

177 The photovoltaic cell's efficiency is compared the perfor-  
 178 mance of one solar cell to another cell. Also, it is determined  
 179 as the ratio of maximum power output to the energy input from  
 180 the light. This experiments were used  $P_{in} = 3.504 \text{ mW/cm}^2$  by  
 181 the following conversion efficiency formula (Dawoud 2016):

$$182 \eta = [(I_{sc} \times V_{oc} \times \text{FF}) / P_{in}] \times 100. \quad (5)$$

### 185 Characterization techniques

186 The characterization of the TiO<sub>2</sub> coated on FTO glass substrate  
 187 with natural dyes immersion (Inthanin bok leaves) was inves-  
 188 tigated under the scanning electron microscope (SEM) for the  
 189 determination of the morphology (Khammee et al. 2020b).  
 190 Besides, the energy-dispersive X-ray spectroscopy (EDX)  
 191 analyzed the elemental composite of the samples. The laser  
 192 scanning microscope (Olympus; OLS 5100) was examined  
 193 the surface and morphology of Inthanin bok dyes coated on  
 194 TiO<sub>2</sub> layers.



## 195 Statistical analysis

196 All statistical analyses were performed using SPSS Version  
197 20.0. A correlation was assumed significant when  $P < 0.05$ .

## 198 Results and discussion

### 199 Spectrophotometric analysis of pigments

200 The plant pigment structure was interacted with sunlight  
201 and the wavelengths were transformed by transmitted or  
202 reflected from the plant tissue. This procedure leads to the  
203 occurrence of plant pigmentation. The natural pigments  
204 such as chlorophylls, carotenoid, flavonoidere specified, and  
205 anthocyanin were specified from the maximum absorbance  
206 of wavelength ( $\lambda_{max}$ ) and the colors perceived by humans  
207 (Shalini et al. 2015; Kumara et al. 2013). In this study, the  
208 absorption wavelength of pigments extraction (Inthanin bok  
209 leaves) was examined by the UV–Vis spectrophotometer  
210 that the wavelength between 380 and 800 nm, as shown in  
211 Fig. 3. Absorbance spectra curves from the Inthanin bok  
212 dyes have shown three peaks of the wavelength of 420 nm,  
213 440 nm, and 470 nm. The wavelength of 420 nm, 490 nm,  
214 and 660 nm is the standard maximum absorption wavelength  
215 of chlorophylls (Khammee et al. 2020a, b). Thus, the maxi-  
216 mum absorption wavelength of Inthanin bok dyes feasibility  
217 is chlorophylls.

218 On the other hand, the absorption peak of Inthanin bok  
219 was also matched with the absorption bands of carotenoids,

220 which is 420 nm, 440 nm, and 470 nm. In most plant tis-  
221 sues, the spectrum's considerably sophisticated blue region  
222 owing to the absorption wavelength of chlorophylls and  
223 carotenoid pigments overlaps absorption wavelength (Kham-  
224 mee et al. 2020a, b). It indicates that the pigments' extraction  
225 from Inthanin bok consists of chlorophylls and carotenoid  
226 pigments.

### 227 The pigment extraction content and estimation 228 of Inthanin bok leaves

229 Chlorophylls are photosynthetic pigments that provide  
230 a green color. The primary functions of chlorophylls are  
231 harvesting light energy, spectral properties, and energy  
232 transduction for photosynthesis processes. Chlorophylls  
233 have two main types, which are chlorophyll-a and chloro-  
234 phyll-b (Ramaraj et al. 2013). Their derivatives of chloro-  
235 phylls are consumed as sensitizers in DSSC because of  
236 their absorbed blue and red light. The most efficient is  
237 the chlorophyll-a derivative, which is the carboxyl group.  
238 There are directly attached to the conjugated macrocycle  
239 to facilitate effective electron injection to  $\text{TiO}_2$  (Shalini  
240 et al. 2015; Wang et al. 2005). Moreover, carotenoids are  
241 a vast group with over 600 members; these are provided  
242 with red, orange, and yellow for fruits and flowers. Carot-  
243 enoids have essential roles in photosynthesis that comple-  
244 ment chlorophylls, and functional involves the light-har-  
245 vesting, photo-protective utilities, and the redox function  
246 (Wang et al. 2005; Frank and Cogdell 1996; Koyama  
247 and Fujii 1999). Inthanin bok leaves dye are composed

248 **Fig. 3** The absorption wave-  
249 length of pigments extraction  
(Inthanin bok leaves)

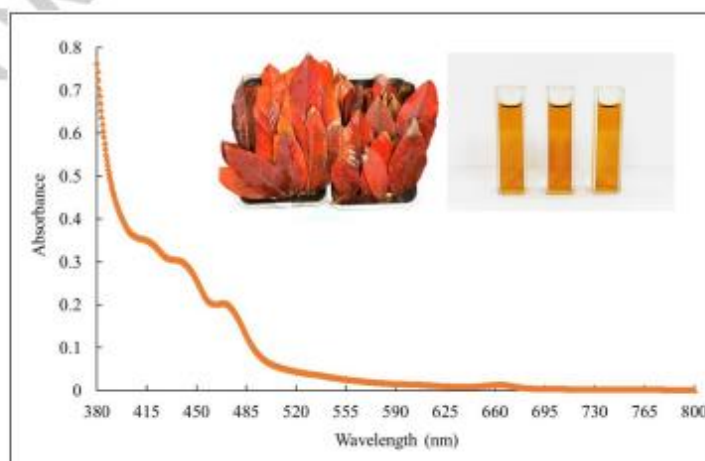


**Fig. 4** The amount of pigments (Inthanin bok leaves)

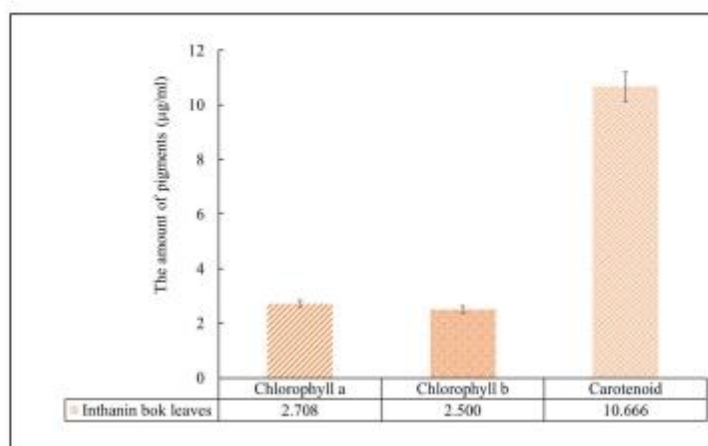
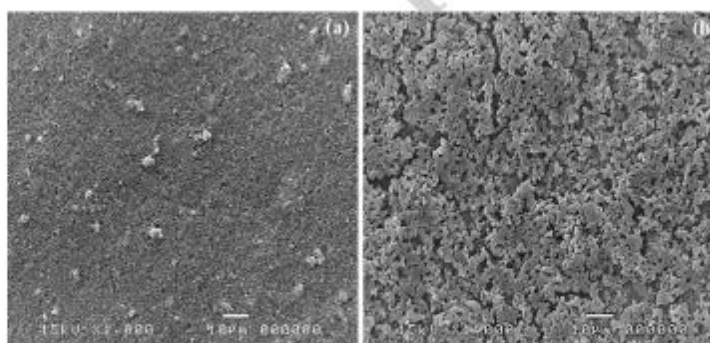


**Fig. 5** Scanning electron microscope of morphological characteristics of TiO<sub>2</sub> thin films without (a) and with natural dye extraction from Inthanin bok leaves dye annealed at 300 °C (b)



248 of pigments, which are chlorophyll-a, chlorophyll-b, and  
 249 carotenoids. Inthanin bok leaves analyzed the pigments  
 250 extraction content using UV–Vis spectrophotometer and  
 251 used the Eqs. (1, 2, and 3). The stated pigments found  
 252 that the remarkably composed of carotenoids, as revealed  
 253 in Fig. 4. The carotenoid content of natural dyes (Inthanin  
 254 bok leaves) was  $10.666 \pm 0.324 \mu\text{g/ml}$ ; followed by  
 255 chlorophyll-a with  $2.708 \pm 0.251 \mu\text{g/ml}$  and lastly, by  
 256 chlorophyll-b with  $2.500 \pm 0.102 \mu\text{g/ml}$ .

#### The surface and morphology analysis of TiO<sub>2</sub> nanoparticles and natural dyes

259 The scanning electron micrographs (SEM) of surface morphology characteristics of TiO<sub>2</sub> nanoparticles pure and with natural dye extracted from Inthanin bok leaves annealed at 300 °C are presented in Fig. 5a, b. The sphere-shaped TiO<sub>2</sub> nanoparticles were observed to be homogeneously distributed and porous. No cracks have been identified and stuck on the FTO glass substrate very well, as exposed in Fig. 5a. The agglomeration of small particles brings about to formation

Author Proof

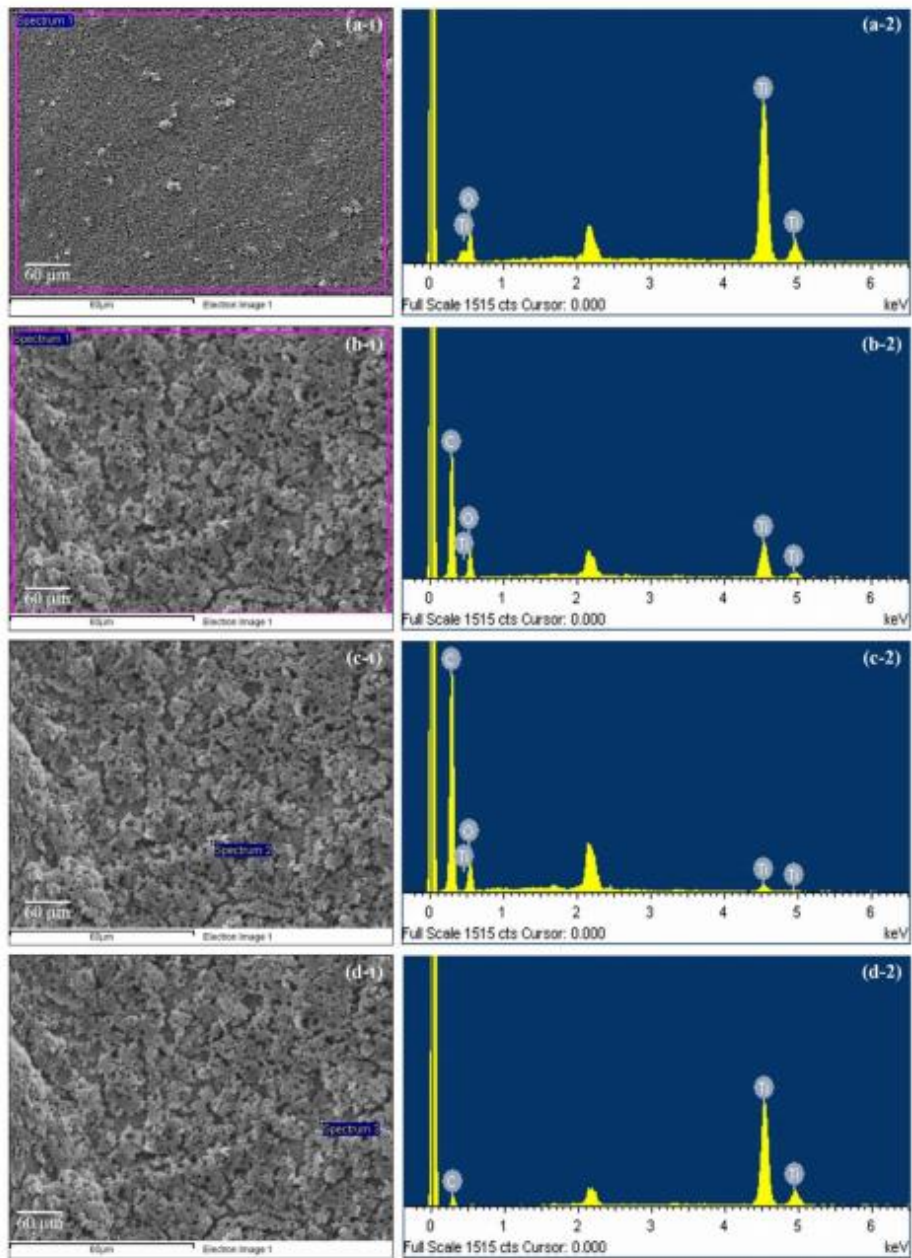




**Fig. 6** The energy-dispersive X-ray spectroscopy (EDX) analysis of TiO<sub>2</sub> coated on FTO glass substrate (a1, 2) and TiO<sub>2</sub>-coated on FTO glass substrates with natural dyes immersion (Inthanin bok leaves) with different spectrum (b1, 2-d1, 2)

of porous structure (Ruhane et al. 2017). The advantages of mesoporous holes of the TiO<sub>2</sub> is to provide the surface of a large hole for higher adsorption of dye molecules and facilitate the penetration of electrolyte within their pores (Jin et al. 2010). Generally, the highest pigment performance consists of the smallest molecule, peak refractive index, scattering coefficient, and brightness. The chemical adsorption of natural dyes becomes potential because of the condensation of hydroxyl and methoxy protons with the hydroxyl groups on the surface of nanostructured TiO<sub>2</sub> (Kushwaha et al. 2013). Therefore, Fig. 5b demonstrates that the pores and surface of the TiO<sub>2</sub> layer were covered with natural dyes extracted from Inthanin bok leaves. The spherical, agglomerate grain morphology can be predicted; it is the Inthanin bok leaves' pigment. Therefore, the spherical, agglomerate grain morphology and cover on their pores and surface of the TiO<sub>2</sub> layer in Fig. 5b can forecast; it is a natural pigment extracted from Inthanin bok leaves.

The energy-dispersive X-ray spectroscopy (EDX) was used to analyze the elemental contents of TiO<sub>2</sub> nanoparticles pure (Fig. 6a-1, 2) and with natural dye extracted from Inthanin bok leaves with different spectrums as shown in Fig. 6b-1, 2, c-1, 2 and d-1, 2 respectively. The data of elemental contents are presented in Table 1 and Fig. 6a-1, 2 indicates that the TiO<sub>2</sub> nanoparticles were coated on FTO glass due to elemental contents of oxygen (O) and titanium (Ti). The atomic ratios were 80.33 and 19.67%, respectively. Follow by Fig. 6b-1, 2, the natural pigments from Inthanin bok leave immersion on TiO<sub>2</sub> nanoparticles. The results show that elemental contents consist of carbon (C), oxygen (O), and titanium (Ti) was 74.42, 24.14, and 1.44%, respectively. This indicated that attendance of natural pigments of functional groups coated on the surfaces of TiO<sub>2</sub> particles. The adsorption of natural dyes on the TiO<sub>2</sub> layer can be boosted electron transfer rates (Al-Alwani et al. 2018).

#### The effect of different nanostructure layers and temperatures on DSSC

Recently, several improvements in this technology (DSSC), such as the innovative natural dyes, can absorb a more extended range of wavelengths and the titanium oxides (TiO<sub>2</sub>) nanostructure for increase surface areas, etc. (Sharma

et al. 2018; Khammee et al. 2020a, b). The main improvement of the research is not only by introducing natural dyes extracted from the waste material, which is Inthanin bok leaves (red or orange colors) that fall from the trees as light harvesters instead of TiO<sub>2</sub> itself but also using different nanostructure layers (1, 2, and 3 layers) and temperatures (100, 200, and 300 °C) to improve the absorption collection and efficiency of DSSC. Consequently, the optimized photoanode (TiO<sub>2</sub> nanostructure) is necessary for developing the high solar efficiency of DSSCs (Jeng et al. 2013).

The data of DSSC parameters of the devices obtained with different thicknesses and temperature of natural dyes extracted from Inthanin bok leaves are shown in Table 2. Extracted natural pigment (Inthanin bok leaves) was applied with the different layers and temperatures on the photocurrent-voltage characteristics curve for the DSSC are presented in Fig. 7. The results showed that the highest efficiency of the pigments extracted from Inthanin bok leaves is  $1.138\% \pm 0.018$ , which the condition of one layer of TiO<sub>2</sub> nanostructure and natural dyes and the temperature; 300 °C. The photocurrent-voltage and power-voltage characteristics curve for the highest efficiency is shown in Fig. 8; also, the thickness, two layers, and the temperature; 300 °C was a similar performance, which is  $1.134\% \pm 0.160$ . Still, the layer of thickness increased, and the protection of the environment, causing chemical waste in TiO<sub>2</sub> paste processing, higher cost value, and protection of the environment.

The increasing rise in the thickness of TiO<sub>2</sub> layers will adsorb more natural dyes. However, the results have shown that the established electron in natural dyes extracted from Inthanin bok leaves cannot be effectively injected into the electrode due too long-distance when the thickness of TiO<sub>2</sub> layers is too thick. The thicker TiO<sub>2</sub> layers will also result in a dwindle transmittance and reduce the pigment dyes' absorption of light intensity. Also, the resistance of charge transfer might be increasing when the thickness of TiO<sub>2</sub> layers increases. Furthermore, the thicker layers of TiO<sub>2</sub> will become difficult for the charge recombination between electrons from the excited dye to the conduction band of TiO<sub>2</sub> and the I<sub>3</sub><sup>-</sup> ions in the electrolyte (Jeng et al. 2013).

Moreover, this research's different temperature affects the pores of TiO<sub>2</sub> nanoparticles and the absorption of natural dyes that result in the performance of DSSC. There examined using the laser scanning microscope to analyzed the surface and morphology of Inthanin bok dyes coated on TiO<sub>2</sub> layers (1 layer and 100 °C) and (1 layer and 300 °C) to the comparison of the low and the highest efficiency of DSSC as shown in Figs. 9 and 10. Also, the area under a



**Table 1** The elemental composition of TiO<sub>2</sub> coated on FTO glass substrate with natural dyes immersion (Inthanin bok leaves)

Methods	Element	Weight %	Atomic %
Blank TiO <sub>2</sub> (spectrum 1) (a-1,2)	O, K	57.70	80.33
	Ti, K	42.30	19.67
Inthanin bok (spectrum 1) (b-1,2)	C, K	66.26	74.42
	O, K	28.63	24.14
	Ti, K	5.11	1.44
Inthanin bok (spectrum 2) (c-1,2)	C, K	77.41	82.29
	O, K	21.98	17.54
	Ti, K	0.61	0.16
Inthanin bok (spectrum 3) (d-1,2)	C, K	35.58	68.78
	Ti, K	64.42	31.22

356 curve of the surface of the low and high efficiency of DSSC  
357 is presented in Table 3.

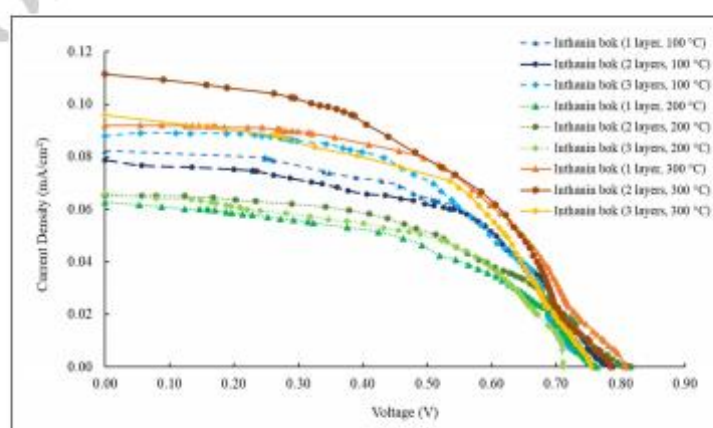
358 In general, for annealing used, the low temperature for the  
359 fabrication DSSCs should override two main problems for

improving photovoltaic performance: the first problem is the  
360 defective connection of TiO<sub>2</sub> particles (Miyasaka et al. 2007)  
361 and the second issue is the residuals of the organic binder  
362 within the TiO<sub>2</sub> film. During the preparation of TiO<sub>2</sub> paste  
363 usually added organic binder, thus the residuals of the binder  
364 would become an insulting core in an annealing process  
365 using the low temperature and would block the transporta-  
366 tion path of electrons that result in the electron transport rate  
367 and electron lifetime would decrease (Longo et al. 2002; Lin  
368 et al. 2012). It can be seen that, in Fig. 10c, the surface area  
369 and morphology of Inthanin bok dyes coated on TiO<sub>2</sub> layers  
370 (1 layer and 300 °C) using the laser scanning microscope  
371 has a roughness than the surface area and morphology of  
372 Inthanin bok dyes coated on TiO<sub>2</sub> layers (1 layer and 100 °C)  
373 in Fig. 9c, due to the difference in temperatures during the  
374 annealing process.

375 The results of the area under a graph of the natural pig-  
376 ments extracted from Inthanin bok leaves were found that  
377 the condition of the thickness of TiO<sub>2</sub> layer; 1 layer and  
378 annealing at 300 °C has the higher result which is two times  
379

**Table 2** The DSSC parameters of the devices obtained with different thicknesses and temperature (natural dyes extracted from Inthanin bok)

Dyes	Thicknesses (layers)	Temperature (°C)	$I_{sc}$ (mA/cm <sup>2</sup> )	$V_{oc}$ (V)	FF (%)	$\eta$ (%)
Inthanin bok	1	100	0.082	0.759	53.20	0.948 ± 0.031
	2	100	0.079	0.788	52.60	0.932 ± 0.127
	3	100	0.088	0.760	53.27	1.014 ± 0.033
	1	200	0.063	0.763	46.41	0.633 ± 0.065
	2	200	0.065	0.816	48.51	0.738 ± 0.157
	3	200	0.066	0.710	53.80	0.721 ± 0.018
	1	300	0.092	0.807	53.71	1.138 ± 0.018
	2	300	0.111	0.785	45.46	1.134 ± 0.160
	3	300	0.096	0.754	52.33	1.080 ± 0.086

**Fig. 7** The photocurrent–voltage characteristics curve for the DSSC extraction natural pigment (Inthanin bok leaves)

**Fig. 8** The photocurrent–voltage and power–voltage characteristics curve for the DSSC extraction natural pigment (Inthanin bok leaves)

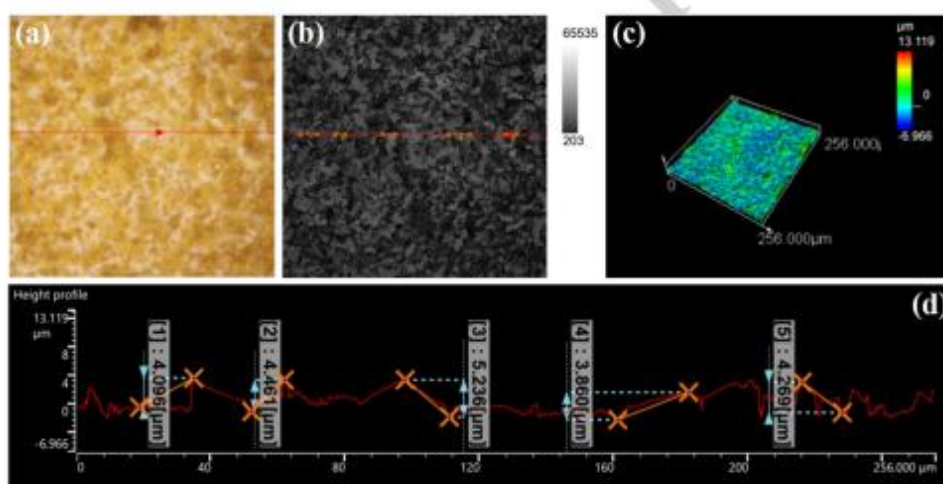
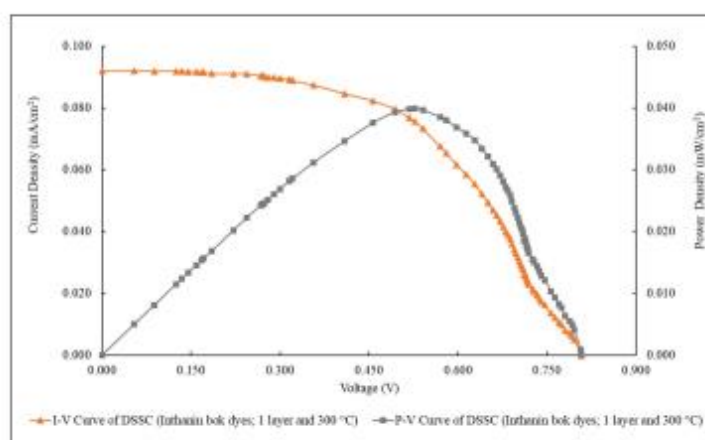


**Fig. 9** The laser scanning microscope analyzed the surface and morphology of Inthanin bok dyes coated on  $\text{TiO}_2$  layers (1 layer and 100 °C)

380 of  $\text{TiO}_2$  layer, 1 layer and annealing at 100 °C as shown in  
381 Table 3. This recommends that the binder's residuals within  
382 the  $\text{TiO}_2$  paste decompose during the annealing process at  
383 high temperatures. There could be correlated with increasing  
384 the layer's surface area. It can increase the dye adsorption  
385 and high photocurrent generation (Krašovec et al. 2009).

386 Table 4 indicates the values of  $I_{sc}$ ,  $V_{oc}$ , FF, and  $\eta$  obtained  
387 from the photovoltaic device (DSSCs) employing photoan-  
388 odes with sensitizer from natural dye extracts (Shalini et al.  
389 2015; Tributsch 1972; Chang et al. 2010; Gómez-Ortiz et al.  
390 2010). Electric current and voltage on DSSC are generated  
391 by irradiation using tungsten lamps, and then, changes in the

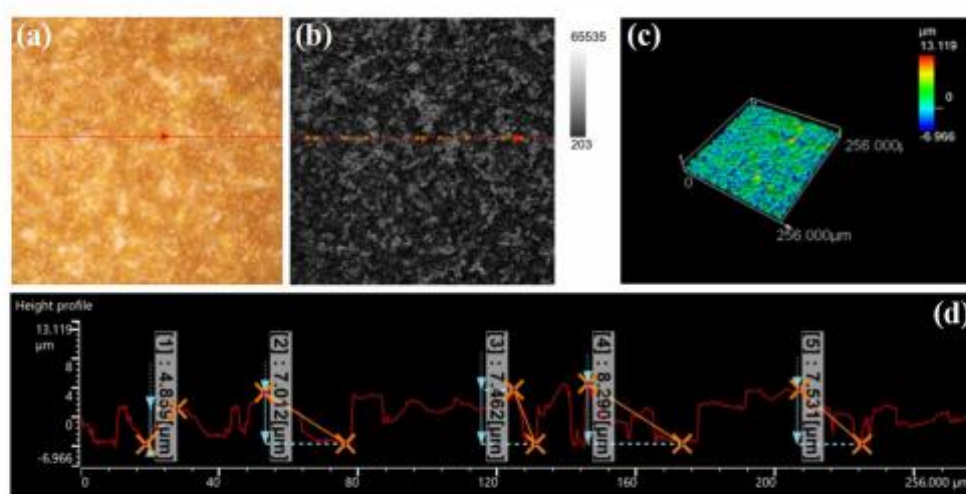


Fig. 10 The laser scanning microscope analyzed the surface and morphology of Inthanin bok dyes coated on TiO<sub>2</sub> layers (1 layer and 300 °C)

**Table 3** The area under a graph (μm<sup>2</sup>) of Inthanin bok dyes coated on TiO<sub>2</sub> layers

Methods	The area under a graph (μm <sup>2</sup> )
Inthanin bok (1 layer, 100 °C)	31.110
Inthanin bok (1 layer, 300 °C)	61.426

392 current and voltage generated are measured the performance  
 393 of DSSC. It was based on natural dyes added with nano-  
 394 TiO<sub>2</sub> that were successfully made. The presence of carbon,  
 395 oxygen, and phosphorus elements in TiO<sub>2</sub> causes the charge  
 396 delivery distance to be shorter to increase the electric cur-  
 397 rent. Our best device, one layer of TiO<sub>2</sub> and annealing at  
 398 300 °C, has the highest performance than other dye pigments  
 399 extracted from different plants.

## Conclusion

400  
 401 In this study, Inthanin bok leaves dye consists of natural  
 402 pigments and these pigments are used as natural dyes  
 403 sensitizers for solar cells. The energy-dispersive X-ray  
 404 spectroscopy was confirmed the elemental of the TiO<sub>2</sub>  
 405 nanoparticles and natural dyes from Inthanin bok leaves.  
 406 SEM images result clearly indicate the surface and morpho-  
 407 logy of natural pigments and TiO<sub>2</sub> nanoparticles. The  
 408 laser scanning microscopy results also revealed that the  
 409 noninvasive spectroscopic methods are important for  
 410 monitoring the physiological state of natural dyes coated  
 411 on the nano-TiO<sub>2</sub> assembled DSSC. Moreover, the high-  
 412 est efficiency of the pigments extracted from Inthanin bok  
 413 leaves is  $1.138\% \pm 0.018$ , which the condition of 1 layer of  
 414 TiO<sub>2</sub> nanoparticles and the temperature; 300 °C. Thus, this  
 415 study recommends that chlorophylls and carotenoids have  
 416 good potential to be photosensitizers in DSSC. Natural  
 417 pigments are cheap, safe, environmentally friendly, easily  
 418 found, and easy extraction process. It can be concluded  
 419 that naturally synthesized pigment-based DSSC will be the  
 420 next generation of bio-solar in the near future, overcoming  
 421 conventional energy sources.



**Table 4** The DSSC parameters of the devices obtained with different natural dyes extraction

Dyes	Dye pigments	$I_{sc}$ (mA/cm <sup>2</sup> )	$V_{oc}$ (V)	FF (%)	$\eta$ (%)	Reference
 Perilla	Chlorophylls	1.36	0.522	69.9	0.50	Shalini et al. (2015)
 Bitterleaf ( <i>Vernonia amygdalin</i> )	Chlorophylls	0.07	0.34	81	0.69	Tributsch (1972)
 Spinach	Chlorophylls	0.470	0.550	51	0.13	Chang et al. (2010)
 Parsley ( <i>Petroselinum crispum</i> )	Chlorophylls	0.530	0.440	34	0.07	Shalini et al. (2015)
 Arugula	Chlorophylls	0.780	0.590	42.0	0.20	Shalini et al. (2015)
 Achiote ( <i>Bixa arellana L.</i> )	Carotenoid	1.100	0.57	59	0.37	Gómez-Ortiz et al. (2010)
 Alkanet	Carotenoid	0.268	0.372	46	0.03	Shalini et al. (2015)
 Turmeric ( <i>Curcuma longa</i> )	Carotenoid	0.200	0.280	65	0.36	Shalini et al. (2015)
 Golden trumpet ( <i>Allamanda cathartica</i> )	Carotenoid	0.878	0.405	54	0.40	Shalini et al. (2015)
 Inthanin bok ( <i>Lagerstroemia macrocarpa</i> )	Carotenoid and Chlorophylls	0.092	0.807	53.71	1.138	This research

422 **Acknowledgements** The authors acknowledged the Program in Bio-  
 423 technology, Energy Research Center, School of Renewable Energy,  
 424 Maejo University, Chiang Mai, Thailand, and supports from advanced  
 425 characterization by Quality Report, Co., Ltd, Bangkok, Thailand.

## 426 References

427 Al-Alwani MA, Ludin NA, Mohamad AB, Kadhum AAH, Mukhlus A  
 428 (2018) Application of dyes extracted from *Alternanthera dentata*  
 429 leaves and *Musa acuminata* bracts as natural sensitizers for dye-  
 430 sensitized solar cells. *Spectrochim Acta A Mol Biomol Spectrosc*  
 431 192:487–498. <https://doi.org/10.1016/j.saa.2017.11.018>  
 432 Alami AH, Aokal K, Zhang D, Taieb A, Faraj M, Alhammedi A et al  
 433 (2019) Low-cost dye-sensitized solar cells with ball-milled tellu-  
 434 rium-doped graphene as counter electrodes and a natural sensitizer

dye. *Int J Energy Res* 43(11):5824–5833. <https://doi.org/10.1002/er.4684>

Ananthi N, Subathra MSP, Emmanuel SC, Kumar NM (2020) Prepara-  
 437 tion and characterization of two dye-sensitized solar cells  
 438 using *Acalypha Godseffia* and *Epipremnum Aureum* dyes as sensi-  
 439 tizers. *Energy Source Part A* 42(13):1662–1673. <https://doi.org/10.1080/15567036.2019.1604876>

Argazzi R, Larramona G, Contado C, Bignozzi CA (2004) Prepara-  
 442 tion and photoelectrochemical characterization of a red sensi-  
 443 tive osmium complex containing 4, 4', 4"-tricarboxy-2, 2', 6',  
 444 2"-terpyridine and cyanide ligands. *J Photochem Photobiol A*  
 445 Chem 164(1–3):15–21. <https://doi.org/10.1016/j.jphotochem.2003.12.016>

Arulraj A, Govindan S, Vadivel S, Subramanian B (2017) Photo-  
 448 voltaic performance of TiO<sub>2</sub> using natural sensitizer extracted  
 449 from *Phyllanthus Reticulatus*. *J Mater Sci Mater Electron*  
 450 28(24):18455–18462



- 452 Arulraj A, Senguttuvan G, Veeramani S, Sivakumar V, Subrama-  
453 nian B (2019) Photovoltaic performance of natural metal free  
454 photosensitizer for TiO<sub>2</sub> based dye-sensitized solar cells. *Optik*  
455 181:619–626. <https://doi.org/10.1016/j.ijleo.2018.12.104>
- 456 Bashar H, Bhuiyan MMH, Hossain MR, Kabir F et al (2019) Study  
457 on combination of natural red and green dyes to improve the  
458 power conversion efficiency of dye sensitized solar cells. *Optik*  
459 185:620–625. <https://doi.org/10.1016/j.ijleo.2019.03.043>
- 460 Cerda B, Sivakumar R, Paulraj M (2016) Natural dyes as sensitizers  
461 to increase the efficiency in sensitized solar cells. *J Phys Conf*  
462 Ser 720(1):012030
- 463 Chang H, Wu HM, Chen TL, Huang KD et al (2010) Dye-sensi-  
464 tized solar cell using natural dyes extracted from spinach  
465 and ipomoea. *J Alloy Compd* 495(2):606–610. <https://doi.org/10.1016/j.jallcom.2009.10.057>
- 466 Dawoud AM (2016) Natural pigments extracted from plant leaves  
467 as photosensitizers for dye-sensitized solar cells. Dissertation,  
468 Islamic University of Gaza
- 469 Frank HA, Cogdell RJ (1996) Carotenoids in photosynthesis. *Photochem Photobiol* 63(3):257–264
- 470 Gómez-Ortiz NM, Vázquez-Maldonado IA, Pérez-Espadas AR et al  
471 (2010) Dye-sensitized solar cells with natural dyes extracted  
472 from achiote seeds. *Sol Energy Mater Sol Cells* 94(1):40–44.  
473 <https://doi.org/10.1016/j.solmat.2009.05.013>
- 474 Gu P, Yang D, Zhu X, Sun H, Wangyang P, Li J, Tian H (2017)  
475 Influence of electrolyte proportion on the performance of  
476 dye-sensitized solar cells. *AIP Adv* 7(10):105219. <https://doi.org/10.1063/1.5000564>
- 477 Jeng MJ, Wung YL, Chang LB, Chow L (2013) Particle size effects  
478 of TiO<sub>2</sub> layers on the solar efficiency of dye-sensitized solar  
479 cells. *Int J Photoenergy*. <https://doi.org/10.1155/2013/563897>
- 480 Jin EM, Park KH, Jin B, Yun JJ, Gu HB (2010) Photosensitiza-  
481 tion of nanoporous TiO<sub>2</sub> films with natural dye. *Phys. Ser*  
482 2010(T139):014006
- 483 Khamme P, Unpaprom Y, Subhasaen U, Ramaraj R (2020a) Potential  
484 evaluation of yellow cotton (*Cochlospermum regium*) pigments  
485 for dye sensitized solar cells application. *Glob J Sci Eng* 2:16–21.  
486 <https://doi.org/10.37516/global.j.sci.eng.2020.008>
- 487 Khamme P, Unpaprom Y, Whangchai K, Ramaraj R (2020b) Com-  
488 parative studies of the longan leaf pigment extraction as a photo-  
489 sensitizer for dye-sensitized solar cells' purpose. *Biomass Conv*  
490 *Biorefinery*. <https://doi.org/10.1007/s13399-020-01060-x>
- 491 Koyama Y, Fujii R (1999) Cis-trans carotenoids in photosynthesis:  
492 configurations, excited-state properties and physiological func-  
493 tions. In: Frank HA, Young AJ, Britton G, Cogdell RJ (eds) *The*  
494 *photochemistry of carotenoids*. *Advances in photosynthesis and*  
495 *respiration*, vol 8. Springer, Dordrecht, pp 161–188. [https://doi.org/10.1007/0-306-48209-6\\_9](https://doi.org/10.1007/0-306-48209-6_9)
- 496 Krašovec UO, Berginc M, Hočevar M, Topič M (2009) Unique TiO<sub>2</sub>  
497 paste for high efficiency dye-sensitized solar cells. *Sol Energy*  
498 *Mater Sol Cells* 93(3):379–381. <https://doi.org/10.1016/j.solmat.2008.11.012>
- 499 Kumara NTRN, Ekanayake P, Lim A, Liew LYC et al (2013) Layered  
500 co-sensitization for enhancement of conversion efficiency of natu-  
501 ral dye sensitized solar cells. *J Alloys Compd* 581:186–191. <https://doi.org/10.1016/j.jallcom.2013.07.039>
- 502 Kushwaha R, Srivastava P, Bahadur L (2013) Natural pigments from  
503 plants used as sensitizers for TiO<sub>2</sub> based dye-sensitized solar cells.  
504 *J Energy*. <https://doi.org/10.1155/2013/654953>
- 505 Lin LY, Lee CP, Tsai KW, Yeh MH, Chen CY et al (2012) Low-tem-  
506 perature flexible Ti/TiO<sub>2</sub> photoanode for dye-sensitized solar cells  
507 with binder-free TiO<sub>2</sub> paste. *Prog Photovolt Res Appl* 20(2):181–  
508 190. <https://doi.org/10.1002/pip.1116>
- 509 Longo C, Nogueira AF, De Paoli MA, Cachet H (2002) Solid-state and  
510 flexible dye-sensitized TiO<sub>2</sub> solar cells: a study by electrochemi-  
511 cal impedance spectroscopy. *J Phys Chem B* 106(23):5925–5930
- 512 Miyasaka T, Ikegami M, Kijitori Y (2007) Photovoltaic performance  
513 of plastic dye-sensitized electrodes prepared by low-temperature  
514 binder-free coating of mesoscopic titania. *J Electrochem Soc*  
515 154(5):A455
- 516 Nguyen TVT, Unpaprom Y, Tandee K, Whangchai K, Ramaraj R  
517 (2020) Physical pretreatment and algal enzyme hydrolysis of  
518 dried low-grade and waste longan fruits to enhance its ferment-  
519 able sugar production. *Biomass Conv Biorefinery*. <https://doi.org/10.1007/s13399-020-011176-0>
- 520 Nong HTT, Unpaprom Y, Chaichompoo C, Ramaraj R (2020) Biome-  
521 thane potential of invasive aquatic weed water primrose. *Glob J Sci*  
522 *Eng* 5:1–5. <https://doi.org/10.37516/global.j.sci.eng.2021.0025>
- 523 Ocakoglu K, Harputlu E, Guloglu P, Erten-Elä S (2012) The photovol-  
524 taic performance of new ruthenium complexes in DSSCs based  
525 on nanorod ZnO electrode. *Synth Met* 162(23):2125–2133. <https://doi.org/10.1016/j.synthmet.2012.10.006>
- 526 Rajkumar S, Kumar MN, Suguna K, Muthulakshmi S, Kumar RA  
527 (2019) Enhanced performance of dye-sensitized solar cells using  
528 natural cocktail dye as sensitizer. *Optik* 178:224–230. <https://doi.org/10.1016/j.ijleo.2018.10.004>
- 529 Ramaraj R, Tsai DD, Chen PH (2013) Chlorophyll is not accurate  
530 measurement for algal biomass. *Chiang Mai J Sci* 40(4):547–555
- 531 Richhariya G, Kumar A, Tekasakul P, Gupta B (2017) Natural dyes  
532 for dye sensitized solar cell: a review. *Renew Sust Energy Rev*  
533 69:705–718. <https://doi.org/10.1016/j.rser.2016.11.198>
- 534 Ruhane TA, Islam MT, Rahaman MS, Bhuiyan MMH, Islam JM et al  
535 (2017) Photocurrent enhancement of natural dye sensitized solar  
536 cell by optimizing dye extraction and its loading period. *Optik*  
537 149:174–183. <https://doi.org/10.1016/j.ijleo.2017.09.024>
- 538 Shalini S, Prasanna S, Mallick TK, Senthilarasu S (2015) Review  
539 on natural dye sensitized solar cells: operation, materials and  
540 methods. *Renew Sust Energy Rev* 51:1306–1325. <https://doi.org/10.1016/j.rser.2015.07.052>
- 541 Sharma K, Sharma V, Sharma SS (2018) Dye-sensitized solar cells:  
542 fundamentals and current status. *Nanoscale Res Lett* 13(1):381
- 543 Sophanodorn K, Unpaprom Y, Whangchai K, Duangsaphasin A, Man-  
544 mai N, Ramaraj R (2020a) A biorefinery approach for the produc-  
545 tion of bioethanol from alkaline-pretreated, enzymatically hydro-  
546 lyzed *Nicotiana tabacum* stalks as feedstock for the bio-based  
547 industry. *Biomass Conv Biorefinery*. <https://doi.org/10.1007/s13399-020-01177-z>
- 548 Sophanodorn K, Unpaprom Y, Whangchai K, Homdoun N, Dussadee  
549 N, Ramaraj R (2020b) Environmental management and valoriza-  
550 tion of cultivated tobacco stalks by combined pretreatment for  
551 potential bioethanol production. *Biomass Conv Biorefinery*. <https://doi.org/10.1007/s13399-020-00992-8>
- 552 Sumanta N, Haque CI, Nishika J, Suprakash R (2014) Spectropho-  
553 tometric analysis of chlorophylls and carotenoids from commonly  
554 grown fern species by using various extracting solvents. *Res J*  
555 *Chem Sci* 4(9):63–69
- 556 Tributsch H (1972) Reaction of excited chlorophyll molecules at elec-  
557 trodes and in photosynthesis. *Photochem Photobiol* 16(4):261–  
558 269. <https://doi.org/10.1111/j.1751-1097.1972.tb06297.x>
- 559 Unpaprom Y, Pimpimol T, Whangchai K, Ramaraj R (2020) Sustain-  
560 ability assessment of water hyacinth with swine dung for biogas  
561 production

APPENDIX B  
CERTIFICATES



**BEST PRESENTATION AWARD**

THIS IS PROUDLY GIVEN TO

**PHITCHAPHORN KHAMMEE**

for the best presentation (2nd position) at

**THE INTERNATIONAL ONLINE CONFERENCE ON  
INNOVATIVE SCIENCE, ENGINEERING, AND TECHNOLOGY  
(IOCISSET-2020) (JULY 03, 2020 - JULY 05, 2020)**

on the topic *"Potential Evaluation of Yellow  
Cotton (Cochlospermum Regium) Pigments  
for Dye Sensitized Solar Cells Application"*



**Knowvel**

TAKE YOUR RESEARCH TO NEXT LEVEL

**KNOWVEL JOURNALS**  
WWW.KNOWVEL.COM  
INFO@KNOWVEL.COM





## CERTIFICATE OF ATTENDANCE, PARTICIPATION, & PRESENTATION

THIS IS PROUDLY GIVEN TO

**PHITCHAPHORN KHAMMEE**

for attending, participating and conducting an oral presentation at

**THE INTERNATIONAL ONLINE CONFERENCE ON  
INNOVATIVE SCIENCE, ENGINEERING, AND TECHNOLOGY  
(IOCISSET-2020) (JULY 03, 2020 - JULY 05, 2020)**

as per the details below:

**Submission Type:** Full Paper

**Title:** Potential Evaluation of Yellow Cotton  
(*Cochlospermum regium*) Pigments for Dye  
Sensitized Solar Cells Application



**Knowvel**

TAKE YOUR RESEARCH TO NEXT LEVEL

  
**KNOWVEL JOURNALS**  
WWW.KNOWVEL.COM  
INFO@KNOWVEL.COM





**INTERNATIONAL CONFERENCE OF BIOMASS AND BIOENERGY 2020**  
"Advanced Technology and Digital Innovations in Biomass, Bioenergy and Agriculture"

# Certificate

This is to certify that

**Phitchaphorn Khammee**

Has participated as a

**Presenter**

10-11 August 2020

Chairman of International Conference of Biomass and Bioenergy

Dr. Dwi Setyaningsih, S.TP, M.Si



## ใบรับรองผลการสอบภาษาอังกฤษ

ใบรับรองนี้ให้ไว้เพื่อแสดงว่า

**นางสาวพิชชาพร คำมี**

ได้เข้ารับการทดสอบวัดสมรรถภาพทั่วไปทางภาษาอังกฤษของมหาวิทยาลัยแม่โจ้

(Maejo University Test of English Proficiency: MJU-TEP)

เมื่อวันที่ ๒๖ มิถุนายน พ.ศ. ๒๕๖๓

และได้ผลการทดสอบดังนี้และได้แสดงผลไว้ทางด้านหลังของใบรับรองนี้ด้วย

- |                           |                |
|---------------------------|----------------|
| ๑. ทักษะการฟังเข้าใจความ  | ๒๐ / ๓๐ คะแนน  |
| ๒. ทักษะกึ่งการพูด        | ๑๙ / ๒๕ คะแนน  |
| ๓. ทักษะกึ่งการเขียน      | ๑๓ / ๓๐ คะแนน  |
| ๔. ทักษะการอ่านเข้าใจความ | ๒๒ / ๓๕ คะแนน  |
| คะแนนรวม                  | ๗๔ / ๑๒๐ คะแนน |

ให้ไว้เมื่อวันที่ ๒ กรกฎาคม พ.ศ. ๒๕๖๓

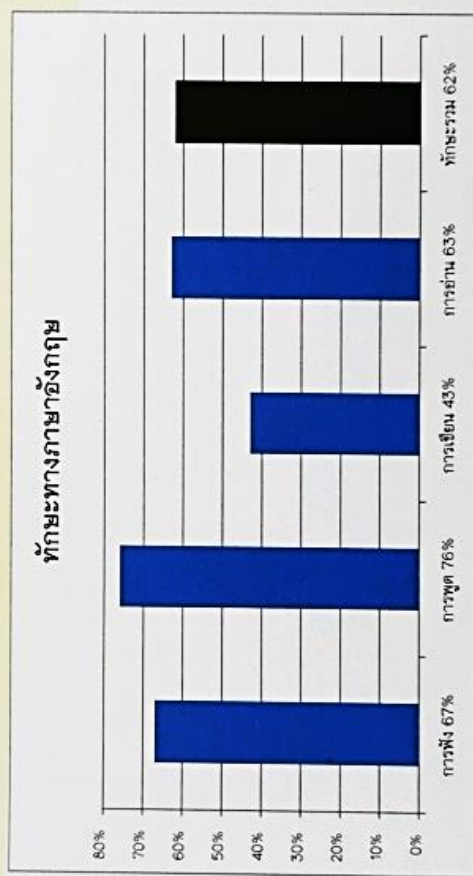


(อาจารย์ ดร.สุเขต สกุลทอง)

รักษาการผู้อำนวยการ ศูนย์ภาษา มหาวิทยาลัยแม่โจ้

## คะแนนผลทดสอบ MJU-TEP

### ของ นางสาวพิชชาพร คำมี



#### ความหมาย

1. ความสามารถระดับเริ่มต้น (Beginning users) 0-20%
2. ความสามารถระดับจำกัดมาก (Very limited users) 21-30%
3. ความสามารถระดับจำกัด (Limited users) 31-40%
4. ความสามารถระดับปานกลาง (Modest users) 41-60%
5. ความสามารถระดับค่อนข้างดี (Competent users) 61-70%
6. ความสามารถระดับดี (Good users) 71-80%
7. ความสามารถระดับดีมาก (Very good users) 81-90%
8. ความสามารถระดับเชี่ยวชาญ (Expert users) 91-100%

## CURRICULUM VITAE

**NAME** Phitchaphorn Khammee

**DATE OF BIRTH** 11 April 1996

**EDUCATION** High School: Lampang Kanlayanee School  
Bachelor: Bachelor of Science Program in Renewable  
Energy, Maejo University

